

# Thermal ignition system for green rocket propulsion

Experimental study on thermal ignition of high concentration hydrogen peroxide and ethanol propellant

Emre Tambag



# Thermal ignition system for green rocket propulsion

**Experimental study on thermal ignition of high  
concentration hydrogen peroxide and ethanol  
propellant**

by

Emre Tambag

to obtain the degree of Master of Science,  
in the field of Aerospace Engineering,  
at the Delft University of Technology.  
to be defended publicly on Tuesday August 23, 2022 at 09:30 AM.

Student number:	4973631	
Project Duration:	November, 2021 - August, 2022	
Thesis committee:	Dr. B. V. S. Jyoti, Prof. Dr. E.K.A. Gill, Ir. R. Noomen,	TU Delft supervisor, Ast. Prof. TU Delft TU Delft, Chairman Committee TU Delft, External Committee Member

An electronic version of this thesis is available at <http://repository.tudelft.nl/>



# Preface

This Master thesis contains the results and observations undertaken at the Aerospace Faculty of TU Delft. This study was realized to obtain a Master of Science degree and hereby also marking the end of a period as a student. The past couple of years were a challenging trip with ups and downs, especially with the COVID period where working from home was the norm. Fortunately, during this period and during my Master's thesis period I had support from experts, coaches and friends who helped and motivated me when necessary. For this, I would kindly thank them.

The most important person that helped me and motivated me, during this research, was my thesis supervisor B.V.S. Jyoti. Her extraordinary motivation and support on an almost daily basis helped me to stay focused and make progress with the research. Especially when experiments failed and the motivation tumbled, you still saw the good in it and motivated me to carry on. Secondly, I would like to thank SolvGE for their support and for providing me with the high concentration of hydrogen peroxide. Without them providing me with this chemical, this exciting research would never have taken place.

I would also like to thank my fellow students, with whom I spent many (online) hours studying together, working on projects and motivating each other when experiencing mental lows. I enjoyed working together and the interesting talks and fun moments we had together.

*“In the field of technology, simplification is always an enormous advance...”*

— Pierre Boule

*Emre Tambag  
Delft, August 2022*



# Abstract

With the field in surge for the replacement of storable liquid bipropellants that are toxic, carcinogenic and hazardous to the environment, like hydrazine and its alternatives, new propellants that are less harmful and toxic are being studied. Together with the research and development of green propellants, as they are called, also other sub-components are in development, like the igniter system. This thesis research focused on the development of a novel igniter system for small storable liquid bi-propellant rocket engines, used in (small) satellites, which is reliable, cost-effective and re-ignitable. During the thesis research, first an alternative green propellant has been selected by means of a trade-off and the ignition system that will be developed. For the selected ignition system and propellant, an experimental test set-up has been made to perform ignition experiments in the chemical laboratory. After the experimental phase, a simplified computer model of the experimental set-up has been made in COMSOL. The results of the computer model are compared with the experimental data for the validation of the model.

Based on the trade-offs made, hydrogen peroxide and ethanol were selected as the oxidizer and fuel, respectively, from a list of green propellants. This propellant combination is less toxic and better for the environment compared to the current propellant combination, which is hydrazine in combination with dinitrogen tetroxide (NTO). While the specific impulse of hydrazine/NTO is better than almost all green storable bipropellants, including hydrogen peroxide/ethanol. The density specific impulse, of the green propellants is comparable with the current propellant combination. For the ignition system a thermal igniter system was selected and developed during this thesis research, because of the low cost, limited mass/volume and the possibility to re-ignite the rocket engine.

During the experimental phase of the study, various experiments have been performed to improve the set-up and the design. The final design was achieved after 10 iterations of improvement. Two experiments have been performed. During the first experiment the optimal angle for the injector head was put to the test. With the aid of a trade-off table, it was selected that the  $20^\circ$  injector head was providing the best results. During the second experiment, with the selected injector head, the power consumption was further reduced to 14 W. Further decreasing the length of the heating coil, made the injected liquid cool down the coil too fast and as a result no ignition was achieved. However, with a small optimization of the heating coil by confining the four wounds of the heating coil at the center of the combustion chamber to have ignition and self-sustained combustion with a power consumption of 10 W was achieved.

A simplified computer model is made of the experimental test set-up. While during the experiments, both hydrogen peroxide and ethanol are injected into the combustion chamber, for the simulation only a single fluid is injected to reduce the complexity of the simulation. Furthermore, it was assumed that ignition would have happened in case the liquid reached the auto-ignition temperature of ethanol which is  $365^\circ\text{C}$ . Three simulations have been performed, each with a different power consumption of the heating coil. Both with a power consumption of 20 W as well as with 15 W the temperature of the liquid reached  $365^\circ\text{C}$  and it could be assumed that ignition would have happened. With the 10 W simulation, the maximum temperature was  $329^\circ\text{C}$ , which is significantly lower than the auto-ignition temperature of ethanol. This is identical to the experimental results, since the lowest power consumption where ignition was achieved, without any optimization, was 14 W.





# Contents

<b>Preface</b>	<b>ii</b>
<b>Abstract</b>	<b>iv</b>
<b>Nomenclature</b>	<b>ix</b>
<b>List of Figures</b>	<b>x</b>
<b>List of Tables</b>	<b>xii</b>
<b>1 Introduction</b>	<b>1</b>
1.1 Research Objectives and Questions . . . . .	1
1.2 System requirements . . . . .	2
1.3 Structure . . . . .	3
<b>2 Literature Study</b>	<b>4</b>
2.1 Igniter systems . . . . .	4
2.1.1 Spark plugs . . . . .	4
2.1.2 Torch igniter . . . . .	5
2.1.3 Hypergolic igniter . . . . .	6
2.1.4 Catalytic igniter . . . . .	6
2.1.5 Thermal igniter . . . . .	7
2.2 Trade-off ignition systems . . . . .	8
2.2.1 Trade-off criterion . . . . .	8
2.2.2 Trade-off table & Discussion . . . . .	9
2.3 Green oxidizer selection . . . . .	10
2.4 Green fuel selection . . . . .	11
2.5 Heating coil selection . . . . .	12
2.6 Combustion of hydrogen peroxide and Ethanol . . . . .	12
2.6.1 Decomposition of Hydrogen peroxide . . . . .	12
2.6.2 Chemical reaction of Hydrogen peroxide and Ethanol . . . . .	13
2.7 Conclusion literature study . . . . .	13
<b>3 Test set-up</b>	<b>14</b>
3.1 Set-up . . . . .	14
3.2 Experiment description . . . . .	16
3.2.1 Experiment 1: Injector angle . . . . .	17
3.2.2 Experiment 2: Reducing length of heating coil . . . . .	17
3.3 Test plan . . . . .	17
3.3.1 Experiment preparation . . . . .	17
3.3.2 Experimental phase . . . . .	18
3.3.3 Expected results . . . . .	19
3.4 Conclusion test plan . . . . .	20
<b>4 Results &amp; Observations</b>	<b>21</b>
4.1 General observations . . . . .	21
4.2 Results with various injector heads . . . . .	22
4.2.1 Flame length . . . . .	22
4.2.2 Flame front fluctuation . . . . .	24
4.3 Trade-off injector head . . . . .	25
4.3.1 Trade-off injector head criteria . . . . .	26
4.3.2 Trade-off table & Discussion . . . . .	26

4.4	Results & Observations optimized power consumption . . . . .	27
4.4.1	Results with reduced coil length . . . . .	28
4.5	Conclusion of Results & Observations . . . . .	29
<b>5</b>	<b>Proof of concept</b>	<b>31</b>
5.1	Iteration 1: Understanding the behaviour of peroxide in combination with a heating coil . . . . .	33
5.1.1	Set-up for first iteration . . . . .	33
5.1.2	Results and observations first iteration . . . . .	34
5.2	Iteration 2: Testing with additional protection around . . . . .	34
5.2.1	Set-up second iteration. . . . .	34
5.2.2	Results and observations second iteration . . . . .	35
5.3	Iteration 3: Increasing power and improving isolation . . . . .	36
5.3.1	Results and observations third iteration . . . . .	37
5.3.2	Conclusion third iteration. . . . .	38
5.4	Iteration 4: Shorter heating coil and smaller tube . . . . .	39
5.4.1	Set-up fourth iteration . . . . .	39
5.4.2	Results and observations fourth iteration . . . . .	40
5.5	Iteration 5: Adding multiple layers . . . . .	41
5.5.1	Results and observations fifth iteration . . . . .	41
5.6	Iteration 6: Decreasing the volume of the droplets . . . . .	42
5.6.1	Set-up sixth iteration . . . . .	43
5.6.2	First tests with water . . . . .	44
5.6.3	Updated safety chamber design . . . . .	44
5.6.4	Results and observations sixth iteration. . . . .	45
5.6.5	Conclusion sixth iteration. . . . .	47
5.7	Iteration 7: Horizontal set-up with fan . . . . .	47
5.7.1	Results and observations seventh iteration . . . . .	48
5.8	Iteration 8: Impinging method . . . . .	48
5.8.1	Set-up eight iteration . . . . .	49
5.8.2	Results and observations eighth iteration . . . . .	49
5.8.3	Conclusion eighth iteration. . . . .	50
5.9	Iteration 9: Hydrogen peroxide and Ethanol combination . . . . .	50
5.9.1	Set-up ninth iteration . . . . .	51
5.9.2	Results and Observations fuel and oxidizer mixture . . . . .	51
5.9.3	Double injector set-up . . . . .	52
5.9.4	Reduced power. . . . .	53
5.9.5	Conclusion ninth iteration . . . . .	54
<b>6</b>	<b>Simulation of thermal igniter for rocket applications</b>	<b>55</b>
6.1	Simplifications & Assumptions . . . . .	55
6.2	Geometry & Mesh . . . . .	56
6.3	COMSOL interfaces & Settings . . . . .	57
6.3.1	Initial- & Boundary conditions . . . . .	57
6.3.2	Materials . . . . .	58
6.4	Simulation results. . . . .	59
6.4.1	Comparison of the three simulations . . . . .	60
6.5	Validation & Sensitivity analyses. . . . .	61
6.5.1	Mesh sensitivity. . . . .	61
6.5.2	Distance heating coil . . . . .	62
6.5.3	Influence of the injected fluid. . . . .	63
6.6	Simulation conclusion . . . . .	64
<b>7</b>	<b>Conclusion</b>	<b>66</b>
7.1	Future work recommendation . . . . .	67

---

<b>Bibliography</b>	<b>69</b>
<b>References</b>	<b>70</b>
<b>A Commercial Available rocket engines for small satellites/cubesats</b>	<b>71</b>
<b>B Hydrogen peroxide Safety Data Sheet</b>	<b>75</b>
<b>C Ethanol Label</b>	<b>86</b>
<b>D Nichrome Data Sheet</b>	<b>87</b>
<b>E Photron FASTCAM NOVA S6 Data Sheet</b>	<b>89</b>
<b>F Comsol Simulation Settings</b>	<b>96</b>
<b>G Thermometer Data Sheet</b>	<b>104</b>

# Nomenclature

## Abbreviations

Abbreviation	Definition
ABS	Acrylonitrile butadiene styrene
ADN	Ammonium dinitramide
AWG	American Wire Gauge
ECHA	European Chemicals Agency
HAN	Hydroxylammonium nitrate
HS	High speed
HTP	High-test (hydrogen) peroxide
LED	Light-emitting diode
MMH	Monomethylhydrazine
NTO	Dinitrogen tetroxide
PLA	Polylactic acid
PFV	Photron FASTCAM Viewer
PZT	Piezoelectric actuator
RCS	Reaction control system
REACH	Registration, Evaluation, Authorisation and Restriction of Chemicals
RFNA	Red fuming nitric acid
RPM	Revolutions per minute
TEA	Triethylaluminium
UDMH	Unsymmetrical dimethylhydrazine
WFNA	White fuming nitric acid

## Symbols

Symbol	Definition	Unit
$D$	Diameter	[mm]
$D_a$	Mesh diameter	[mm]
$D_{in}$	Inner diameter	[mm]
$D_{out}$	Outer diameter	[mm]
$E_a$	Activation energy	[kJ/mol]
$I$	Current	[A]
$I_{sp}$	Specific Impulse	[s]
$k$	Reaction rate constant	[-]
$P$	(Electrical) Power	[W]
$R$	Universal gas constant	[8.314 $JK^{-1}mol^{-1}$ ]
$T$	Temperature	[°C] [K]
$t$	Time	[s] [ms]
$V$	Voltage	[V]
$\rho$	Density	[g/cm <sup>3</sup> ]
$\rho I_{sp}$	Density Specific Impulse	[s · g/cm <sup>3</sup> ]
$\Phi$	Angle	[°]

# List of Figures

2.1	Schematic view of spark plug [1]	5
2.2	Schematic view of torch igniter [2]	6
2.3	Schematic view of catalytic igniter [3]	7
2.4	Schematic view of thermal igniter [4]. 1: Connector, 2: Injector, 3: (ceramic) Insulator, 4: Heating wire, 5: Nozzle, 6: Holding plates.	8
3.1	Schematic of final set-up design for the ignition tests	15
3.2	Final set-up design for the ignition experiments	16
3.3	All five injector heads side-by-side. From left to right: 0°, 10°, 20°, 30° and 40°	17
4.1	Explosion, when ethanol is injected slightly later than hydrogen peroxide in the combustion chamber.	22
4.2	Exported frames from video recording to illustrate the flame length with the 0° and 10° injector heads.	23
4.3	Frames from video recording to illustrate the flame length with the 20°, 30° and 40° injector heads.	23
4.4	Exported frame from high-speed camera of the flame front with each injector head angle.	25
4.5	Self-sustained combustion with reduced heating coil length	29
5.1	'U' shaped heating coil inside a glass tube, with the power supply connected to it.	33
5.2	First version of the safety chamber. On three sides, a steel plate is used and at the front side a safety glass is used to have a clear view inside the chamber.	35
5.3	Wound heating coil placed inside the safety chamber. With small thermocouples below the heating coil for temperature measurements.	35
5.4	Second version of the safety chamber with the glass tube and the long heating coil. On top, a plastic lid is placed to reduce the heat dissipation.	37
5.5	Exported frames from high-speed camera footage	38
5.6	Curled heating coil inside the glass tube, to have more space covered with it.	38
5.7	Testing the heating coil with the new glass tube. A part of the glass is broken, since the process of cutting and drilling the glass was still not optimized at this moment of time.	40
5.8	Droplet of hydrogen peroxide falling on heating coil and split into multiple smaller droplets before exiting the glass tube.	40
5.9	Side and top view of the glass bottle with the three layers of heating coil.	41
5.10	Exported still frames from high-speed camera footage. Hydrogen peroxide concentration is 95% and the current used from the power supply is 4.02 A.	42
5.11	Schematic and picture of piezoelectric disc	43
5.12	Set-up with the piezoelectric disc. The syringe and needle are above the piezoelectric disc, outside the frame of this picture.	44
5.13	Third version of the safety chamber. Compared to the previous version, the bottom part has been raised.	45
5.14	Different frames have been taken from a video, which shows how the heating coil is cooling when being in contact with the atomized liquid.	46
5.15	Burned rubber ring and ABS cover	46
5.16	Horizontal set-up with the fan. The fan is inside the converging nozzle at the left side and blowing air to the right through the glass bottle.	48
5.17	Three major design changes of the atomizer of the impinging method and the cross-section.	49
5.18	Spray cone angle with water (and without heat) of the three major versions.	50
5.19	The splitter allows to place two piezoelectric discs on one side, which injects the liquids on the other side where the glass bottle is placed.	51

---

5.20	Combustion of pure ethanol with atmospheric oxygen . . . . .	52
5.21	First successful test with double injector set-up and the shattered glass right after the test.	53
5.22	Successful ignition and combustion with 1 and 2 layers of heating coil. . . . .	53
5.23	Failed experiments with 95 + % concentration hydrogen peroxide. . . . .	54
6.1	Geometry of computational model . . . . .	56
6.2	Extremely coarse and Normal mesh visualized . . . . .	57
6.3	Heat distribution around a small part of the heating coil . . . . .	60
6.4	Highest temperatures around the heating coil . . . . .	61
6.5	Geometry of computational model . . . . .	61
6.6	Temperature comparison with three different mesh element sizes. . . . .	62
6.7	Temperature comparison with a simulation at 30 mm and 15 mm distance from the inlet.	63
6.8	Temperature comparison with three different fluids: Water, Hydrogen peroxide and Ethanol	64

# List of Tables

2.1	Trade-off igniter systems . . . . .	10
2.2	Green monopropellants comparison [5] . . . . .	11
2.3	Comparison of hydrogen peroxide with several types of fuel and NTO in combination with hydrazine as a baseline [6] . . . . .	11
4.1	Overview of successful ignition followed by combustion of different injector head angles with changing current. . . . .	22
4.2	Trade-off table injector head selection . . . . .	27
4.3	Test results and power consumption of optimized heating coil . . . . .	29
5.1	Summary of all the iterations for the experimental test set-up . . . . .	32
5.2	Dimensions of the three glass bottles. . . . .	39

# Introduction

There are various ignition systems currently that are used in rocket engines. The selection of the ignition system is based, among other reasons, on the phase of the chemicals, the propellant and the objective of the mission. For satellite propulsion, hypergolic propellants are often selected. This propellant type would ignite when the fuel and the oxidizer get in touch with each other without the need of additional energy. A well-known hypergolic propellant, that is also often used for satellite propulsion, is hydrazine ( $N_2H_4$ ) in combination with dinitrogen tetroxide ( $N_2O_4$ ), which is also known as NTO. Or the derivatives of this propellant which are monomethylhydrazine (MMH), unsymmetrical dimethylhydrazine (UDMH), red fuming nitric acid (RFNA), white fuming nitric acid (WFNA). The main concern with (most) hypergolic propellants, including the above mentioned chemicals, is that they are highly toxic, carcinogenic and hazardous for the environment [7].

The REACH regulation, which was established by the European Chemicals Agency (ECHA), aims to improve the protection of human health and the environment through the better and earlier identification of the intrinsic properties of chemical substances. This regulation also encourages the development of alternative chemicals as replacement for the most dangerous chemicals, which can be found in the list of "substances of very high concern" [8], which is published and maintained by ECHA in accordance with the REACH regulations. Hydrazine is one of the chemicals that is on this high concern list, for the hazards that have been mentioned above. For this reason, alternative green propellants are being studied that can replace hydrazine over time. Within the space industry, alternative propellants that are less harmful to humans and less dangerous to the environment are called green propellants.

Most green propellants that are currently studied are not hypergolic and would require a separate ignition mechanism to ignite the propellants and to generate thrust. For this reason, various ignition systems are studied and in development to work with those alternative green propellants. This leads to the research objective and research questions of this study, which are presented in Section 1.1. In this section, a brief explanation will be provided on how the research question and sub-questions will be answered during this study. For the feasibility study, some requirements are made which can be read in Section 1.2. Lastly, the structure of this report will be described in Section 1.3.

## 1.1. Research Objectives and Questions

During this study, an experimental and numerical research will be performed to develop a novel ignition system that can ignite storable liquid green bipropellant. This research aims to lay the fundamentals of alternative ignition systems for rocket engines to simplify the transition from harmful propellants to greener alternatives. The objective of this thesis research can be expressed as follows:

*This research aims to investigate the feasibility of a novel and simple reusable ignition system that is suitable for storable green liquid bi-propellant rocket engines.*



Based on this research objective, the following research- and sub-questions are set-up to be answered within this report:

*How to develop a simple, reliable and cost effective ignition system that is reusable and also compatible with storable green bi-propellant?*

1. Which ignition system, which fulfills the requirements of the main question (above), should be developed?
2. How to develop such an (conceptual) ignition system, which can be tested in a laboratory environment?
3. How to test the ignition system for self-sustained combustion and re-ignitability?
4. What is the performance of the ignition system, in terms of power consumption?
5. How to model, in COMSOL, the ignition of the propellant?
6. How does the simulation compare to the experimental results?

At the beginning of this study, a literature study will be performed to have a list of ignition systems that are used to ignite rocket propellants. With the aid of a trade-off, the most suitable ignition system for this thesis research will be selected. A set-up will be developed in the laboratory to be able to experiment with the selected ignition system. The final test set-up will be used to gather data on the minimum required electrical power, re-ignitability and self-sustained combustion. A computer model of the experimental test set-up, in COMSOL, will be made to validate the model and to compare the simulated model to the experimental set-up.

As it already made clear by the research- and sub-questions, mentioned above, the purpose of this study is to investigate in an ignition system for a green storable liquid bi-propellant within a time frame of roughly 30 weeks. Within this time period, the selection of the ignition system and propellant will be made and an experimental set-up followed by a computer model will be made to demonstrate the feasibility of the ignition system.

## 1.2. System requirements

To be able to determine the criteria for the trade-off of the ignition system and the selection of the propellant, it is of importance to determine the requirements that are applicable for the (experimental) set-up. The requirements, in the list below, are based on the research- and sub-questions listed above and are applicable for the feasibility study that will be performed during this research and is not directly comparable with igniter systems and (small) rocket engines that are available on the market.

- REQ-01 The igniter system shall be able to re-ignite the propellants for at least 5 times, without requiring maintenance in between.
- REQ-02 The power consumption of the igniter system shall not exceed 30 W. Preferably even lower than 30 W.
- REQ-03 The pre-heating of the propellant shall be less than 1 minute. Preferably even lower.
- REQ-04 The propellant shall be a liquid storable propellant.
- REQ-05 The propellant (fuel and oxidizer) shall be approved green by the European chemicals agency (ECHA).
- REQ-06 The cost of hardware for the feasibility study/experiment shall be less than 500 EUR.

For this feasibility study, an experimental ignition system was developed for small thruster applications, which are usually used for small satellites. The propellants in a satellite will be used during its whole lifespan. Cooling those propellants to cryogenic temperatures will require additional hardware and increase the power consumption of the satellite. For this reason, it is preferred to have storable propellants. This type of propellants are in a liquid phase at room temperature and atmospheric pressure. During the lifespan of the mission, the rocket engine is used multiple times for orbit changes, orbit

corrections, etc. depending on the purpose of the satellite mission and the purpose of the rocket engine itself. To start the engine the igniter system should be able to restart the rocket engine. During the lifespan of a satellite, the rocket engine will be re-ignited more than 1000 times. However, since this is an early feasibility study, the requirement for the re-ignitability will be limited to only five times to be able to demonstrate that the igniter is able to ignite the propellant multiple times. The power consumption of the ignition system is also an important factor, especially for small satellites. Although, the experiments that will be performed during this study are not completely representable since there will not be a pressurized system, no vacuum and no micro-gravity this feasibility study will provide an indication of what the possibilities are in terms of power consumption. For this reason, the power consumption requirement (REQ-02) is set to 30 W which is the upper limit of the average power consumption of small rocket engines that are used for small satellites and CubeSats. The complete list of rocket engines, including their power consumption can be found in Appendix A.

To have an alternative to harmful propellants, like hydrazine, the European Union made a list of green propellants for rocket propulsion applications [9]. For this study, the propellant that will be selected to perform the experiments with, has to be one of the green propellants that have been approved by the European Union. This will increase the interest in this study and this propellant in the future, especially since hydrazine and its alternatives are slowly being phased out.

### **1.3. Structure**

A literature review will be conducted at the start of this study to compile a list of the ignition methods used to ignite rocket propellants. The most appropriate ignition system for this thesis research will be selected via a trade-off. The literature review and the trade-off are addressed in Chapter 2. The final test setup for the experiments is explained in Chapter 3. This set-up will be used to perform all experiments and to gather data about the minimum required electrical power, re-ignitability and self-sustained combustion. The results of those data are discussed in Chapter 4. Before the final test set-up multiple iterations and tests have been performed. The details of all the iterations can be found in Chapter 3. In the laboratory to be able to experiment with the selected ignition system, the explanation of the final test set-up for the experiments is discussed in Chapter 5. A computer model of the experimental test set-up, in COMSOL, is made to validate the model and to compare the simulated model to the experimental results. More details and the discussion of the simulation can be found in Chapter 6. Finally, Chapter 7 contains the conclusion and recommendation of the thesis research.

# 2

## Literature Study

A literature review was conducted on ignition systems and green propellants. This literature study will serve as a basis for the selection of the ignition system and the green propellants that will be used for the experimental set-up. In this chapter, besides the summary of the findings about several types of ignition systems also the trade-offs for the ignition system and the selection of the propellants will be discussed.

### 2.1. Igniter systems

The igniter is a small part of a (rocket) engine system. As its name suggests, its purpose is to initiate the combustion in the (main) combustion chamber which eventually results in power/thrust. Which ignition system a rocket engine needs depends on multiple factors and requirements of the manufacturer and customer like the propellant, reusability, mass and volume among others. In this section, a brief description of various ignition systems that are of interest for this study will be provided. In the end, a comparison with all the ignition systems will be performed by means of a trade-off table. Since the purpose of this research is to develop an ignition system that can be used for satellite propulsion applications, like for example a reaction control thruster (RCS). Only ignition systems will be discussed that have the potential to reignite the (main) combustion chamber and are suited for liquid propellants as it is defined in REQ-01 and REQ-04 in Section 1.2.

#### 2.1.1. Spark plugs

The working principle of a spark plug, also known as direct spark plug, for a rocket engine is the same as it is for a (petrol) car engine. Two wires of the spark plug are separated by a small gap. The power source or exciter that is connected to the spark plug applies an electric voltage to it, because of the gap a current jump between the two wires, which is illustrated in Figure 2.1. The spark plug is installed in the combustion chamber in the flow path of the vaporized mixture of the propellants. When the spark plug produces an arc in the vaporized mixture, the mixture will start to ignite. Each spark is about 100 mJ and the spark plug itself can produce about 50 sparks each second. Obviously, the required amount of power and the number of sparks per second depend on the engine and the conditions that apply. To start-up the rocket engine, the spark plug produces a spark for up to 10 seconds. Additional spark plugs are usually installed in the rocket engine for redundancy.

One of the main advantages of a spark plug is that it can be reused without the need of any maintenance in between. This makes this ignition method perfectly suitable for starting up the engine multiple times. However, unlike hypergolic propellants the spark plug is not able to produce infinite number of times a spark, it still is limited to the capabilities of the materials used for the spark plug. On the other hand, since the spark plug is installed in the combustion chamber itself, additional measures are needed to protect the spark plug from the high pressures and heat. Another disadvantage of a spark plug is that the generated spark is very local and as a result for bigger engines a single spark plug will not be sufficient to ignite the whole engine, multiple spark plugs need to be distributed over the

combustion chamber to be able to ignite the engine properly [1] [10].

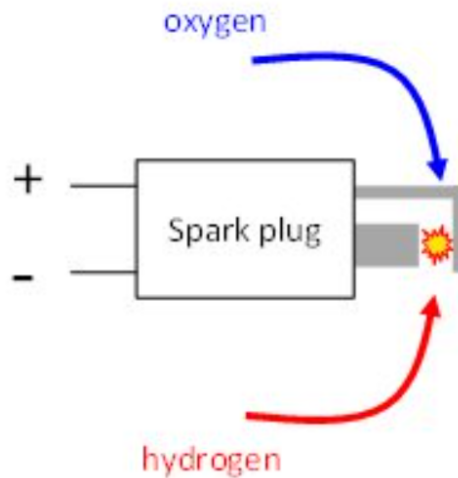


Figure 2.1: Schematic view of spark plug [1]

### 2.1.2. Torch igniter

A torch igniter, also known as augmented spark igniter, is very similar to a spark plug. The difference is that the torch igniter has its own small combustion chamber where the propellant can be ignited in a controlled environment, with the aid of a spark plug, before the hot gas/fire is expelled to the main combustion chamber through a tube, see also Figure 2.2. The diameter of the igniter is usually between a quarter inch to one inch in diameter and is installed on the centerline of the injector head with the exit facing downward to the center of the main combustion chamber. The propellant for the torch igniter can be the same as the main propellant which will be tapped from the main feeding lines. Or the propellant for the torch igniter can be stored separately, which makes it possible to use different propellants which are better suited for the torch igniter. Like the direct spark plug, multiple spark plugs in the torch igniter can be used for redundancy purposes [11].

The advantage of a torch igniter is that it is also suited for bigger rocket engines. In fact, the main engine of the space shuttle was also ignited by a torch igniter [12]. Furthermore, since the igniter has its own (small) combustion chamber, the tips of the spark plug are better protected against the high pressures and temperatures that occur in the main combustion chamber [10].

For even bigger engines where bafflers are used or if multiple engines are used under a rocket a variant of a torch igniter can be used, which is called a combustion wave igniter [13]. Instead of using multiple torch igniters for each compartment of the engine or for each engine, a single ignition system is used which directs the flame front to all compartments/engines. This will greatly reduce the required amount of hardware required for the ignition system of the rocket. Also, the required amount of mass and volume will reduce accordingly. This method will increase the distance a flame front needs to travel from the combustion chamber of the torch igniter to the main combustion chamber of the rocket, but from the research it can be concluded that the length is not influencing the result in any significant way, while still having all the advantages of a "normal" torch igniter.

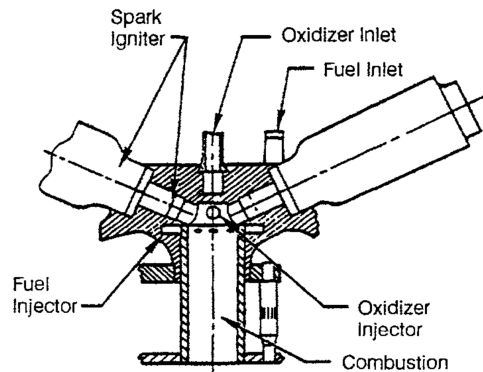


Figure 2.2: Schematic view of torch igniter [2]

### 2.1.3. Hypergolic igniter

The definition of hypergolic is that when two substances get in touch it spontaneously ignites. In case of rocket propulsion, when hypergolic fuel and oxidizer are used and they get in touch the mixture spontaneously starts combusting. This property can be used as an ignition system to ignite the main propellant of the rocket engine. But that will require additional tanks and feeding lines specifically for the propellant of the ignition system. This will first of all increase the weight of the rocket and secondly, it will require additional volume inside the tank. Instead, the main propellant of the rocket can be replaced with a propellant combination that is hypergolic. This will be a lighter option and at the same time, require less tanks which will reduce the required amount of volume.

In the event that a hypergolic propellant cannot be used as the main propellant, hypergolic cartridges installed at the fuel lines can be used as an alternative to ignite the rocket engine. When the rocket engine needs to be (re)started, the cartridge breaks open and gets injected into the combustion chamber while at the same time the (main) oxidizer gets injected. This combination will then spontaneously ignite. Right after the cartridge breaks open, the valve of the main fuel will be opened, so that the main fuel can take over and have a stable self-sustaining combustion with the oxidizer. This method will bypass the complex second feed system that was necessary if both hypergolic fuel and oxidizer are different than the main propellant, but the number of re-ignitions is limited to the number of available cartridges with hypergolic fuel.

Hydrazine based hypergolic fuels, like mono-methylhydrazine (MMH) and unsymmetrical dimethylhydrazine (UDMH), are often used. Hypergolic oxidizers then can be used with those fuels are nitrogen tetroxide (NTO) and nitric acid. Triethylaluminium (TEA) is another hypergolic fuel, which at the same time is also an organometallic compound. This hypergol can react with (liquid) oxygen, which makes the hypergolic fuel very attractive to use it in a cartridge since liquid oxygen is an often used oxidizer for the main propellant [14] [15].

Although hypergolic ignition, is very reliable and it can have a low ignition delay time it also has some major disadvantages. Some hypergol reactions produce solid particles which can clog some of the (feeding) lines, this makes it also not possible to use it as the ignition system of a gas generator. Furthermore, (almost) all hypergolic fluids are very toxic and could potentially ignite with air. This makes it difficult to produce, handle, store and to load it on the engine. Special safety requirements and procedures are required for all the phases the hypergol goes through. Aside from the safety issues that arise, also the cost and time will increase significantly [10].

### 2.1.4. Catalytic igniter

A catalyst lowers the activation energy of the propellant that needs to be decomposed. An often used monopropellant is hydrogen peroxide ( $H_2O_2$ ). The catalyst is able to decompose this liquid to hydrogen ( $H_2$ ) and oxygen ( $O_2$ ) at ambient temperatures, while without a catalyst it would require a temperature of about  $500\text{ K}$  to decompose hydrogen peroxide. This decomposition process is an exothermic reac-

tion, as a result the decomposed hydrogen peroxide can reach temperatures of more than  $700\text{ K}$  and even  $1000\text{ K}$  with higher concentrations of hydrogen peroxide [16]. In a rocket engine, the hydrogen peroxide would be the oxidizer and since the fuel will not be compatible with the same catalyst as for hydrogen peroxide, the fuel is injected into the engine after the catalyst when hydrogen peroxide is already decomposed. The injected fuel and the available free oxygen molecules combust directly without the need for any additional heating.

A wide variety of materials can be used as catalysts. Even liquids can be used as a catalyst, although it needs to be mixed with the propellant with the right amount and time, which makes it overcomplicated and not preferred for rocket propulsion. Instead, solid catalysts are used, either metals like silver, platinum and manganese oxide or ceramics. But this depends on the propellant that needs to be decomposed, the required heat for the catalytic bed, the decomposition temperature and the pressures. The catalytic activity of the material for hydrogen peroxide depends on the material of the catalyst itself. Furthermore, other parameters that affect the performance of the catalyst are the dimensions of the catalyst, the surface area and whether the catalyst oxides to something which has a lower catalytic activity.

Points to consider during the selection of the catalyst material, besides the performance are its temperature resistance and capability to cope with thermal shock. Silver has a relatively low melting point, which makes it not very applicable for very high concentrations of hydrogen peroxide. Also, the thermal shock the catalyst goes through can break it, which is especially applicable for ceramic catalysts [3] [17].

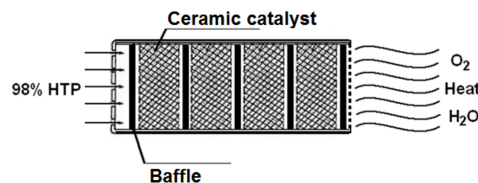
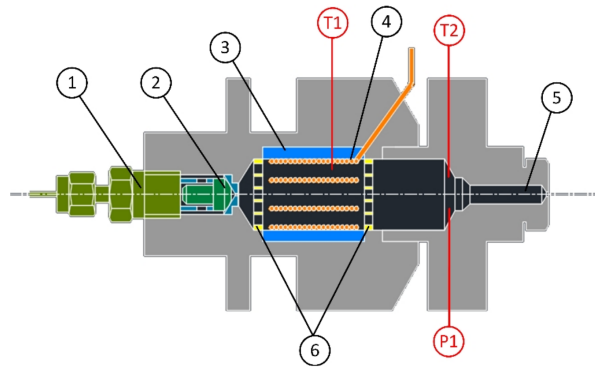


Figure 2.3: Schematic view of catalytic igniter [3]

### 2.1.5. Thermal igniter

A thermal ignition method is an ignition method that decomposes the propellant by heating up the propellant. Instead of making use of a catalytic bed to decompose the propellant, which usually also needs to be heated up, the propellant will be directly heated up. The heating of the propellant is done by making use of a heating wire, which basically is a metal wire with a high electrical resistance, see Figure 2.4 for a schematic view. Initial research with this ignition method has been conducted successfully [18], but further research will be required to get a better understanding of this ignition method and how to improve/optimize it in such a way before it can be used in a real mission.

This method can be both used in monopropellant configuration as well as in bipropellant configuration. In case of the later configuration, after one of the propellant is heated up and decomposed, the other propellants will be injected which will cause a chemical reaction with the decomposed propellant. This principle is very similar to an ignition method with a catalytic bed, since this can be also used for both configurations.



**Figure 2.4:** Schematic view of thermal igniter [4]. 1: Connector, 2: Injector, 3: (ceramic) Insulator, 4: Heating wire, 5: Nozzle, 6: Holding plates.

The advantage of this ignition method is that first of all, no expensive materials are required, which is the case for the catalyst. Secondly, it is a lightweight solution which does not require that much space. Since this type of ignition method is not researched that much, very little is known about it and the behaviour of thermal decomposition. Furthermore, since the propellant is directly heated up with a heating wire, the electrical power consumption will increase significantly in case of higher mass flows and bigger rocket engines, which probably makes this engine not very well suited for bigger rocket engines, but could be a good ignition method for smaller rocket engines used for spacecrafts and low thrust applications.

## 2.2. Trade-off ignition systems

In this section, based on those requirements mentioned in Section 1.2, the trade-off for the ignition system and the propellant selection will be performed. For the ignition system, the hypergolic ignition system will be also competing in the trade-off together with other ignition systems. Even though there are no green liquid bipropellants that are hypergolic, hydrazine as propellant is currently often used which is hypergolic. The scoring of the hypergolic ignition system will serve as a basis and will provide a good comparison with the alternative ignition systems.

### 2.2.1. Trade-off criterion

The grading for each criterion, will be between 0 and 6. Since most criteria can not be expressed in hard numbers and not all information is directly provided by the manufacturer, it will not be possible to have a clear grading scheme and as a result it will be a more qualitative grading than a quantitative grading. In the worst case, the grade will be 0, which is the lowest possible grade. The better the ignition system is, the higher it will be graded. This grade will then be multiplied with the weighting factor of that criterion, to get the score for that criterion. This weighting factor is a number between 1 and 5 and allows to make a distinction between the importance of each criterion. The summation of all scores, provides the total score for each ignition system. This total score makes it possible to compare and see how much the difference is between each ignition system. In the list below, a brief explanation will be provided why this criterion has been selected for the trade-off and what the weighting factor of this criterion will be.

- **Mass/ Volume**

The mass and volume of a rocket engine are always an important factor. This is also applicable to the ignition system of the rocket engine. To keep the trade-off table simple and since the mass and volume of an ignition system are not provided explicitly, the mass and volume will be considered as a single criterion with a weighting factor of 5.

- **Handling**

The second criterion is the handling of the ignition system. As mentioned earlier in this chapter, the ignition systems could potentially also have some hazards during the handling of it. This could

be related to the propellant used for the ignition system, however it could be also related to the ignition system itself. Since safety concerns, makes handling more difficult and increases the cost, the handling will have a weighting factor of 3.

- **Reusability**

Being able to restart the rocket engine, is getting more important to all rocket sizes that range from rocket engines for small spacecrafts to launch vehicles. Especially since more spacecrafts are getting launched into space and the need for more (affordable) spacecrafts is increasing. Since there is already a requirement for the re-ignitability of the igniter system. Only igniter systems that can be reused are considered for this trade-off. However, since there are still differences in reusability of an igniter system it will be considered as a criterion with a weighting factor of 2.

- **Price**

The fourth criterion will be the price of the ignition system. This criterion will compare the prices of the hardware and materials that are required and the transportation costs for that hardware. Although, the igniter system is only a small part of the complete rocket engine and even a smaller part of a (small) satellite. Since companies and organizations that develop those small satellites have a limited budget this criterion has also been selected for the trade-off with a weighting factor of 1.

### 2.2.2. Trade-off table & Discussion

In (open) literature there is almost no information and hard numbers/specifications for each ignition method. Because of this reason, the trade-off table will not be graded on the basis of quantitative values, but based on qualitative values which are mainly discussed in Section 2.1. Table 2.1 provides the grades of each ignition method for each criterion. This grade is multiplied by the weighting factor of the criterion. This results in the score of the ignition system for that criterion. The score can be found in the second column of each criterion. In the last column, the total score of each ignition method can be found. The grading for each criterion will be discussed in the following paragraphs.

For the mass/volume criterion, the catalytic igniter has the lowest grade of 0. This is due to the fact that the catalyst in a rocket engine occupies a significant amount of area and because it is usually made out of metals it is also heavy. On the other hand, the hypergolic igniter has 6 points, because it does not need any additional hardware. The spark plug and torch igniter do require small hardware, however since the torch igniter has its own combustion chamber it received a slightly lower grade compared to the spark plug. The thermal igniter has the 5 points, since the hardware requirements for it are less than a spark plug.

For the handling criterion, where safety is an important parameter, the hypergolic igniter received the lowest points. The reason for it being the hazards of hypergolic chemicals and the additional safety precautions that are required as explained in Section 2.1. The catalytic igniter scored the highest points, since it is completely passive. The other three igniter systems, spark plug, torch igniter and thermal igniter all received 5 points. Although, all three are safe and easy to handle they do require electricity which resulted in a slightly lower grade compared to a passive system.

It is important for a rocket engine, which is developed for satellite propulsion, to be able to re-ignite during its life-time. For this, the ignition system needs to be reusable. The hypergolic ignition system receives the maximum points, since it will always ignite as long as there is propellant left in the tanks. The catalytic igniter degrades over time which resulted in having the lowest grade for this criterion. The spark plug, torch igniter and thermal igniter are all able to re-ignite the combustion chamber, but they are limited by the number of times they are designed to do so. This resulted in 3 points for all those ignition systems for this criterion.

Hypergolic ignition does not require any additional hardware, but is restricted by the propellants that can be used. The handling, transport and the chemicals itself do add to the price. On the other hand, a spark plug, torch igniter and thermal igniter all need some hardware, but are not that costly. This



resulted in 6 points for all three igniters. The hypergolic igniter gets 3 points and the catalytic igniter has the lowest grade of 0 points, since it requires expensive materials as the catalytic bed.

**Table 2.1:** Trade-off igniter systems

Ignition Method	Mass/Volume		Handling		Reusability		Cost		TOTAL
	5		3		2		1		
Hypergolic igniter	6	30	0	0	6	12	3	3	45
Spark plug	4	20	5	15	3	6	6	6	47
Torch igniter	3	15	5	15	3	6	6	6	42
Catalytic igniter	0	0	6	18	0	0	0	0	18
Thermal igniter	5	25	5	15	3	6	6	6	52

From the trade-off table, it is clear that the thermal igniter system has the highest total score of 52. The hypergolic igniter, which is currently mostly used, has a total score of 45 points. This is due to the low score of the hypergolic igniter received for the handling criterion. The spark plug and torch igniter have a total score of 47 and 42 respectively. Both had a lower score for the mass/volume criterion. The catalytic igniter has the lowest total score, with 18. For each criterion it scored 0, except for the handling criterion.

### 2.3. Green oxidizer selection

Conventional storable oxidizers, which are currently mostly used for satellite propulsion, are mostly NTO and its derivatives like RFNA and WFNA. As explained in Section 2.1, those oxidizers in combination with hydrazine are hypergolic. This makes a separate ignition system unnecessary, which was until now, besides the high performance, a reason to work with this propellant combination. However, the downside of this propellant is the handling of this chemical, hazards to the environment and health concerns to humans due to its toxicity, flammability and carcinogenic effects [4] [7]. On top of mentioned hazards of hydrazine, this chemical will be banned at some point in time by the European Union, as discussed in Chapter 1. Additionally, as mentioned by REQ-05 in Section 1.2 the propellant has to be a green propellant according to the European Union. A list of those green propellants can be found in [9].

Space companies and researchers are searching for alternative green propellants that can replace hydrazine, while having about the same performance characteristics compared to its predecessor. While all space propellants can be dangerous, green propellants are usually classified as propellants that are significantly less toxic and less hazardous to work with compared to conventional propellants. As an additional benefit this makes storage and handling easier and fewer special safety precautions will be required. This results in a lower overall cost.

Green propellants that are currently introduced and researched are most of the time based on hydroxylammonium nitrate (HAN), Ammonium dinitramide (ADN) and Nitrous Oxide ( $N_2O$ ). Those chemicals are mixed with an aqueous solution and fuel like methanol is added to increase the specific impulse of the propellant while still having the benefits of a monopropellant, like a single tank. Hydrogen peroxide ( $H_2O_2$ ) is also an alternative green propellant. Unlike the previous mentioned propellants, hydrogen peroxide is not a mixture of chemicals. This results in a lower specific impulse compared to the other green monopropellants. Even compared to hydrazine, hydrogen peroxide is under performing in terms of specific impulse. When comparing the density specific impulse, all green propellants gain more compared to hydrazine since the density of the green propellants are higher. AF-M315E is a HAN based propellant that has 50% higher density specific impulse compared to hydrazine [19]. While hydrogen peroxide has a lower specific impulse compared to hydrazine, the density specific impulse is slightly higher than hydrazine. In Table 2.2, a comparison of the (density) specific impulse ( $I_{sp}$ ) is made with green monopropellants and hydrazine.

**Table 2.2:** Green monopropellants comparison [5]

Propellant	Density [ $g/cm^3$ ]	Theoretical $I_{sp}$ [s]	$\rho I_{sp}$ [ $s \cdot g/cm^3$ ]
AF-M315E	1.47	357	377
LP1846 (HAN)	1.4	262	376
SHP163 (HAN)	1.442	254	366
HNF-based	1.4	260	354
LMP-103S (ADN)	1.24	253	313
HAN/HN-based	1.4	210	294
Hydrogen peroxide (98%)	1.431	182	260
LTHG	1.3	191	254
Hydrazine	1.01	239	241

In a liquid bi-propellant configuration, currently hydrazine is mostly combined with dinitrogen tetroxide as storable oxidizer, commonly referred to as nitrogen tetroxide (NTO), and its derivatives. Green alternatives for oxidizers are limited. HAN and ADN based propellants, discussed in the paragraph above, can not be effectively used in a bi-propellant configuration, since it is a mixture of chemicals including the fuel. One often used green oxidizer is liquid oxygen, however this oxidizer is cryogenic and as a result not suitable for this study. This leaves hydrogen peroxide and nitrous oxide as green oxidizers. Although nitrous oxide can be in a liquid phase at room temperatures, it will require pressures greater than 50 bar for it [20]. At atmospheric conditions, the boiling temperature of nitrous oxide is  $-88\text{ }^\circ\text{C}$  [21]. Since the experimental set-up will not be done in a pressurized system, it will leave hydrogen peroxide as the only green oxidizer that is suited for this research. For the properties and the safety data sheet of hydrogen peroxide, please see Appendix B.

At high concentrations (80 + %), hydrogen peroxide can be also considered as a high performance oxidizer. Since the beginning of liquid rockets, hydrogen peroxide has been experimented with as a possible oxidizer for rocket propulsion. However, after the discovery of hypergolic propellants, like hydrazine interest in hydrogen peroxide dropped. Recently, again interest has been shown for hydrogen peroxide as a propellant due to its low toxicity, low irritation, low corrosivity and low volatility.

## 2.4. Green fuel selection

There are various storable green fuels that can be used in combination with hydrogen peroxide. Most commonly used are alcohol based fuels, like ethanol and methanol. As it was the case with the monopropellants, the green propellants usually do not have the specific impulse of hydrazine in combination with NTO. However, the density specific impulse of the green propellants is very close to the density specific impulse of hydrazine and NTO. Hydrogen peroxide in combination with butanol has a slightly better density specific impulse compared to hydrazine and NTO combination, with  $379\text{ }g \cdot s/cm^3$  and  $372\text{ }g \cdot s/cm^3$  respectively. The complete list with the (density) specific impulse and combustion temperature can be seen in Table 2.3.

**Table 2.3:** Comparison of hydrogen peroxide with several types of fuel and NTO in combination with hydrazine as a baseline [6]

Oxidizer	Fuel	$r_{opt}$ [-]	$I_{sp\ vac}$ [s]	$\rho I_{sp}$ [ $g \cdot s/cm^3$ ]	Tc [K]
NTO	MMH	2.1	313.6	372.2	3314
98% H2O2	Ethanol	3.79	288.9	367.7	2761
98% H2O2	Methanol	2.81	284.3	353.9	2682
98% H2O2	1-Propanol	4.29	291.2	374.9	2798
98% H2O2	2-Propanol	4.3	290.6	372.8	2790
98% H2O2	1-Butanol	4.6	292.4	378.6	2817
98% H2O2	2-Butanol	4.61	291.9	377.9	2811
98% H2O2	t-Butanol	4.62	291.4	375.8	2804

Within the chemical laboratory of the Aerospace faculty, as green fuels ethanol and methanol are readily available for use. Which made Ethanol being selected as the fuel for hydrogen peroxide, since it has slightly better performance in terms of (density) specific impulse compared to hydrogen peroxide with methanol. The label of the ethanol that will be used during the experiments can be found in Appendix C.

## 2.5. Heating coil selection

For a thermal ignition system, a heating element is required. A heating element is made out of a material that has a high resistance, which results in heat when current is flowing through this material. There are various materials that can act as a heating element for this study. However during the selection of the heating element, it should be considered whether the material of the heating element is compatible with hydrogen peroxide, the high temperatures it will be exposed to and corrosive resistance. In general there are two categories of heating elements, the metal based and the ceramic/silica based materials. The later are more exotic and harder to acquire. Metal based heating elements are generally broadly available and used in consumer products.

Two well known metal based heating elements are nichrome and kanthal. The first material is a combination of nickel and chromium usually in a ratio of 80/20. The latter material is a mixture of iron, chromium and aluminium. In terms of compatibility, no data was able to confirm the compatibility of kanthal with hydrogen peroxide. For nichrome wire, a paper was available that confirms the compatibility with hydrogen peroxide [22]. For this reason, it was decided to select nichrome as the material for the heating element. The properties of the nichrome wire can be found in Appendix D.

Although the heating element will have a significant influence on the power consumption and the lifespan of it. Since this study will be a feasibility study of an ignition system, the material of the heating element is fixed during this study.

## 2.6. Combustion of hydrogen peroxide and Ethanol

At atmospheric temperatures and pressures, the reaction between hydrogen peroxide and ethanol will happen at temperatures higher than the auto-ignition temperature of ethanol assuming no catalyst is used. At those high temperatures hydrogen peroxide is also decomposing spontaneously and releases oxygen to react with ethanol. In literature there is a discrepancy about the auto-ignition temperature of ethanol, most sources mention temperatures of  $363\text{ }^{\circ}\text{C}$  or  $365\text{ }^{\circ}\text{C}$  [23] [24]. A paper that has performed a study on the auto-ignition temperature of some chemicals including ethanol mentions an auto-ignition temperature of  $368.8 \pm 7.4\text{ }^{\circ}\text{C}$  [25]. In this section, first the decomposition process of hydrogen peroxide and afterwards the reaction with ethanol will be briefly discussed.

### 2.6.1. Decomposition of Hydrogen peroxide

For both mono-propellant as well as bi-propellant propulsion applications, hydrogen peroxide needs to be decomposed to release its energy and to be able to react with the fuel. This decomposition process leads to the reaction presented in Equation 2.1. This exothermic reaction releases a heat of ( $\Delta H$ ) of  $-2884.5\text{ kJ/kg}$  [26], which results in hot water vapor (steam) and hot oxygen. During this decomposition process of high concentration hydrogen peroxide can lead to temperatures of more than 1000 K, depending on what concentration of hydrogen peroxide is used [16]. From a mass percentage the oxygen, within hydrogen peroxide makes up 47%. This makes it a good oxidizer in case it is used in a bi-propellant configuration [27].



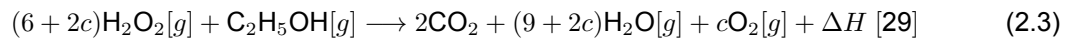
For spontaneous decomposition of hydrogen peroxide, either a catalyst can be used or by adding heat. In case of the first method, the catalyst reduces the required activation energy ( $E_a$ ), which results

in a higher reaction rate ( $k$ ) at the same temperature ( $T$ ). This is defined with the Arrhenius Equation 2.2. Various materials can act as a catalyst for hydrogen peroxide, those include among others silver, platinum and manganese dioxide [16] [17]. While a catalyst ignition system is used with alternative propellants for space applications. It is not always a preferred method, because of its drawbacks discussed in Section 2.1. Alternatively, hydrogen peroxide can be decomposed spontaneously by increasing the temperature of the high concentration hydrogen peroxide to  $200\text{ }^{\circ}\text{C}$  or higher [28]. It has been proven that by only making use of heat that hydrogen peroxide can be decomposed within a short period of time for rocket application by [18].

$$k = A \exp(-E_a/RT) \quad (2.2)$$

### 2.6.2. Chemical reaction of Hydrogen peroxide and Ethanol

In a bi-propellant set-up, after the hydrogen peroxide has decomposed, the oxygen that is released will be reacting with ethanol once it reaches the auto-ignition temperature. The chemical reaction and the reaction products can be found in Equation 2.3. In case of a complete combustion, the only reaction products, besides the heat that is released, are carbon dioxide ( $\text{CO}_2$ ) and water. This chemical reaction shows that also the reaction products of this green bi-propellant are very clean relative to currently existing storable bi-propellants.



## 2.7. Conclusion literature study

In this chapter, a literature study has been performed on reusable igniter systems for liquid bipropellant rocket engines. With the aid of a trade-off table the thermal ignition system was selected as the best suited for the criteria and requirements that have been defined. For the propellant that will be used to be ignited by the thermal igniter system, a list of green propellants has been consulted. This list is made by the European Union, to encourage the development of alternative propellants that are less harmful. Although as monopropellant there are various propellants that can be used. As oxidizer for a bipropellant configuration the selection of green propellants is limited. As the oxidizer high concentration hydrogen peroxide is selected. For the fuel, ethanol is selected, because of its easy availability and a density specific impulse that is similar to the current propellant (hydrazine/NTO). The heating coil that will be used as the igniter system of this set-up is a wire made out of nichrome. This metal is made out of 80% nickel and 20% chromium and is well known as a heating element that is able to withstand high temperatures and is compatible with hydrogen peroxide.

For the thermal ignition of hydrogen peroxide and ethanol, the temperature of the liquid has to be raised above the auto-ignition temperature of ethanol which is about  $365\text{ }^{\circ}\text{C}$ . At this temperature hydrogen peroxide is spontaneously decomposing and releasing oxygen and heat since it is an exothermic reaction. This oxygen molecule reacts with ethanol and a combustion takes place.

# 3

## Test set-up

To perform the experiments, a (safe) set-up has to be made. Before reaching to the final design of the set-up, multiple experiments and iterations of the set-up have been performed. With each iteration small steps have been made and the knowledge gained was used as an input for the next iteration to further improve the design. In this chapter, the final set-up that has been built and the equipment that is used will be discussed. The details of all the (previous) iterations will be provided in Chapter 5.

### 3.1. Set-up

The set-up should be well integrated to have accurate and repeatable results. On the other hand, it should provide some level of modularity that allows to adjust the parameters. The set-up should also provide a safe environment for the personal around the set-up and also for the (expensive) equipment that is around the set-up. Furthermore, since this research is focusing/developing on the thermal ignition system. It is important to be able to observe the (physical) phenomena that is happening within the combustion chamber.

The walls of the combustion chamber are made out of glass. This will provide the before mentioned transparency. At the beginning/inlet of the combustion chamber, a 3D printed injector head is placed that is made out of Polylactic acid (PLA). This injector head has place for two piezoelectric discs, which will inject the atomized liquids inside the combustion chamber. From one of the piezoelectric discs high concentration hydrogen peroxide will be injected, while through the other piezoelectric disc ethanol will be injected. The amount of injected fluid can not be adjusted with the piezoelectric discs. This results that the ratio of oxidizer and fuel flowing through the combustion chamber is fixed. More details about the piezoelectric discs can be found in Section 5.6 and Figure 5.11a. The supply of liquids to the piezoelectric discs are provided by two syringes which are filled with the fuel and oxidizer. In the middle of the combustion chamber, about  $29 \pm 1 \text{ mm}$  from the inlet, two holes are drilled opposite to each other. Through those drilled holes, the heating coil is placed and the ends of it are connected to a power supply. The end of the combustion chamber is open. This will allow all the reaction products and gasses to escape and prevent the system from being pressurized. For safety purposes, around this combustion chamber a safety chamber is made. This safety chamber is the external protection which has metal plates on the sides and at the front a safety glass. More details about the safety chamber are provided in Chapter 5.

To record all the phenomena that is happening during ignition and combustion of the propellant, two cameras are placed in front of the set-up. The first camera is the Photron FASTCAM NOVA S6 high-speed camera with a monochrome sensor that is able to record with 6400 frames per second and its maximum resolution of 1024 by 1024 pixels. The camera is only capable to record for about 3.4 seconds at a time before the internal (short-term) memory is full. The data sheet of the high-speed camera can be found in Appendix E. During the experiments, the high-speed camera should be well timed to be able to record all the phenomena of the ignition and the combustion. To interact with the

high-speed camera and to save the recordings, the high-speed camera is connected to a computer with an Ethernet cable. This high-speed camera can only record in monochrome. No colored high-speed camera was available at the Aircraft hall of the Aerospace Faculty of TU Delft. However, to still be able to capture the ignition and combustion of the propellant in color, a (smart)phone camera is used. This phone camera is capable of recording with 240 frames per second at a resolution of 1920 by 1080 pixels. The schematic and a photo of the set-up can be seen in Figure 3.1 and Figure 3.2 respectively. The whole set-up is placed inside a fume hood at the chemical laboratory.

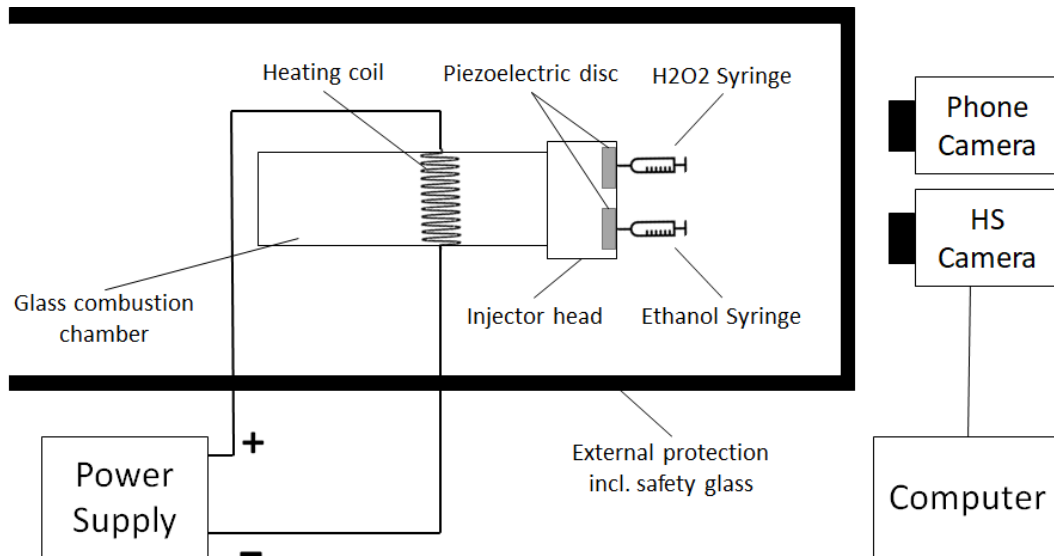
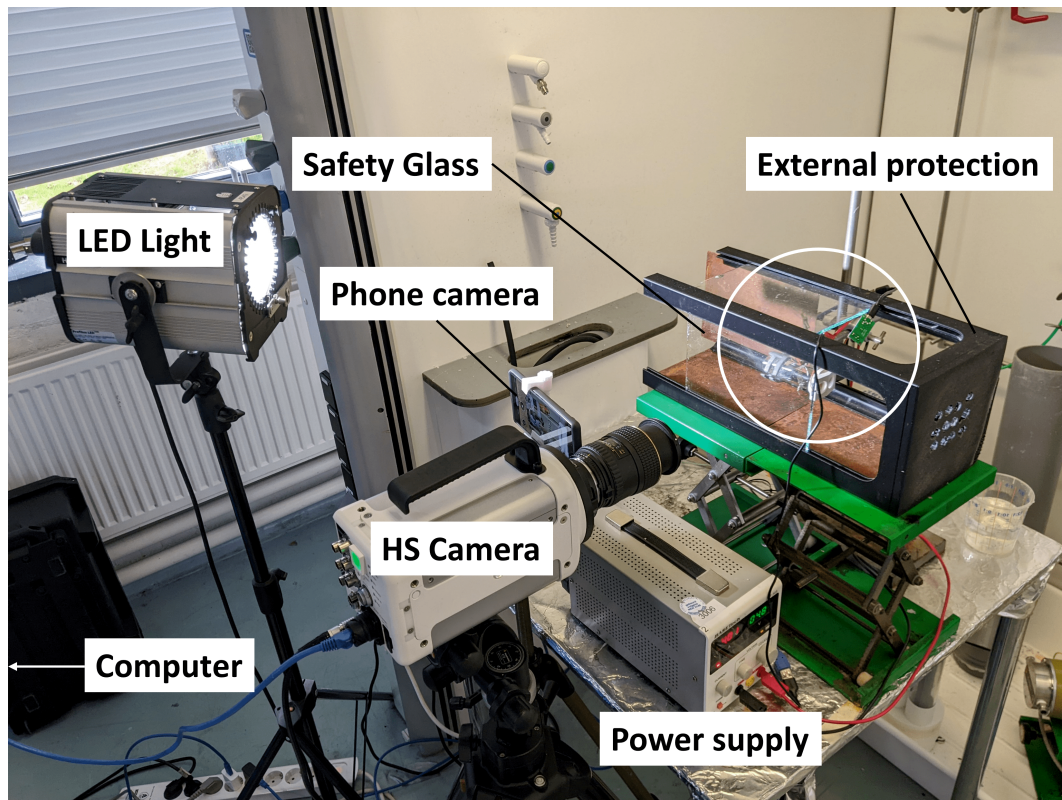
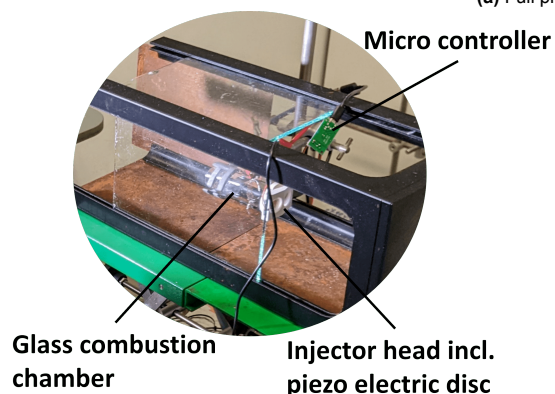


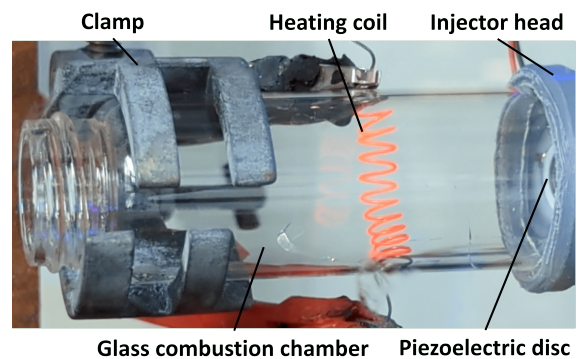
**Figure 3.1:** Schematic of final set-up design for the ignition tests



(a) Full picture of the set-up



(b) Zoom at white circle



(c) Close-up combustion chamber

Figure 3.2: Final set-up design for the ignition experiments

## 3.2. Experiment description

Two experiments will be performed during this study with the experimental set-up. The first experiment will be about the optimal angle of the injectors. The angle that provides the best results will be used for the second experiment, where the focus is on optimizing the power consumption by reducing the length of the heating coil.

The distance between the heating coil and the injector head will be fixed, and no changes will be made to it during the experiment. Placing the heating coil closer to the injectors will increase the probability of the plastic injector head catching fire. This will make it very difficult to have valid results. Secondly, because of the time limit of the thesis it was decided not to change this parameter.

The concentration of hydrogen peroxide that will be used during the experiments is also fixed, to 90%. Since this ignition system is being developed for space applications, the goal is to use the highest

possible concentration. However, increasing the concentration higher than 90% increases the risk of the plastic injector head acting as the fuel for hydrogen peroxide. This results in violent flames and loud explosions, which are discussed in more detail Section 5.9. For this reason, it is decided to use 90% concentration of hydrogen peroxide as a safe concentration.

### 3.2.1. Experiment 1: Injector angle

For this experiment, five different injector heads will be used. The angle of the injectors are varying between  $0^\circ$  to  $40^\circ$ , with step sizes of  $10^\circ$ . All the five injector heads can be seen side by side in Figure 3.3. The mentioned angle is the angle that each injector makes when determined from the middle of the injector head.

The second parameter that will be modified during the experiment is the amount of electrical power that is used to heat up the heating coil. Since the temperature of the coil is determined by the current that is going through it, for the experiments the current will be reduced each time with 0.25 A each time when there is a successful ignition to determine the minimum power that allows for ignition of the propellants.

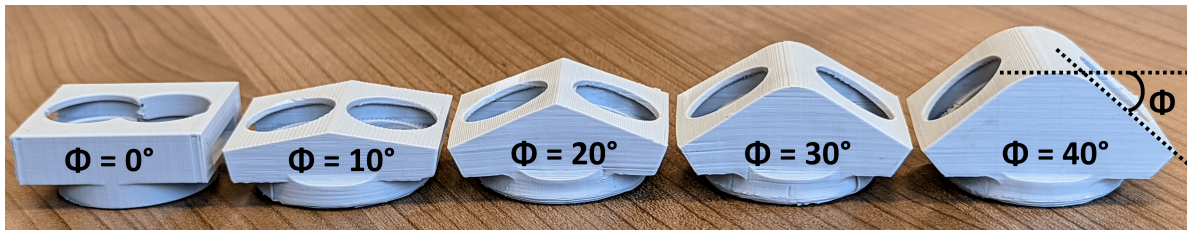


Figure 3.3: All five injector heads side-by-side. From left to right:  $0^\circ$ ,  $10^\circ$ ,  $20^\circ$ ,  $30^\circ$  and  $40^\circ$

### 3.2.2. Experiment 2: Reducing length of heating coil

With the selected injector head angle from the previous experiment, the second experiment will be performed. During this experiment, the minimum power consumption for which ignition followed by combustion is achieved. This will be done, by reducing the length of the coil. This will reduce the voltage, assuming no changes are made to the current, which will reduce the overall power consumption.

The second objective of this experiment is to determine whether it is possible to have a self-sustained combustion and if yes, what is the minimum power consumption to achieve self-sustained combustion. To accomplish this, the power supply for the heating coil will be turned off after ignition has been achieved. However, this will be only a limited self-sustained combustion, since the maximum amount of liquid that will be used during each run is 2 mL.

## 3.3. Test plan

For the ignition experiment, two separate experiments will be performed. The brief description of the two experiments is already explained in Section 3.2 above. In this test plan, a brief explanation of all the steps that need to be taken before, during and after the experiment will be provided. Lastly, a step-by-step guide will be provided that will describe all the steps that need to be taken for each run of the experiment. This will help not to forget any handling and to keep the experiment safe.

### 3.3.1. Experiment preparation

In addition to the entire set-up discussed above, the experiment also needs the chemicals. In this case, that is 90% hydrogen peroxide and absolute (100 %) ethanol. The high concentration hydrogen peroxide is provided by SolvGE. This company is located on the 12<sup>th</sup> floor of TU Delft, and they provide the hydrogen peroxide at the requested concentration. The ethanol is available in the chemical lab of the



Aerospace Faculty of TU Delft and is free of charge for (Master thesis) students.

The high-speed camera, which belongs to the Aircraft hall of the Aerospace Faculty of TU Delft, also needs to be reserved in case that high-speed footage is required. The glass combustion chambers are modified glass bottles which are readily available in the chemical lab. The backside of the bottles are cut with a grinder and two holes are drilled at the side of the glass tube for the placement of the heating coil. From a spool of nichrome wire, 20 cm is cut and curled into a spring shape before placing it inside the combustion chamber. Lastly, 3D-prints of the injector head are printed that tightly fit at the inlet of the combustion chamber.

### 3.3.2. Experimental phase

On the day of the experiments right before starting, some preparations need to be done first. In this paragraph, each required preparation will be elaborated.

#### Integration of set-up

The injector head should fit tightly on the glass combustion chamber. In some cases, sanding it with sanding paper will be required to make it fit. The piezoelectric discs can be placed from the slit at the sides of the injector head in its place. The piezoelectric discs then need to be connected to the microcontroller that is delivered with it. The microcontroller itself is connected to a wall socket and turned on with the button on top of the microcontroller. With a 20 cm long nichrome wire 12 windings are made with an inner diameter of 3.2 mm. This coil is then placed inside the combustion chamber and the ends of the coil are sticking out of the two holes that were drilled previously. The power supply is connected to both of those ends.

#### Preparation high-speed camera

The reserved high-speed camera, comes with its own computer. This computer comes pre-installed with Photrons own software that is used to interact with, record and save the footage of the high-speed camera. The software is called: Photron FASTCAM Viewer software (PFV). Since the frame rate of the camera is very high, the shutter time is very low. To capture sufficient light, a dedicated bright light source is required which does not flicker. Otherwise, when playing back the recordings in slow motion the flickering of the light will be visible. In the aircraft hall, bright (LED) lights which do not flicker are available for use.

The high-speed camera is placed on a tripod and connected to the computer with an Ethernet cable. After adjusting the height of the tripod, the focus of the high-speed camera and the brightness of the light. The high-speed camera will be ready for use.

#### Preparation phone camera

For the preparation of the phone camera. The pre-installed camera software is opened after the phone is placed on a tripod. Since the frame rate of the phone camera is lower than the high-speed camera, there is no need of an external light source, however since the recordings will be made simultaneously the external light source will be on. In the camera application, selecting the slow motion function is the only change that needs to be made. The focus, brightness and exposure are all automatically regulated by the camera software itself.

#### Preparation safety measures

After the ignition system is fully integrated. It has to be clamped horizontally with a metal clamp. It is important for the clamp that it does not contain cork, since it can catch fire when (hot) hydrogen peroxide leaks on it. After the ignition system is clamped, a metal plate can be placed at the back side of the set-up. On the top side and front, a safety glass is placed.

Because of the chance of the propellant and the plastic parts catching fire, two bottles/beakers with water are placed at two different locations. One inside the fume hood on the table next to the

experimental test set-up, while the second bottle of water is placed outside the fume hood. Lastly, it is important to have easy access to the on/off switch of the power supply.

### Steps during ignition experiment

In this sub-section the step-by-step guide for an experimental run will be provided. For both experiments the steps are the same, in case there is a difference this will be indicated with brackets.

1. Fill a small container with 90% hydrogen peroxide.
2. Fill a second small container with ethanol.
3. Turn on both microcontrollers of the piezoelectric discs.
4. Turn on the power supply. First start with 4.0 A and reduce the current with steps of 0.25 A until no ignition is happening. (For experiment 2: the length of the coil is reduced and the current is fixed at 4.0 A)
5. Fill two syringes with the propellant. One with hydrogen peroxide and the other with ethanol.
6. Press the 'Record' button in the PFV software. This will put the high-speed camera in a ready position. The high-speed camera is NOT recording yet. It is only an additional safety measure that is built in the software.
7. Start the recording with the phone camera, by pressing on the round record button.
8. Call the current, voltage, the concentration of hydrogen peroxide and the angle of the injector head.
9. Press 'Ready' in the PFV software, to start the recording with the high-speed camera. The recording will at maximum last for 3.4 seconds before its internal memory is full.
10. Inject both liquids from the syringe to both piezoelectric discs.
11. (For experiment 2: Turn-off power supply once ignition is achieved for self-sustained combustion)
12. After all the liquids has been injected, turn off the power supply for the heating coil.
13. Stop the recording on the phone camera. The footage will be automatically saved on the storage.
14. Inspect the footage of the high-speed camera on the computer. Crop the footage to the part that is of interest and save it on the hard drive of the computer.

### 3.3.3. Expected results

As explained at the beginning of this chapter, the objective of the first experiment is to observe and capture with a (high-speed) camera the phenomena that are happening during ignition and combustion. The second objective of this experiment is to determine the lowest required electrical power for which stable combustion is achieved.

The experiment will use various injector head angles, hence a brief anticipated outcome will be given below for each angle.

- **0° injector head angle**

With the 0° injector head angle, the liquid is injected perpendicular to the inlet of the combustion chamber and there is no direct impingement of the two injectors. The mixing of the two liquids happens only by the spray angle of the injectors itself. Because of this low mixing, it is expected that it will require the highest amount of electrical power to make the propellant ignite in this set-up. However, since the mixing is happening slowly and as a result it needs more of the length of the combustion chamber to mix, it is also expected that the fluctuations of the flame front will be limited because of the slow mixing.

- **10° injector head angle**

Increasing the injector head angle to 10°, the two liquid jets coming out of the injectors will impinge. This will improve the mixing and it is expected that this will slightly reduce the required electrical power. Furthermore, it is expected that the fluctuations of the flame front will be very similar to the 0° injector head angle.

- **20° injector head angle**

The impinging of the two streams of atomized liquid will be even more significant with a 20° injector head angle. The mixing will be further improved, while the stability of the flame is still comparable to the previous two injector heads. However, since the mixing is happening earlier in the combustion chamber, it is expected that after the flame has fully developed that the begin of the flame is closer to the injector.

- **30° injector head angle**

In previous experiments, where two streams of nitrogen were impinging at an angle of 30°, it resulted in a good and stable spray cone angle. Because of this, the expectation is that with this injector head it will provide a good balance between mixing and flame stability while also lowering the required electrical power for the heating coil.

- **40° injector head angle**

At 40° injector head, the injector head has a significant bulge. This is also apparent in Figure 3.3. This makes the expectations for this injector head that the mixing will be very good, but it will be spraying against the (glass) walls of the combustion chamber. This will probably result in an unstable flame with a lot of fluctuations of the flame front. Secondly, since the atomized droplets will be hitting the walls the length of the flame will be very short since there will be not that much speed in the longitudinal direction.

### 3.4. Conclusion test plan

This experiment will capture the phenomena that are happening during the ignition followed by a combustion of hydrogen peroxide and ethanol. The high-speed camera recordings will visualize the fine and very fast details that are normally not observable with normal cameras and naked eye, which will be of importance when comparing the combustion and flames with the different ignition head angles.

For the second experiment, where the length of the heating coil will be reduced. It is expected to have ignition and combustion till about 15 W. However, going lower than 15 W, will result in ignition failures because the heating coil is cooling down too much. This results in the liquid mixture not reaching the auto-ignition temperature of ethanol. In terms of self-sustained combustion, within the short duration of the test it is expected that for every power consumption where ignition is achieved it will be also possible to have a self-sustained combustion since the flame temperature is significantly higher than the temperature of the heating coil with only electrical power applied.

# 4

## Results & Observations

In this chapter, the results and observations gathered during both experiments will be discussed. As discussed in Chapter 3, five different injector heads have been tested to find out which angle provides the best balance between combustion stability and required electrical input. In this section, for each injector head the observations will be shown and discussed. At the end of this section, a comparison of the required electrical power for each injector head will be done.

The second part of this chapter will discuss the results achieved with the second experiment where the length of the heating coil is reduced to find the minimum power consumption where ignition and self-sustained combustion are achieved. During both experiments no temperature measurements were performed, since the thermocouple was not able to withstand the high temperatures caused by the flame. In the best case scenario, it did not show the measured temperature and in the worst case the connection point of the thermocouple melted apart, resulting in two loose wires.

### 4.1. General observations

During the experiments, a number of phenomena can be observed. Some of those phenomena are related to the injector head that is used, while other phenomena are related to other factors. In this section, some of the phenomena that are not specific to the injector head (angle) will be discussed.

In all cases, the initial ignition happened near the heating coil since that is the location where the highest temperatures are reached. The flame expands and propagates to other parts of the combustion chamber until a relatively stable flame front is established. The propagation of the flame can be clearly seen with the high-speed camera, and this phenomenon is even more pronounced when there is an explosion taking place. An explosion occurs mostly when ethanol is injected inside the combustion chamber with a slight delay compared to the injection of hydrogen peroxide. In this instance, the hydrogen peroxide is accumulating and beginning to decompose inside the combustion chamber. When afterwards ethanol is injected into the combustion chamber and it reaches the auto-ignition temperature (near the heating coil), it ignites. Because of the significant amount of (decomposed) hydrogen peroxide that is inside the combustion chamber, the flame front propagates very quickly until it covers the whole volume of the combustion chamber. In case of a strong explosion, no flame is following up afterwards. In case of a weaker explosion, on some occasions a flame is established after the explosion. This phenomenon can be seen in the high-speed footage in Figure 4.1. This entire process from ignition till the end of the explosion only takes about 20 ms and usually goes in tandem with a loud explosion sound caused by the pressure waves.

However, if the delay between the injection of hydrogen peroxide and ethanol is even further increased, the hydrogen peroxide cools down the heating coil too much which prevents the later introduced ethanol from reaching its auto-ignition temperature. As a result, there will be neither a combustion nor an explosion happening.

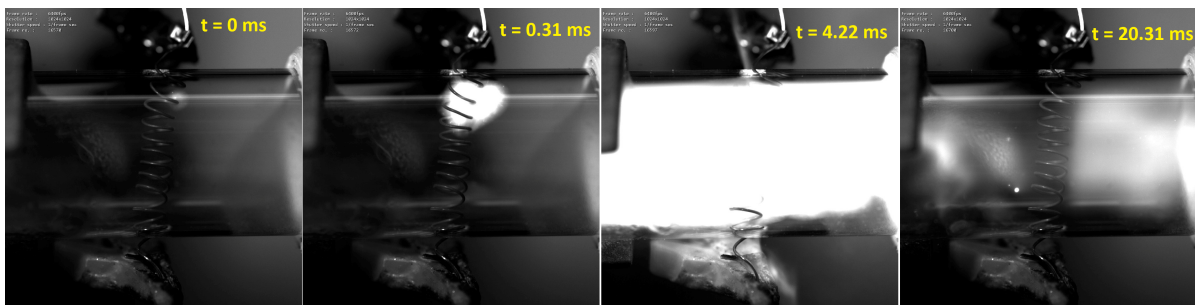


Figure 4.1: Explosion, when ethanol is injected slightly later than hydrogen peroxide in the combustion chamber.

## 4.2. Results with various injector heads

With each injector head, the starting current was 4.0 A, since it is known that this always leads to an ignition of hydrogen peroxide and ethanol. Afterwards, the current is reduced in steps of 0.25 A, until the propellant did not ignite anymore.

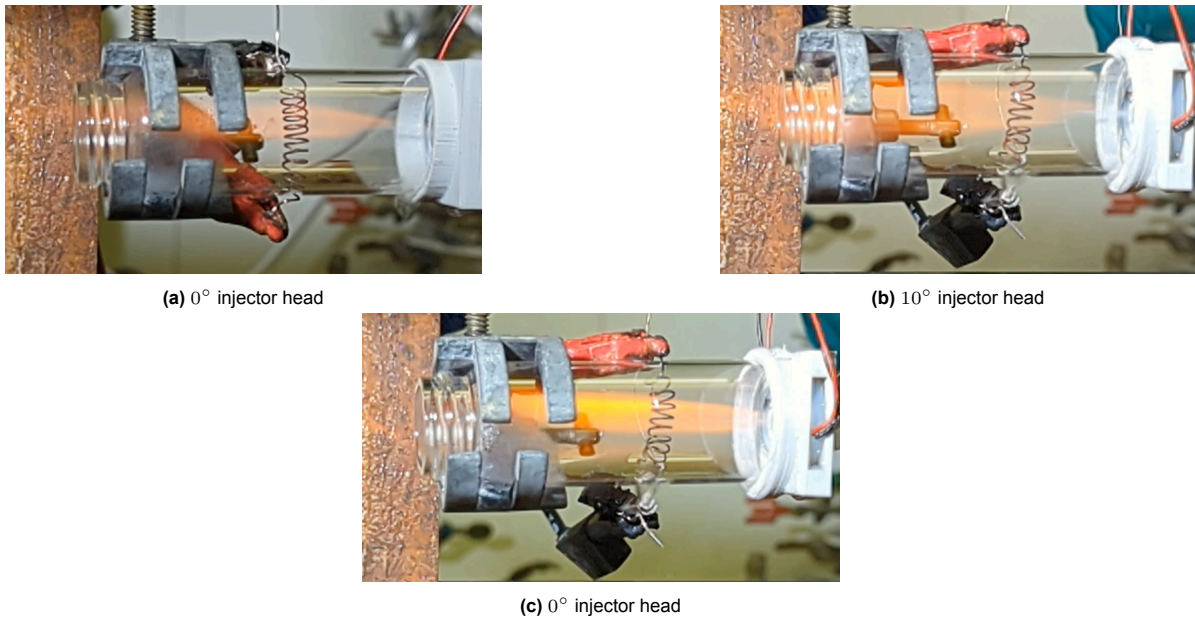
Table 4.1 makes it evident that greater injector head angles results in successful ignition with lower power consumption. While with the  $0^\circ$ ,  $10^\circ$  and  $20^\circ$  injector head no repeated ignition could be achieved with 3.25 A. With the two highest injector head angles, an ignition was achieved multiple times with a current of 3.25 A. However, besides having an ignition at the lowest possible electrical power it is also important to have a stable combustion. The higher the angle of the injector head was, the more turbulent and unstable the flame became. For a propulsion application, these kinds of flames are not desired since this causes instabilities, anomalies with the thrust, local flames which damage the engine and excessive vibrations. Because of this reason, the  $10^\circ$  injector head angle is selected as the best between all five angles. Although it does not have the lowest electrical power for ignition, it is providing a reasonable stable flame. In the paragraphs below, some more details and observations of the ignitions and flames for each injector head angle will be provided.

Table 4.1: Overview of successful ignition followed by combustion of different injector head angles with changing current.

Injector head angle	Successful ignition					Comments
	4.0 A	3.75 A	3.5 A	3.25 A	3.0 A	
$0^\circ$	Yes	Yes	Yes	No	No	Ignition once achieved with 3.25 A
$10^\circ$	Yes	Yes	Yes	No	No	Ignition once achieved with 3.25 A
$20^\circ$	Yes	Yes	Yes	No	No	-
$30^\circ$	Yes	Yes	Yes	Yes	No	-
$40^\circ$	Yes	Yes	Yes	Yes	No	-

### 4.2.1. Flame length

In terms of flame length, the  $0^\circ$  and  $10^\circ$  injector heads were very similar to each other. There was no significant difference between the length of the flame. In both cases, the length of the flame filled the entire length of the combustion chamber, once the flame was fully developed. On some occasions, the flame was even longer than the combustion chamber itself. The length of the fire, for both injector head angles can be seen in Figure 4.2.



**Figure 4.2:** Exported frames from video recording to illustrate the flame length with the 0° and 10° injector heads.

In both of the injector head angles, it was not expected that the begin of the flame would be close to the injector head, since the mixing of the propellants was expected to happen later in the combustion chamber. Inspecting the high-speed footage showed that the atomized liquid injected from the two injectors was mixing earlier than expected. This was due to the spray cone angle of the injectors which allowed the mixing to happen very close to the injector head. As a result, the flame itself was also getting very close to the injector head, which can be also seen in Figure 4.2c.

With the higher injector head angles, the flame was as expected not as long as it was the case with the 0° and 10° injector heads. The flame for the higher injector head angles usually appears in the area between the injector head and the heating coil. In Figure 4.3 a couple of examples of the flame for each injector head angle can be seen.

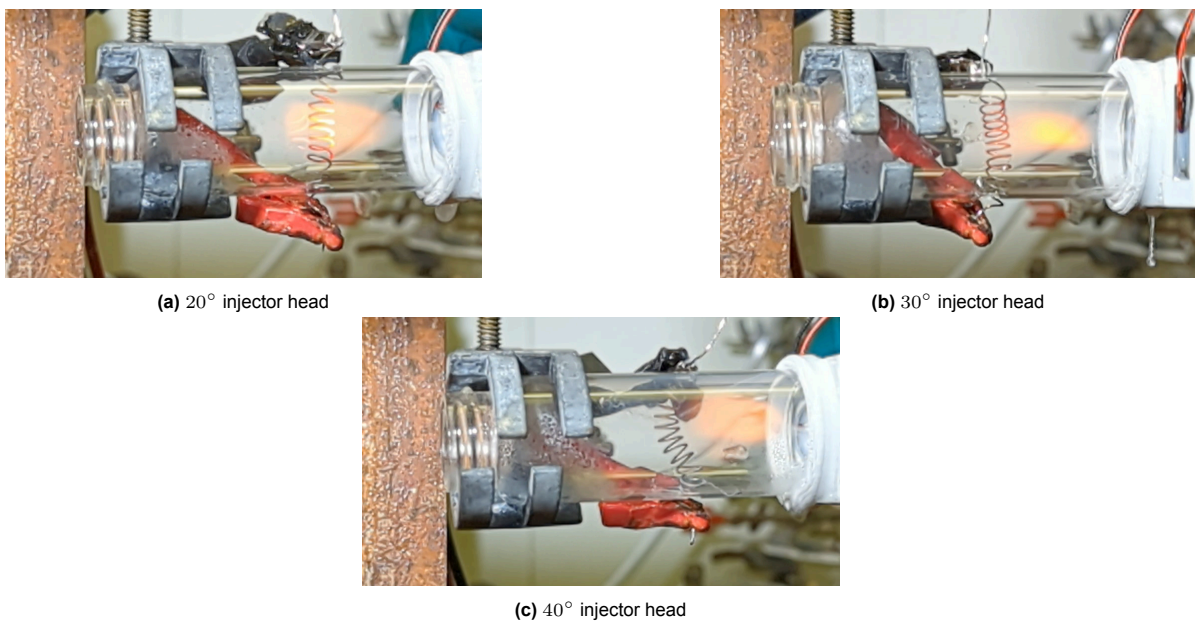


**Figure 4.3:** Frames from video recording to illustrate the flame length with the 20°, 30° and 40° injector heads.

The impinging of the two liquids happens closer to the injector head with the increasing injector head angle. This results in the flame being closer to the injector head, with increased angles. From all the five injector heads, the flame with the  $20^\circ$  injector head was the furthest away from the injector head.

#### **4.2.2. Flame front fluctuation**

As discussed at the beginning of this chapter, the fluctuation of the flame front is an important factor. With the different injector head angles, there is a significant difference in the fluctuations of the flame. While the injector heads with the lower angles were showing considerably fewer fluctuations, the higher angles resulted in significant fluctuations of the flame front. As discussed in the previous paragraph, the flames with the  $0^\circ$  and  $10^\circ$  injector head had a long flame and consisted mostly of a single flame without interruptions in the flame front. The flame front itself was not completely stable, since the flame moves during a time interval, however it was less severe compared to the higher angle injector heads.

In case of injector heads with the higher angles, the location and the direction of the flame can significantly change in very short periods of time. This in combination with local interruptions in the flame front, which looks like local extinctions shows that the flame is not very stable. This is especially the case for the injector heads with  $30^\circ$  and  $40^\circ$  angles. In Figure 4.4 the frames of the high-speed camera have been exported to display the behaviour of the flame front with each injector head angle.

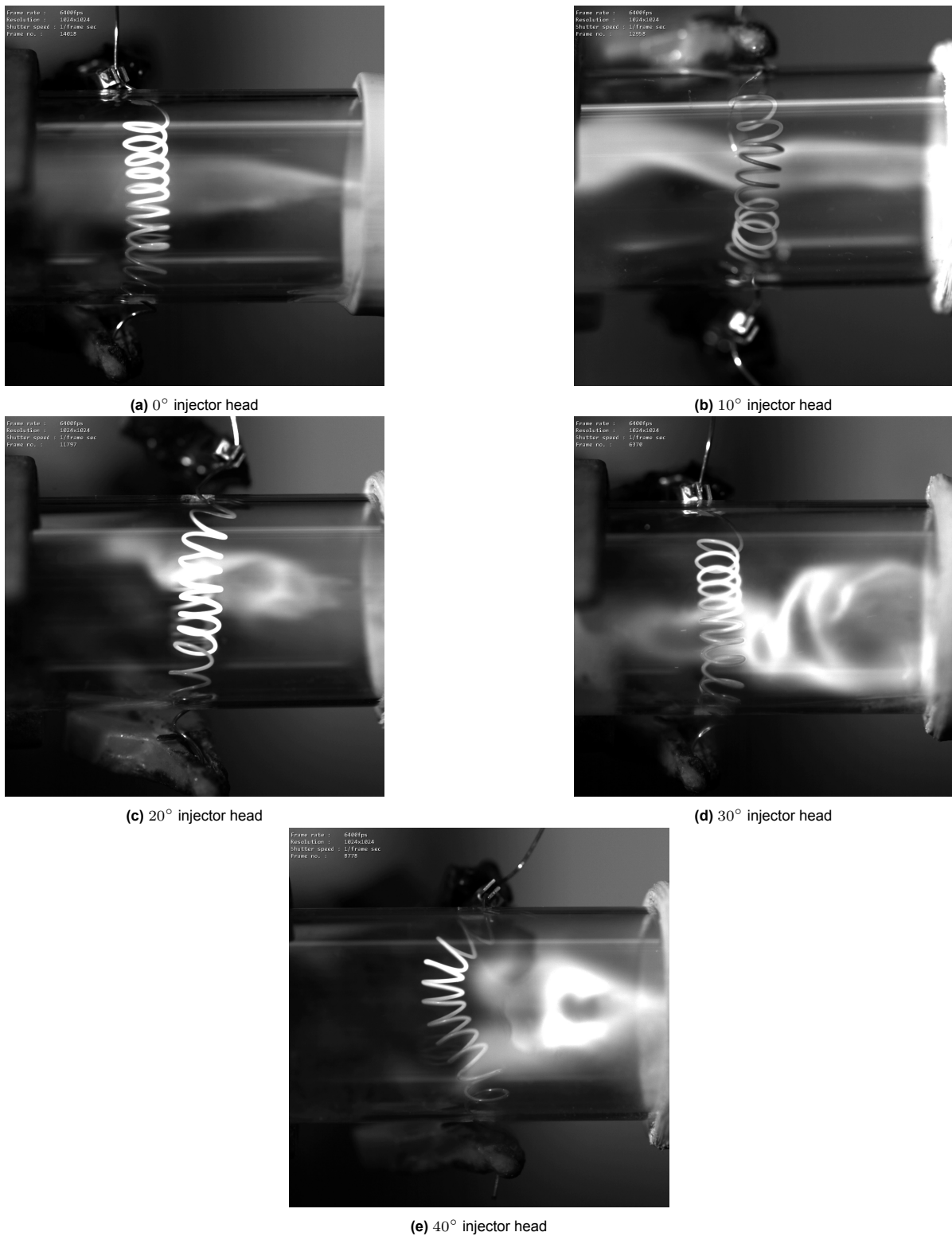


Figure 4.4: Exported frame from high-speed camera of the flame front with each injector head angle.

### 4.3. Trade-off injector head

All five injector heads have been tried out with different current levels. With those achieved results, a trade-off will be performed and the injector head with the highest points will be used to perform some more experiments. Those follow up experiments and the achieved results with it are discussed in Sec-



tion 4.4.

As it was the case for the ignition type trade-off, first each selected criterion will be explained and the weighting factor between 1 and 5 will be determined. Afterwards, the trade-off table will be made where each injector head angle will get a grade between 1 and 6 for each criterion. This grade will be multiplied with the weighting factor of the criterion. The score of each criterion will be summed up to get the total score of each injector head angle.

### 4.3.1. Trade-off injector head criteria

For the trade-off table, three criteria will be used to compare the performance of each injector head. In this section, a short explanation of each criterion together with its weighting factor will be provided.

- **Power**

The electrical power consumption is an important factor, since small satellites are often limited by their (peak) electrical power consumption. The less the ignition system consumes the more power budget there will be left for other components. While power consumption is an important criterion, there are also other factors that are influencing the temperature and the ignition of the propellant. Because of this reason, the weighting factor for the power criterion has been set to 3.

- **Fluctuation**

For a combustion engine, it is important to have a smooth combustion without the flame front fluctuating from its position too intensely. The more the flame front is fluctuating, the more vibrations and instabilities will be introduced. This can also cause (too many) local fuel bubbles and/or local extinctions. Both of those phenomena can again possibly introduce additional problems like vibrations and instabilities in the combustion chamber. For this reason, the highest weighting factor of 5 was given for this criterion.

- **Impinging**

Preferably the beginning point of the flame is at some distance from the injector head and not very close to it. In case the flame gets too close to the injector head, it can damage the injectors and the injector head itself. This is especially the case with the current set-up, since the injector head is made out of 3D-printed plastic and the injector itself is surrounded by a rubber ring which can catch fire. Compared to the other two criteria, this is the least important one and that is why the weighting factor for this one is set to 1.

### 4.3.2. Trade-off table & Discussion

The grading for each injector head is done on the basis of the results obtained/observed from the experiments that have been discussed in Section 4.1 and Section 4.2. Since no hard numbers have been obtained during the experiments, the grading for the trade-off will be mostly qualitatively based.

For the power consumption, there were only two results. The lowest possible current, with which successful ignition was achieved multiple times, was either at 3.5 A or at 3.25 A. This resulted in having the full six points, in case it was able to achieve ignition at 3.25 A, like the 30° and 40° injector head angles. Or it scored zero points, when achieving ignition at 3.5 A. This was the case for all other injector head angles.

For the fluctuation criterion, both the 0° and 10° injector head angles received the full 6 points. Both had the lowest fluctuations and the flames were (almost) indistinguishable from both injector head angles. The 20° injector head was fluctuating from position more than the previous two injector heads, however the fluctuations of the flame front were not too intense and was possible to follow the movement of the flame front with the naked eye. That is why it received 4 points for this criterion. The flame front with the 30° and 40° injector head was fluctuating more intensely and it was difficult to follow the fluctuations of the flame front with the naked eye. Especially with the 40° injector head the fluctuations

and local extinctions were severe. This resulted in zero points, while the 30° injector head has 1 point.

The distance between the beginning of the flame and the injector head will determine the number of points each injector head will receive. Since the distance changes during fluctuations and during each experiment, it would be too hard to measure the exact distance. Because of this, the grading for this criterion will be also qualitative. While the flame for both the 0° and 10° injector head looks very similar and in both cases the flame propagates close to the injector head, in general the 10° injector head had a flame that was slightly farther away from the injector head itself. This resulted in 0 and 1 point respectively. The 20° injector head was able to maintain a reasonable distance from the injector head during the whole duration of the experiment. This resulted in scoring the highest grade with 6 points. The 30° injector head was generally able to maintain a sufficient distance from the injector head, however sometimes the flame front was moving very close to the injector head for a short period. As a result, it got 3 points for this criterion. The atomized particles from the 40° injector head were hitting the walls of the combustion chamber very close to the injector head. Although the flame front was heavily fluctuating during the experiments it was also multiple times during a single test getting very close to the injector head itself. This resulted in having a grade of two points.

**Table 4.2:** Trade-off table injector head selection

Injector angle	Power		Fluctuation		Impinging		TOTAL
	0	3	4	5	0	1	
0°	0	0	6	30	0	0	<b>30</b>
10°	0	0	6	30	1	1	<b>31</b>
20°	0	0	4	20	6	6	<b>26</b>
30°	6	18	1	5	3	3	<b>26</b>
40°	6	18	0	0	2	2	<b>20</b>

From the trade-off table, it can be concluded that the 10° injector head has the highest total score of 31. It is closely followed by the 0° injector head with a total score of 30. Both scored similarly for each criterion, except for the distance. For this criterion, the 10° injector head scored slightly higher. The injector head with a 40° angle has the lowest total score of 20. Because of the intensity of the fluctuations of the flame front, it lost a lot of points. The 20° and 30° injector head, have both a total score of 26.

The follow up experiments, from now on will be performed with the 10° injector head, since it had the highest total score. The other injector heads will not be used anymore to experiment with.

## 4.4. Results & Observations optimized power consumption

With the selected injector head in the previous section, the follow up experiments can be performed. The main objectives with the follow up experiments is to even further lower the power consumption while still being able to have ignition and combustion of the propellant. During the previous experiments, the current was reduced and as a result also the total electrical power consumption dropped. However, since the temperature of the heating coil is dependent on the current going through it, at some point the coil will be close to or even lower than the auto-ignition temperature of ethanol and no ignition will be happening. For the follow up experiments, the electrical power consumption will not be reduced by dropping the current, but instead the length of the heating coil will be shortened. This will result in a lower voltage, with the same current levels.

The second objective of the follow up experiments is to determine whether a self-sustained combustion can be realized with the current set-up. This implies that the power supply needs to be turned off at some point after the ignition. For this experiment the combustion will be called "self-sustained", if the combustion continues, after the power supply has been turned off, for the whole duration till both liquids are completely injected. In case the combustion stops directly after the power supply is turned off

or at some point before all the liquids are injected it will be not categorized as self-sustained combustion.

It is important to note that with the current set-up, because of safety reasons, a maximum of 1 mL of each liquid can be used for each run. Which results in a combustion time of a couple of seconds. For this experiment, during this period the ignition needs to happen and a sustained combustion needs to be established, before the power supply can be turned off. The time that is left to continue the experiment after this point will be very limited and not completely representative of a real case scenario. However, this will show whether the combustion will stop abruptly the moment the power supply has been turned off or whether it can still carry on and be self-sustained, even though it is for a short duration.

#### 4.4.1. Results with reduced coil length

During the experiments, the length of the heating coil was stepwise reduced. With each small change to the coil length, a couple of experiments were performed to check whether an ignition and combustion was achieved. In the initial case, the heating coil had about 12 windings, which resulted in 5 V at 4 A. By reducing the number of windings, the length of the heating coil is reduced and as a result also the voltage dropped (with the same current level).

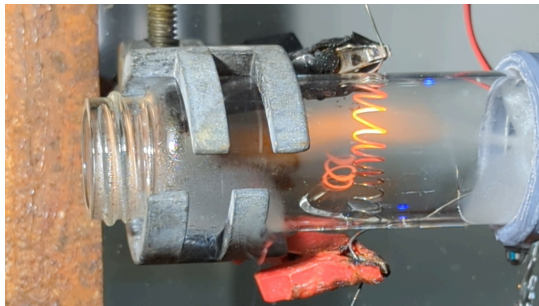
As explained above, the starting point was with 4.0 A and 5.0 V. As soon as a combustion was established the power supply was turned off manually. The combustion carried on till all the liquids were injected in the combustion chamber. A self-sustained combustion was also achieved with a slightly reduced coil length that resulted in a power consumption of 4.0 A and 3.8 V.

Another experiment was performed with 4.0 A and 3.9 V, with a new glass combustion chamber since the previous one broke. Also, in this case a self-sustained combustion was achieved. Reducing the coil length even further, resulted to a voltage of 3.5 V with a power consumption of 14 W. Also, in this case a self-sustained combustion was achieved. Dropping the voltage to 3.1 V, by reducing the coil length even more, was the point where no ignition was achieved. Multiple tries resulted in an explosion. However, it was observed that the red glow of the coil reduced the further the windings of the heating coil were pulled apart. This indicates that the temperature of the heating coil is also dropping. Since the ignition of the propellant usually happens at the middle of the heating coil, the distance between the four windings was reduced. The ends of the heating coil were only extended till it sticks out of the combustion chamber in order to be able to connect the ends to the power supply. This allowed to reduce the total length of the heating coil and thus resulting in a lower power consumption of 10 W. At the same time, at the windings the temperature was clearly higher than the previous case, since a more apparent red glow was visible which was not the case previously. The confined heating coil, with a power consumption of 10 W, was able to achieve ignition followed by a self-sustained combustion. This experiment was performed multiple times to prove that it was not only a single time coincidence, but a self-sustained combustion that was reliable and repeatable.

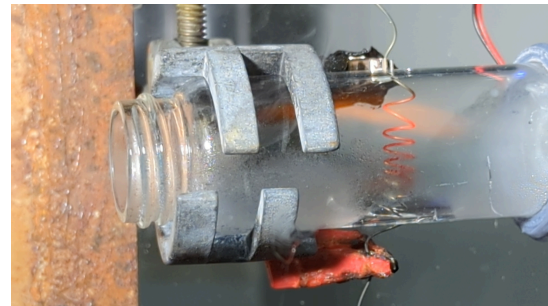
Table 4.3 provides a summary of the details of each run during the experiment and the achieved results. In Figure 4.5 a picture has been added of the combustion (or explosion) with each power consumption. It should be mentioned that the interval between ignition and the photos taken varies for each image. As a result, the photographs cannot be directly compared to one another. However, the later the picture is taken after the ignition, the brighter the heating coil is at the place where the flame and heating coil are in contact.

**Table 4.3:** Test results and power consumption of optimized heating coil

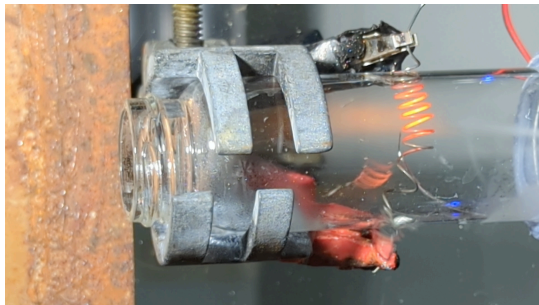
Current [A]	Voltage [V]	Power [W]	Combustion	Self-sustained	Comments
4.0	5.0	20.0	Yes	Yes	
4.0	3.8	15.2	Yes	Yes	
4.0	3.9	15.6	Yes	Yes	
4.0	3.5	14.0	Yes	Yes	
4.0	3.1	12.4	No	-	
4.0	2.5	10.0	Yes	Yes	Confined heating coil



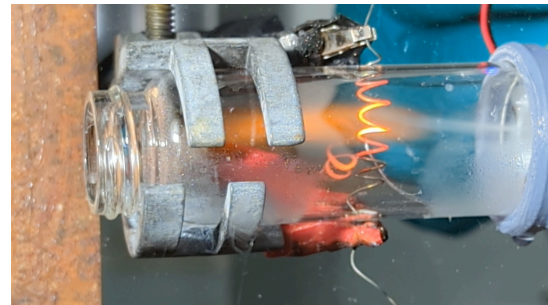
(a) 4.0 A and 5.0 V. Combustion successful



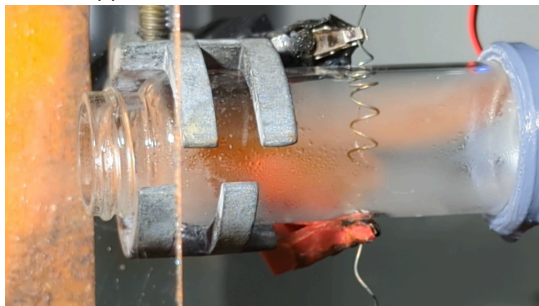
(b) 4.0 A and 3.8 V. Combustion successful



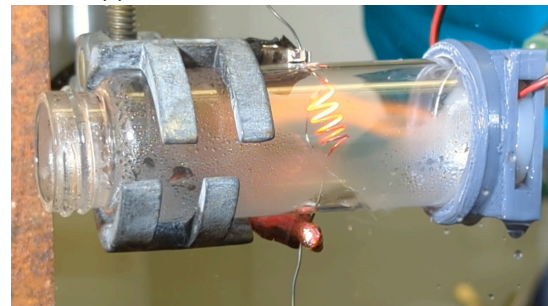
(c) 4.0 A and 3.9 V. Combustion successful



(d) 4.0 A and 3.5 V. Combustion successful



(e) 4.0 A and 3.1 V. Combustion failed



(f) 4.0 A and 2.5 V. Combustion successful

**Figure 4.5:** Self-sustained combustion with reduced heating coil length

## 4.5. Conclusion of Results & Observations

Two experiments have been performed, during the first experiment tests have been performed with different injector head angles. With the aid of a trade-off table, the most effective angle for the injector head was selected. The second experiment was then conducted using the selected injector head to determine the minimum amount of electrical power required for ignition and self-sustained combustion.

The colored slow motion and the footage with the high-speed camera clearly showed the phenomena that happened in (very) short period, which are too fast and small for the human eye. Multiple tests were performed with different injector head angles and different currents. This information is used to

grade each injector head on the criteria: (electrical) power, fluctuations of the flame and the distance of the impinging from the injector head. While the power consumption was slightly lower with the higher angle injector heads, the fluctuation and the impinging was not great. On the other hand, the injector heads with the lower angle had good scores with for the fluctuation and lower grades for the other two criteria. In the end, it resulted in the  $10^\circ$  injector head having the highest total score.

The  $10^\circ$  injector head was then used for the second part of the experiments. The current was fixed at 4.0 A and the length of the coil was stepwise reduced to reduce the voltage. Starting with 4.0 A and 5.0 V till 4.0 A and 3.5 V, a self-sustained combustion was achieved. Self-sustained combustion implies that after a combustion has been established the power supply is turned off, and the combustion still continues till all the liquids are injected in the combustion chamber. At 4.0 A and 3.1 V, not enough heat was in the system to start the ignition of hydrogen peroxide and ethanol. However, reducing the number of windings to four and confining those windings at the center of the combustion chamber allowed to have a successful ignition followed by a self-sustained combustion with only 10 W.

# 5

## Proof of concept

While in Chapter 3, the final set-up has been discussed in detail, the explanation of the earlier iterations has been left out. In this chapter, all the earlier iterations of the experimental set-up will be discussed. In Table 5.1, on the next page, an overview is given of all the nine iterations. This table briefly explains what the changes were for each iteration and what the obtained results were. More details of each iteration are discussed in the sub-sections below in chronological order.

**Table 5.1:** Summary of all the iterations for the experimental test set-up

#	Description	Changes	Comments	Results
1	First test set-up	-	- Initial tests with a heating coil and hydrogen peroxide.	- Not enough heat transfer from heating coil to liquid droplet within the short period of time.
2	Curled heating coil	- Heating coil is curled to increase surface area and residence time	- Heating coil is wound, like a spring, to increase the residence time of the droplet on the heating coil.	- Heat transfer still not sufficient to have decomposition of hydrogen peroxide
3	Improved isolation	- Set-up is surrounded by glass tube. - Length of heating coil increased.	- The glass tube will reduce the heat dissipating to the environment. - Increased heating coil increases the temperature inside the glass tube and residence time of droplet.	- Decomposition is achieved.  - Electrical power consumption is too high with 100+ W.
4	Smaller glass tube	Small glass bottle is used as combustion chamber	- The glass tube is replaced by a small glass bottle, this reduces the volume inside the glass tube for improved thermals. - With the smaller glass tube also the length of the heating coil has been reduced by placing it in a radial direction	- Power consumption was reduced, because of the reduced coil length.  - The residence time was also reduced, which resulted in droplets of hydrogen peroxide not decomposing.
5	Multiple layers heating coil	- Multiple layers of heating coil is used	- Instead of a single layer, multiple layers of heating coil is used to increase the chance of a droplet hitting multiple times the heating coil.	- Droplets that are hitting the heating coil multiple times or hitting the (glass) wall are getting decomposed.  - Droplets that hit the heating coil once and do not hit the wall, are not decomposed.
6	Atomized droplets	- Piezoelectric disc is used to generate a fine mist of liquid droplets	- A piezoelectric disc is used to produce very fine droplets. The droplet sizes are much smaller than the ones from a syringe.	- The atomized liquid was causing the heating coil to cool down up to the point where no decomposition could happen. - The heat from the heating coil and decomposed hydrogen peroxide caused the piezoelectric disc to catch fire.
7	Set-up with fan	- Horizontal test set-up with a fan	- Instead of a vertical test set-up where a droplet is falling on the heating coil. A horizontal set-up is opted where the fan blows the fine droplets towards the heating coil.	- The airflow because of the fan, is cooling down the heating coil too much which prevents the hydrogen peroxide to decompose.
8	Impinging method	- Impinging of the liquid with gaseous nitrogen	- The atomization of the liquid is achieved by impinging two lines of nitrogen. The liquid droplet in the middle is split into smaller droplets.	- The nitrogen flow is cooling down the heating coil too much to have a proper decomposition of hydrogen peroxide.
9	Injector head	- Horizontal test set-up where the piezoelectric discs are directly placed behind the inlet of the combustion chamber. - Ethanol is also injected	- Instead of using a fan, two piezoelectric discs are placed right behind the inlet of the combustion chamber.  - From one disc, hydrogen peroxide is injected, while from the second disc ethanol is injected.	- With the oxidizer and fuel both injected, ignition and sustained combustion was achieved.  - Low power consumptions were achieved, since the flame was able to maintain the required temperatures - High concentrations of hydrogen peroxide (95+ %), lead to fires at the test set-up.

## 5.1. Iteration 1: Understanding the behaviour of peroxide in combination with a heating coil

The first iteration allowed to have a general understanding on how to build a set-up that makes it possible to have small droplets falling on a heating coil. Water was utilized in the majority of test runs with this setup, and hydrogen peroxide was only used to study how hydrogen peroxide behaves when heat is applied.

### 5.1.1. Set-up for first iteration

While it is already proven in the Master's thesis of Jaime [28] that it is possible to decompose and combust hydrogen peroxide and ethanol. During that study, a droplet of hydrogen peroxide and ethanol was dropped on a heating plate. In the case of rocket propulsion and ignition, this is not completely representative since the droplet on a heating plate has as much time as required to decompose and combust. A new setup was made to confirm whether a falling drop of hydrogen peroxide on a thin heating coil can be heated enough in a short period of time to get decomposition.

A simple setup, seen in Figure 5.1, was created to gain experience and obtain a better understanding of how hydrogen peroxide behaves when it comes into contact with a heated coil. The glass tube will trap the heat within the glass tube and will provide safety. The coil itself, is a nichrome heating coil. Which is 80 % nickel and 20 % chromium. The coil is bent into a "U" shape so that the drop can fall on top of the (heated) coil. To control the heat of the coil, a power source is linked to both ends of the coil. A clamp held a syringe in place at the top. At the top, a syringe was fixed in place by a clamp. Droplets will be expelled from the syringe that will fall on the heating coil. Below the glass tube, a small bowl has been placed to catch the droplets that did not evaporate or decompose.

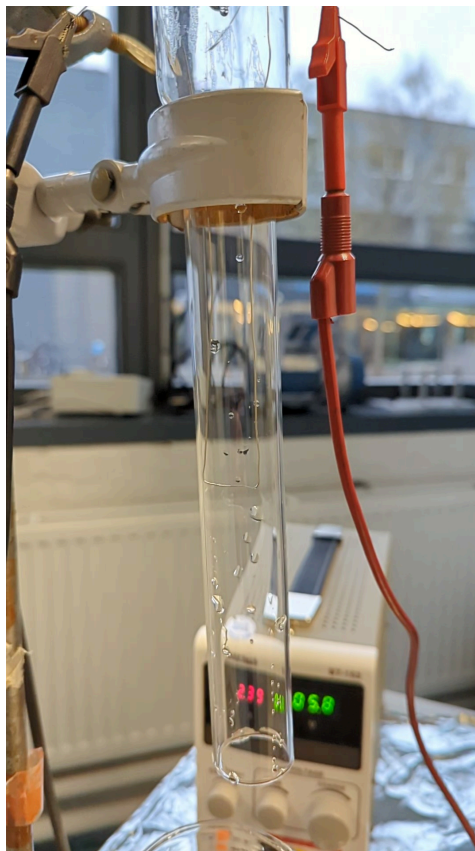


Figure 5.1: 'U' shaped heating coil inside a glass tube, with the power supply connected to it.



### 5.1.2. Results and observations first iteration

To ensure that the setup is operating as anticipated and to see if anything unexpected was occurring that required further intervention, the first tests were carried out using only water.

The first tests with water showed how a droplet was interacting when getting in touch with the (heated) heating coil. The droplet was not sticking on the coil and it was also not splitting the droplet into smaller drops. Secondly, there is also no clear sign of the droplet being partly evaporated. Either the droplet hit the wall of the glass tube after changing direction when it struck the heating coil, or it was dropping into the bowl beneath the tube. The same results were obtained from tests using hydrogen peroxide instead of water. There were no indications that anything was decomposing. Another problem that occurred with this setup is that it was very difficult to aim a droplet on the coil. In some cases, the droplet was hitting the coil, but most of the time the droplet was missing the coil.

The surface area of the heating coil has to be increased for the following iteration in order to increase the likelihood of droplets hitting it and to increase the residence time of the droplet on the heating coil. This will make the set-up less susceptible to small disturbances to the trajectory of the droplet.

Another observation that was made during the first iteration was that the droplet was splashing under the glass tube and leaving small droplets on the table. When it comes to hydrogen peroxide, this might be particularly hazardous. It could potentially damage the (electrical) equipment that is positioned around the test set-up and could be also a potential problem for the people that are working on the set-up.

## 5.2. Iteration 2: Testing with additional protection around

Additional protection around the setup will be required for safety concerns, as was addressed in the preceding section. However, the additional safety should not obstruct the view of the set-up itself. Making use of a safety glass on at least one side, it will provide a view inside.

### 5.2.1. Set-up second iteration

For the additional protection, a 3D-design is made that can be printed with a 3D-printer. The safety chamber features four pillars at each corner of its rectangular base. Each of those pillars includes two rails that may be used to slide safety glass or metal plates on each side to provide additional protection for the area around it. On at least one side, a glass plate will be placed to have a view inside and to record safely with a (high-speed) camera. An impression of the 3D-printed safety chamber is shown in Figure 5.2.



**Figure 5.2:** First version of the safety chamber. On three sides, a steel plate is used and at the front side a safety glass is used to have a clear view inside the chamber.

The initial plan was to use the glass tube again as a thermally isolating layer, however it is difficult to have a heating coil inside the glass tube. Because of this reason, it was decided to first try it without a glass tube.

The heating coil was wound like a spring and placed on one of the metal plates that serve as protection, as shown in Figure 5.3. To electrically isolate the heating coil from the metal plate, a high temperature resistant tacky tape was used. Like in the previous set-up a syringe was fixed in place by a clamp at some distance above the heating coil. The distance between the syringe and the heating coil will also protect the hydrogen peroxide inside the syringe from heating up and decomposing inside the syringe. The only droplet that is exposed to the high heat emitted by the heating coil is the one that is expelled out of the syringe.

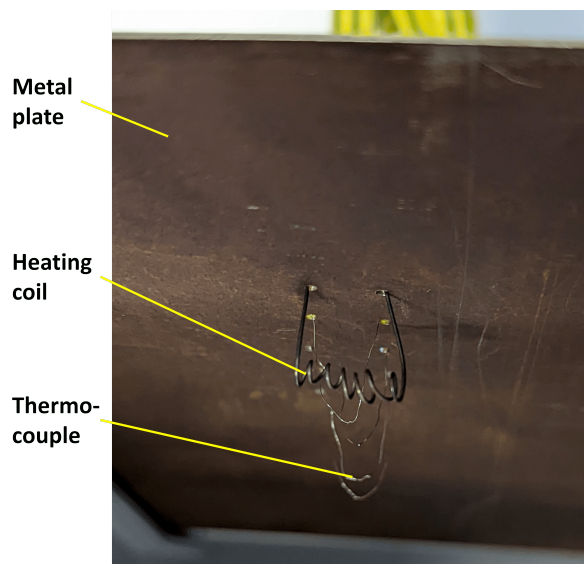


**Figure 5.3:** Wound heating coil placed inside the safety chamber. With small thermocouples below the heating coil for temperature measurements.

### 5.2.2. Results and observations second iteration

At the beginning of the second iteration, a few tests were carried out with water. Despite the droplet touching the heating coil more frequently, there was still no indication that it was evaporating. This situation was confirmed by the thermocouples located beneath the heating coil. Within the brief period

of contact with the heating coil, the temperature of the droplet did not change considerably.

The absence of (glass) tubing around the heating coil allowed the heat produced to disperse into a larger environment. This led to a decrease in temperature around the heating coil. It is crucial to keep the heat better contained, by making use of a glass tube that surrounds the heating coil. Which might be the cause of the failure to evaporate or decompose water and hydrogen peroxide.

Additionally, the residence time of the droplet on the heating coil is very short. A longer coil should be used to increase the residence time. From the Master thesis of Jaime, the minimum residence time of a droplet of 90 + % hydrogen peroxide to have decomposition on a heated plate of  $250^{\circ} C$  is about 100 ms [28]. In case of a heating coil, there is no full contact between the droplet and the coil itself, as it is the case with a heated plate. As a result, the expectation is that the contact time should be even higher in case of a coil, since the surface area of a droplet that is in contact with the coil will be significantly smaller than the surface area that is in contact with the heated plate with the current set-up.

To reduce the residence time with the coil, besides increasing the length of the coil itself, the electrical power could be also increased to achieve higher temperatures to reduce the required residence time to achieve decomposition.

### **5.3. Iteration 3: Increasing power and improving isolation**

The glass tube, which was introduced at the first iteration, is also used for the third iteration to have some thermal isolation and as a result achieve higher temperatures. However, the existing 3D-designed safety chamber cannot accommodate the length of the glass tube. A new and longer 3D design was made and printed with a 3D-printer. This new design is twice as long as the old one, and a top cover was created to minimize heat loss from the top portion. A slit was cut out of the plastic cover in the center to allow the droplet to pass through. However, the temperature was too high for the plastic top cover and was starting to melt after a short period of time. The plastic cover was replaced by a metal plate afterward. The new design of the set-up and the melted plastic cover can be seen in Figure 5.4.

Since it was very difficult to make holes inside the glass tube, it was decided to use a long heating coil, which would also increase the residence time of the droplet and as a result increase the chance of having decomposition of hydrogen peroxide.

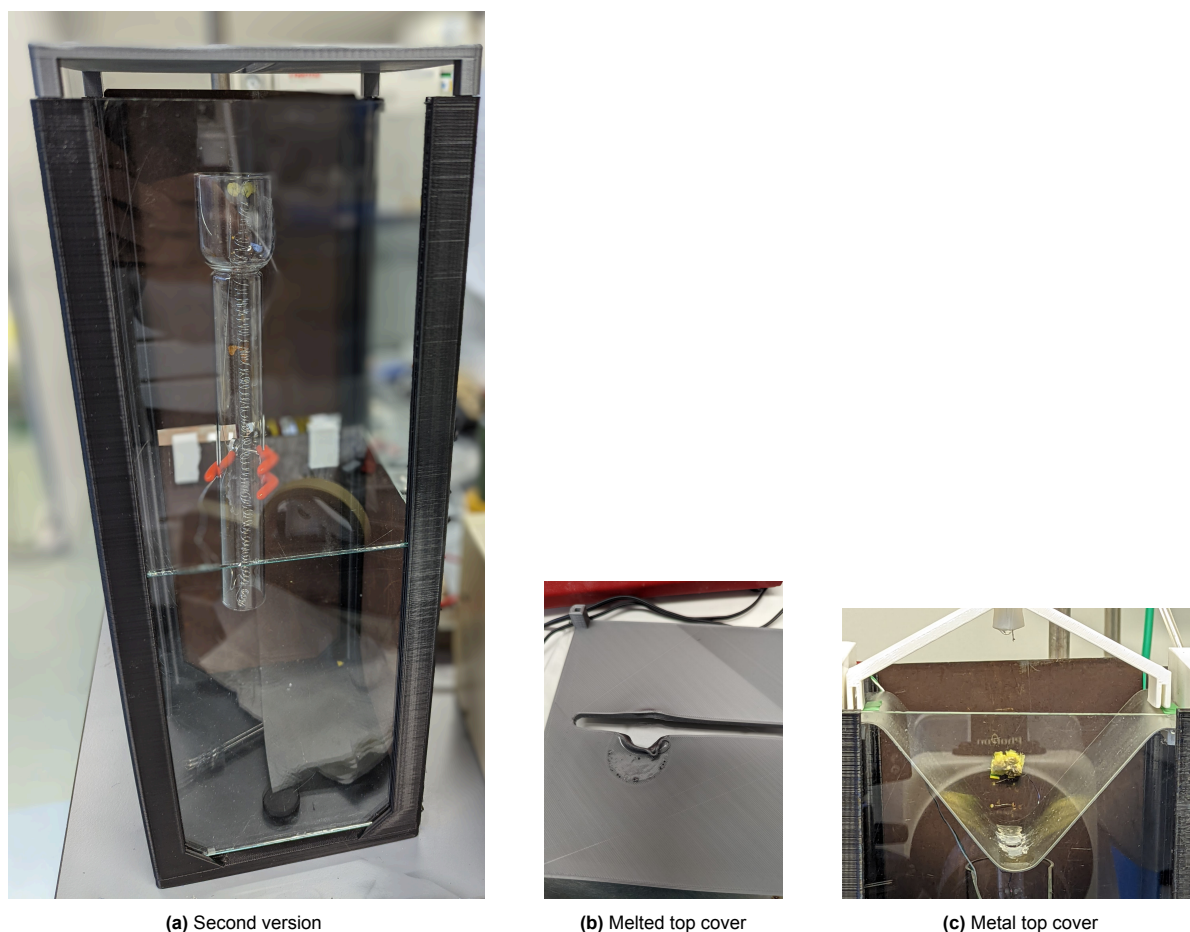


**Figure 5.4:** Second version of the safety chamber with the glass tube and the long heating coil. On top, a plastic lit is placed to reduce the heat dissipation.

### 5.3.1. Results and observations third iteration

First, the heating coil was heated using a single power source. However, a significant amount of voltage is needed due to the length of the coil, as is depicted in Figure 5.4a. The maximum power output of the power supply was 30 V with a current of 2.3 A. The temperature of the heating coil was not very high, which could be also observed by the naked eye since the heating coil was not glowing red. As a result, during experiments with water and hydrogen peroxide there were no signs of evaporation or decomposition.

The current has to rise in order to reach the requisite high temperature. Two power supplies were linked together in series to accomplish this. As a result, the heating coil began to glow red and the voltage and current could be increased to 40 V and 3.9 A, respectively. Tests with water showed that the drops were evaporating. This could be seen by the vapor and the condensation on the glass tube. The same experiment with hydrogen peroxide produced vapor and condensed on the glass tube once more, indicating that decomposition was taking place. More crucially, while the hydrogen peroxide was decomposing, a volume expansion took place and a distinct small explosion sound could be heard. Footage from the high-speed camera showed that the falling droplet was only hitting the first quarter of the heating coil. The droplet was not hitting the last three quarters of the heating coil, because the trajectory of the liquid droplet changed by hitting the heating coil at the beginning. As a result, the droplet splits into smaller drops at the first impact with the heating coil and then hits the side walls of the glass tube. The footage of this behaviour can be seen in Figure 5.5.

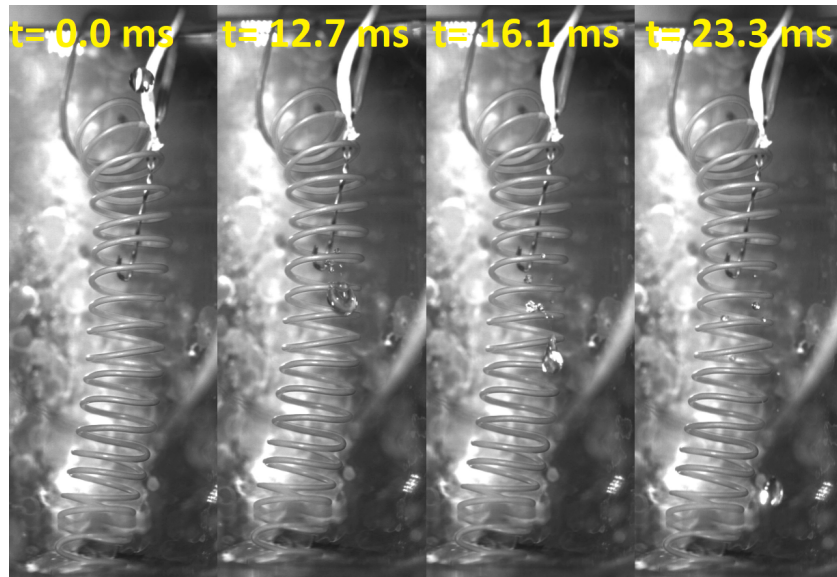


Figure 5.5: Exported frames from high-speed camera footage

To be able to hit the heating coil more often with the falling droplet, the heating coil has been bent. The coil is now also occupying the space close to the walls of the tube, see Figure 5.6. With this modification, also the total length of the heating coil was reduced since most of the length of the heating coil was not used anyways. This resulted in a lower voltage, while still maintaining the same current level. Consequently, the second power source was taken out and only one power supply was used for the tests.



Figure 5.6: Curled heating coil inside the glass tube, to have more space covered with it.

This small change resulted in louder and multiple explosion sounds of the decomposition of hydrogen peroxide that took place. With the high-speed camera footage, it was clearly visible that droplets were exploding into smaller droplets because of decomposition. Additionally, droplets that stuck to the hot glass wall made decomposition obvious. It was decomposing as a result of the heat transmission, and the process resembled boiling water.

### 5.3.2. Conclusion third iteration

With the third test set-up, the required amount of electrical power was very high. With the long heating coil, used at the beginning, two power supplies were connected in series with a power consumption

of 125 W. With the bent heating coil, the total length of the coil was also reduced which resulted in a power consumption of about 100 W. While the reduction in electrical power consumption is in the good direction, the power consumption needs to be reduced further to reach the target power consumption discussed in Section 1.2.

To further reduce the power, the next step will be to further reduce the length of the heating coil. Another step that can be taken is to use a (glass) tube that has a smaller diameter. This will first of all reduce the volume that needs to be heated up and as a result, less heat will be lost to the environment. Secondly, the heating coil can occupy more area of the tube which will increase the chance of the droplet impacting the heating coil.

## 5.4. Iteration 4: Shorter heating coil and smaller tube

Smaller glass tubes were not available at the chemical laboratory of the Aerospace faculty. Instead glass bottles, in different sizes were available for use. Three different glass bottles were selected for the initial tests of which the dimensions can be found in Table 5.2. Some modifications are made to the glass bottles to make them suitable for the test set-up. Details about the modification will be provided later in this section.

**Table 5.2:** Dimensions of the three glass bottles.

Glass bottle	Diameter	Length
Short small bottle	28 mm	46 mm
Long small bottle	28 mm	73 mm
Big bottle	44 mm	52 mm

### 5.4.1. Set-up fourth iteration

A glass tube like open end will be cut out of the bottom portion of the glass bottle. This will allow the liquids injected from the top side to fall down out of the glass tube. In the event of decomposition, this open end will prevent pressure build-up inside the glass tube. Secondly, holes at the sides of the glass bottle need to be drilled. The holes will allow to place the heating coil. The ends of the heating coil will be sticking out of those drilled holes to be able to connect it to the power supply, instead of extending the heating coil till the end of the glass tube, as it was done with the previous iterations.

Several methods have been tried to cut and drill the glass. Most of those methods either broke the glass or bend the glass into unusable shapes because of the high temperatures involved in it. In the end, a rotary tool was used in combination with a diamond drill bit and a diamond cutting disc. Using about 15000 RPM with the rotary tool and submerging the glass bottle under water during the drilling and cutting of the glass for cooling purposes provided the best results.

After the bottom part of the glass bottle had been cut off and two holes were drilled in the glass. The heating coil was wound and placed inside the glass tube, with the ends of the coil sticking out of the two holes that were previously drilled. In Figure 5.7 the glass tube with the heating coil connected to the power supply for a short test can be seen.

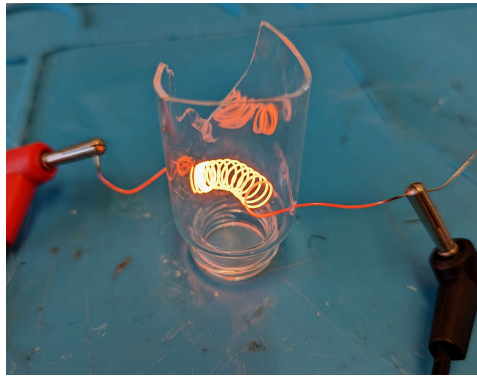


**Figure 5.7:** Testing the heating coil with the new glass tube. A part of the glass is broken, since the process of cutting and drilling the glass was still not optimized at this moment of time.

### 5.4.2. Results and observations fourth iteration

After the glass tube has been clamped to the test set-up from the previous iterations, first tests with water have been performed to check the alignment of the set-up. Afterwards the water was replaced by hydrogen peroxide. Although no high-speed camera was used to see in slow motion how the droplet was interacting with the heating coil, it was clear that the hydrogen peroxide droplet was not decomposing with this set-up, since it did not make the familiar exploding sound and no vapor or condensation on the glass walls was visible. The droplet was split into multiple smaller droplets after hitting the heating coil and exited the glass tube from the bottom of the glass tube as it can be seen in Figure 5.8. It can be concluded that again the residence time of the droplet on the heating coil was not sufficient and this needs to be increased to have a decomposition of the droplet of hydrogen peroxide. With the previous iterations, it was proven that increasing the length of the coil, will increase the chance of a droplet hitting the coil (multiple) times and resulting in decomposition.

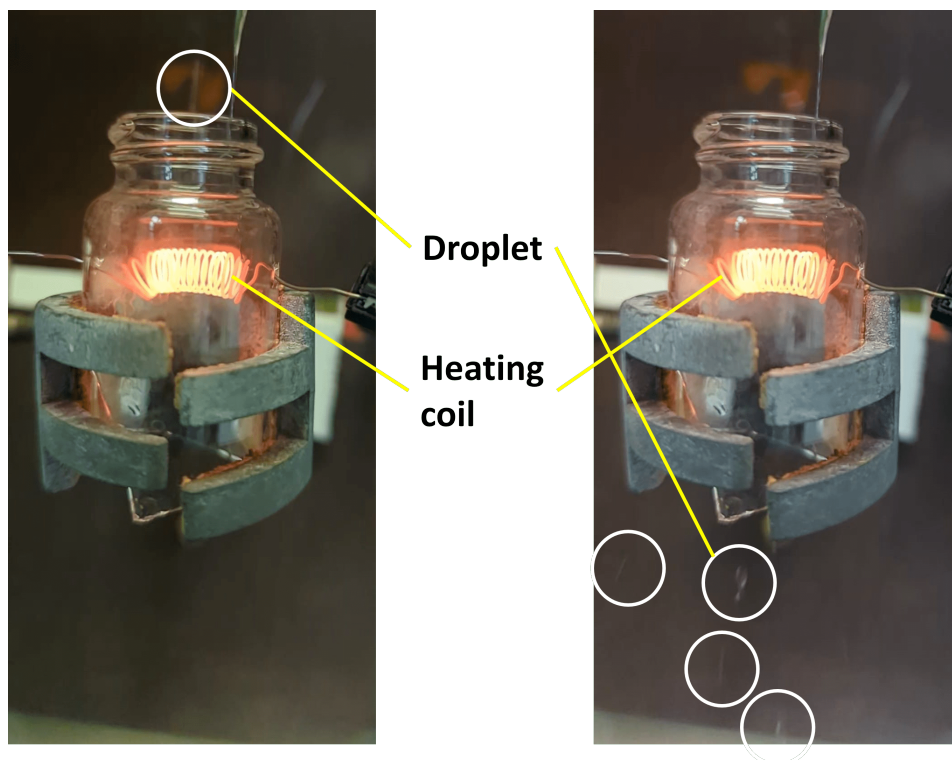


**Figure 5.8:** Droplet of hydrogen peroxide falling on heating coil and split into multiple smaller droplets before exiting the glass tube.

## 5.5. Iteration 5: Adding multiple layers

Instead of increasing the length of the heating coil inside the combustion chamber by bending it, more holes were drilled at the sides of the glass combustion chamber. This will allow to have multiple wound layers of heating coil. The heating coil, at each layer, has been rotated with about  $90^\circ$  on its plane. This results in more area covered with the heating coil and as a result will also increase the chance of hitting the droplet (multiple times). The glass combustion chamber with the three layers of heating coil is shown in Figure 5.9 below.

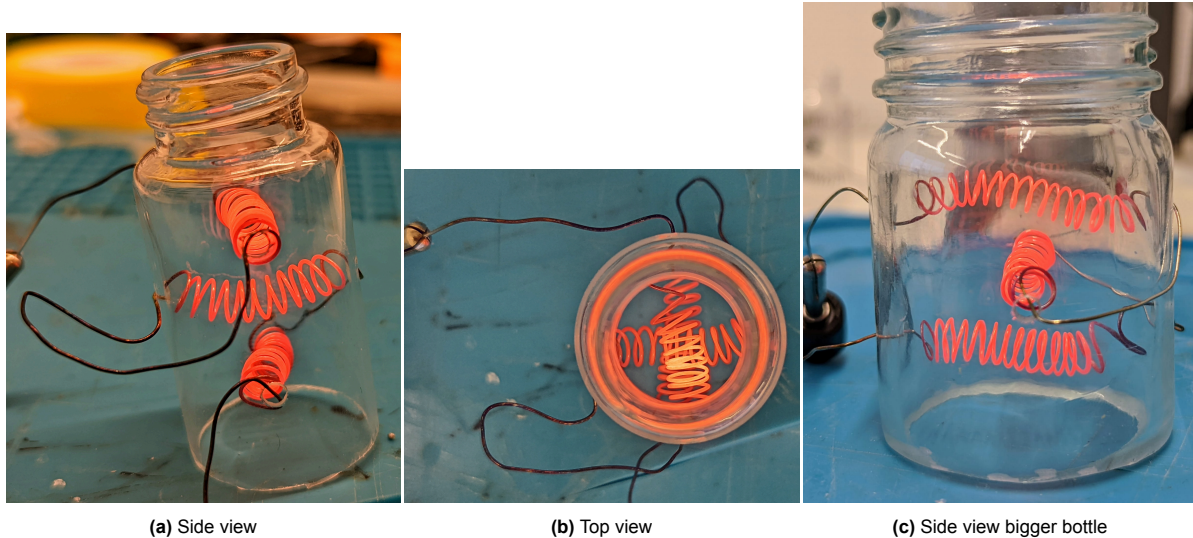


**Figure 5.9:** Side and top view of the glass bottle with the three layers of heating coil.

### 5.5.1. Results and observations fifth iteration

From tests with (high-speed) camera, it can be concluded that with this set-up the droplets are hitting the heating coil multiple times the majority of the time, but occasionally it happens that the droplet after hitting the first layer of heating coil gets directed in such an angle that it misses the other two layers of heating coil. Depending on the trajectory of the droplet, it either hits the wall or it falls through the outlet of the combustion chamber. Droplets that were hitting the other layers of heating coil and/or the glass wall do decompose. The familiar exploding sound, vapor and boiling of the liquid at the glass wall serve as indicators for this decomposition process. The boiling of the small droplets can be clearly seen in the footage of the high-speed camera. In Figure 5.10 some frames have been taken from this slow motion recording, to show how the droplet is hitting the heating coil and how the droplet is boiling on the wall at the left bottom from  $t = 17.97 \text{ ms}$  onward. However, the boiling and the other phenomena is not as clear as the running video compared to the exported frames in Figure 5.10.



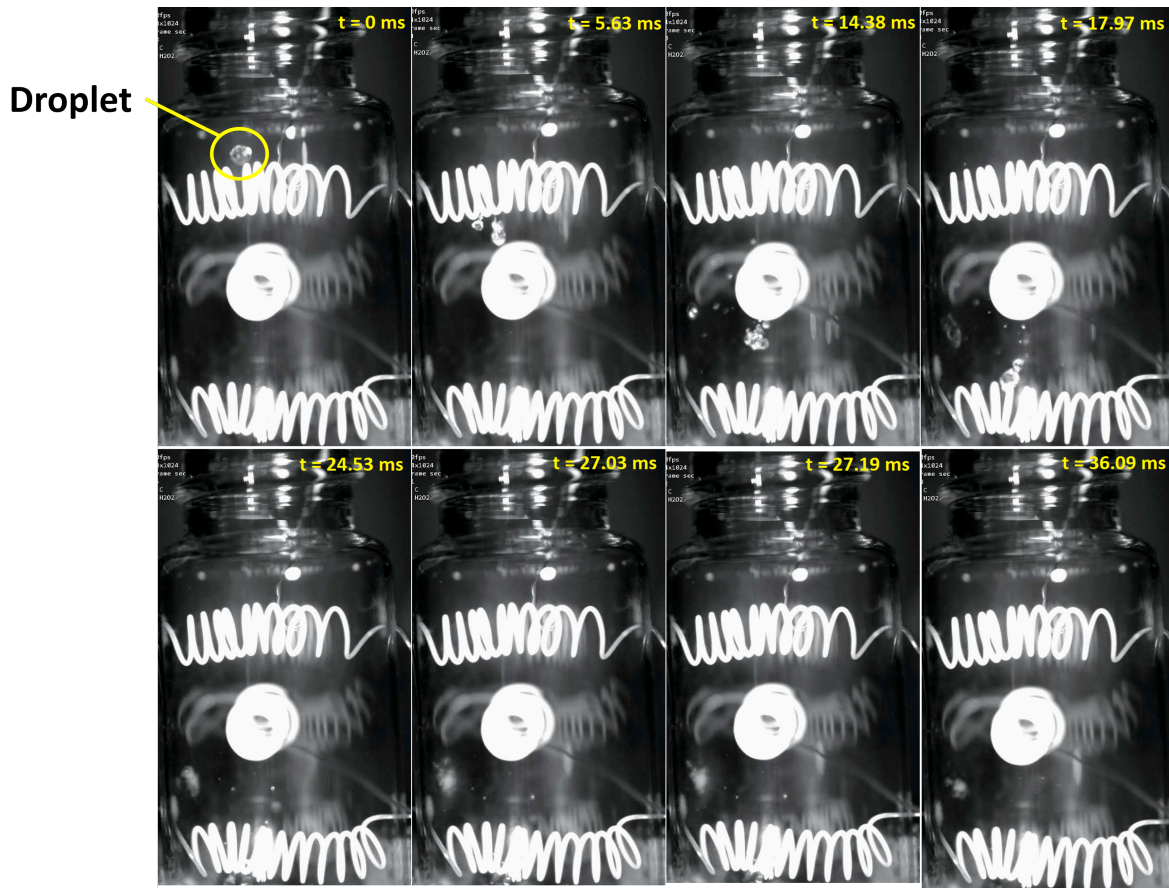


**Figure 5.10:** Exported still frames from high-speed camera footage. Hydrogen peroxide concentration is 95% and the current used from the power supply is 4.02 A.

The same tests were also performed with the bigger glass bottle, which can be seen in Figure 5.9c. Since this bottle has thicker glass walls it was assumed that it would keep the heat better trapped and the heat loss through the walls will be reduced. However, after performing some experiments with this bottle, the conclusion was that because of the higher inner volume and the bigger openings at the top and bottom the heat loss is significantly higher. As a result, unlike with the smaller bottle, the drops were not decomposing. The bigger bottle was abandoned, and further experiments only involved the smaller bottle. The small bottle has two length sizes available. To make the clamping easier and to have more space to place the heating coil, it was decided to continue with the longer version of the small bottle. The exact dimensions of this bottle can be found in Table 5.2.

## 5.6. Iteration 6: Decreasing the volume of the droplets

To increase the temperature of the liquid, two possibilities do exist. The residence time can be increased as discussed during the previous iterations. Increasing the residence time of the droplet on the heating coil, will increase the temperature of the droplet. However, to increase the residence more area needs to be covered with the heating coil, which results in the use of a longer heating coil. This is undesirable since increasing the length of the heating coil will result in increased electrical power consumption.

The second possibility is to reduce the volume of the droplet. By decreasing the volume of the droplet, less mass needs to be heated up which will result in less energy being required. Currently, a needle is used to produce small droplets. To have smaller droplets alternative methods should be investigated. Due to the safety standards within the chemical laboratory, pressurized systems should not be used in procedures to minimize droplet size.

One possible method to reduce the droplet volume is by atomizing the liquid with a piezoelectric disc. The piezoelectric actuator, in Figure 5.11 it is called PZT, will vibrate at very high frequencies of about 113 kHz [30]. The metal plate to which the PZT is attached will also vibrate with the PZT. In the middle of this metal plate, there is a mesh. The liquid on top of this mesh is not able to go through the small holes of the mesh when no power is applied. When the disc starts vibrating small amounts of energy will be released into the liquid, which breaks the surface tension and results in small droplets that go through the mesh and are ejected at the other end of the piezoelectric disc [31]. These atomized liquid drops have a very small and consistent droplet size, like a mist. A second method to reduce the droplet volume is by impinging the liquid. This method will be further elaborated in Section 5.8.

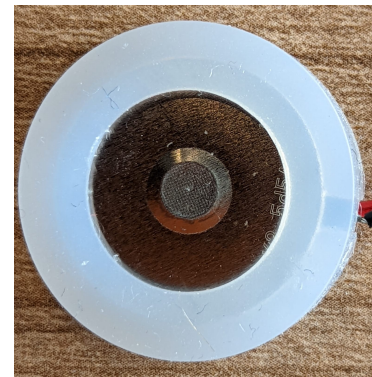
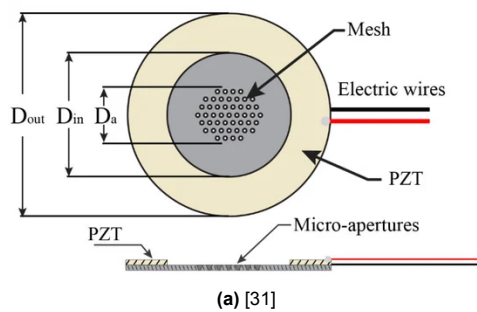
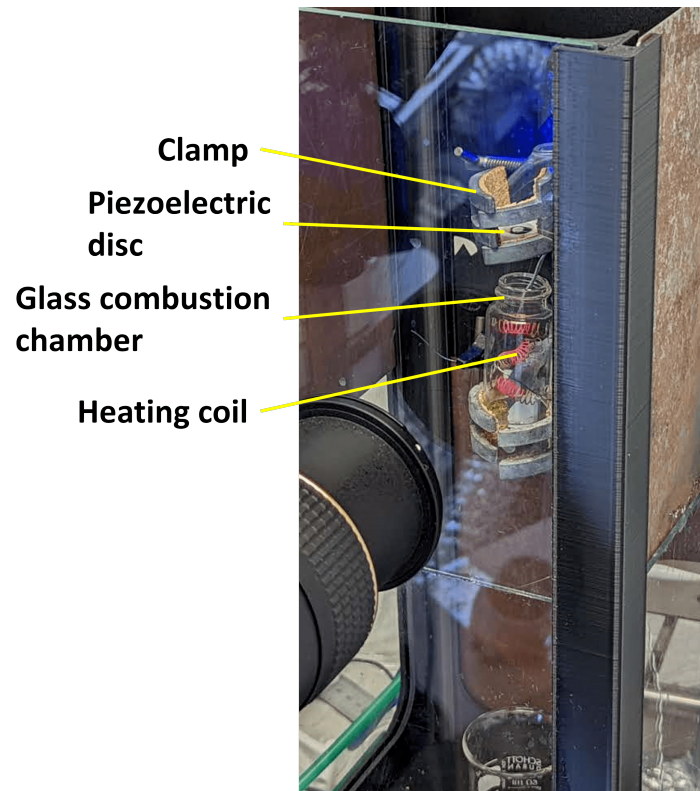


Figure 5.11: Schematic and picture of piezoelectric disc

One of the main advantages of the piezoelectric disc is that it produces very fine droplets with an average diameter of  $10 \mu\text{m}$  [32]. This reduces the volume per droplet significantly and as a result, the surface area to volume ratio increases. This would require less energy to heat up the droplet and decompose the hydrogen peroxide. The flow rate of a piezoelectric disc is also very low, with  $0.025 \text{ mL/s}$ . This will also require less energy from the heating coil and as a result, reduce the power consumption of the total system.

### 5.6.1. Set-up sixth iteration

The required changes to the set-up are minimal. The piezoelectric disc needs to be placed between the needle and the glass combustion chamber. Which is an additional safety benefit, since this allows the syringe with the needle to be placed higher up further away from the heat source. Only the piezoelectric disc with a small amount of hydrogen peroxide will be in close approximation to the heating coil. The new set-up can be seen in Figure 5.12.



**Figure 5.12:** Set-up with the piezoelectric disc. The syringe and needle are above the piezoelectric disc, outside the frame of this picture.

### 5.6.2. First tests with water

A few tests with water were conducted first before moving on to the hydrogen peroxide experiment. Similar to the earlier experiments, this one aims to determine whether the setup is functioning as intended, whether the alignment is accurate, and whether any unforeseen safety issues exist.

After the first couple of tests, it could be observed that the atomized water was hovering just above the ground and escaping from the small gaps between the base of the 3D-printed protection and the safety glass. The atomized liquid that escapes from the small gaps is potentially a safety problem, and it can also damage the (electronic) equipment right next to the set-up.

### 5.6.3. Updated safety chamber design

A third version of the 3D-printed safety chamber has been created to improve safety and lower the possibility of harming the equipment. In the new version, the borders of the base have been elevated and a slit has been made in to this raised edge. The safety glass and metal plate will now slide into this slit and no gap will be left open at the bottom. The liquid and gas will be prevented from leaking from the bottom area by this new design. Figure 5.13 depicts the updated design.

By performing some droplet tests with water, it was confirmed that the water in neither liquid phase nor the gaseous phase was able to escape from the bottom part of the safety chamber.



**Figure 5.13:** Third version of the safety chamber. Compared to the previous version, the bottom part has been raised.

#### 5.6.4. Results and observations sixth iteration

The surface area has grown as a result of atomization, whereas the volume of each drop has greatly decreased. Since there was decomposition happening with the previous iteration, it was expected that in this case with the smaller drops and the more even distribution over the heating coil it would result in better decomposition.

After the first couple of iterations, it was clearly observable that the heating coil was immediately cooling down when the atomized droplets were hitting the heating coil. The same results were obtained after more tests. Figure 5.14 provides four frames of a video made during the experimentation. The first frame, at  $t = 0$  s is from the moment right before the mist of atomized liquid was generated. In the second frame, the first layer of the heating coil has significantly cooled down. While for the third frame also, the second layer of the heating coil has significantly cooled down. The last frame is the moment right before the atomized liquid droplets stopped. In this shot, the first as well as the second shot are not glowing red at all anymore. Even the third layer has cooled down. The handheld thermometer that was hooked to the first layer of the heating coil, was confirming the observations by showing temperature drops of more than  $200$  °C.



**Figure 5.14:** Different frames have been taken from a video, which shows how the heating coil is cooling when being in contact with the atomized liquid.

When increasing the distance between the piezoelectric disc and the inlet of the glass combustion chamber, the generated atomized liquid, is not going through the inlet. This is partly due to the spray angle, the further the distance becomes the more the atomized liquid is spread out. The heat that is generated inside the combustion chamber is raising upwards and making it more difficult for the atomized liquid to enter the combustion chamber. Instead, the atomized liquid is redirected to the sides of the atomized liquid is carried upwards by the heated bubble of air. Which resulted in only a small amount of the atomized liquid hitting the heating coil. Bringing the piezoelectric disc closer to the inlet of the combustion chamber, like in Figure 5.14, was also not altering the results.

Other observations that could be made from the experiments were that the droplets were so small and light that it was behaving like aerosols. This resulted that a part of the droplets was floating in the air and following (partly) the air currents. This was especially the case, nearby a heating element like the heating coil. In this case, the small droplets would even move upward together with the heated air.

The rubber cover around the piezoelectric disc started to catch fire at some point and burned down until a white powder was left. The first hypothesis was that the incompatibility of the rubber with hydrogen peroxide was the cause of this. Since it has already been established that Acrylonitrile butadiene styrene (ABS) plastic is compatible with hydrogen peroxide, a ring made of ABS plastic has been designed and printed using a 3D printer. However, after a while of experimentation, the 3D-printed ABS cover started to catch fire as well.



(a) Rubber ring



(b) ABS ring

**Figure 5.15:** Burned rubber ring and ABS cover

At the same time, two separate experiments were performed with the rubber ring. The first experi-

ment was to check compatibility with hydrogen peroxide, by submerging the rubber in a bath with high concentration of hydrogen peroxide for a couple of days. The second experiment was to heat up the rubber ring with a torch blower and see whether it melts or catches fire. The first experiment showed that the rubber ring was compatible with hydrogen peroxide since there was no reaction happening during a period of three days. The second experiment showed that it catches fire when heated up to about  $700^{\circ} C$ . Those two small experiments showed that the rubber ring required additional thermal protection to prevent it from catching fire.

Since the ABS printed ring was also catching fire. It was decided to continue the experiments with the rubber ring. To prevent the rubber ring to catch fire, additional measurements were taken. Radiant barrier foil was used and a metal plate. The foil was wrapped around the metal plate and a hole was drilled through it. By placing the plate between the piezoelectric disc and the glass bottle, the atomized liquid generated could go through the hole but the heat and the hot gasses would be partly blocked. With the first couple of tries, the rubber ring caught fire again and required a different method to prevent it from catching fire.

A second attempt to thermally protect the rubber ring was to put aluminium tape directly on the rubber ring itself. The tape will be resistant to high temperatures and will be reflecting the heat coming from the heating coil. After repeated tests, it could be concluded that this solution was indeed working.

### 5.6.5. Conclusion sixth iteration

The piezoelectric disc is providing a nice evenly distributed small droplets. However, it cools down the heating coil too much to make the droplets decompose. Changing the distance between the inlet of the combustion chamber and the piezoelectric disc did not improve the decomposition of hydrogen peroxide. However, when getting too close to the combustion chamber, the rubber as well as the ABS ring get too hot and catch fire. This was later during the experimentation solved by making use of an aluminium tape on the rubber ring.

The atomized liquid generated from the piezoelectric disc was still cooling down the heating coil and as a result it was preventing it from decomposing. For the next iteration, the goal is to keep the heat better trapped within the combustion chamber, so that the generated atomized liquid will be decomposing instead of cooling the whole system down.

## 5.7. Iteration 7: Horizontal set-up with fan

Since hot air is raising and together with the raising air also a part of the atomized liquid generated from the piezoelectric disc is carried away from the combustion chamber. Instead of placing the combustion chamber vertically, it can be also placed horizontally. With this set-up, the inlet and the outlet of the combustion chamber will be on the sides and the heat will not be able to escape as quickly as with the vertical set-up. An additional benefit of the horizontal set-up is that the piezoelectric disc is not directly exposed to the hot gas, which was the case for the vertical set-up. This could potentially also reduce the risk of potential fires of the rubber ring around the piezoelectric disc.

However, by placing the combustion chamber horizontally the atomized liquid generated from the piezoelectric disc would also be directed through the combustion chamber horizontally. Placing the piezoelectric disc vertically right in front of the inlet, so that the atomized liquid is directly injected inside will make it difficult to put the liquid on the piezoelectric disc since it will glide off the piezoelectric disc and no fluid will be left that the piezoelectric disc can inject to the side facing the combustion chamber. To counteract this problem, it was preferred to place the piezoelectric disc horizontally, but the atomized liquid generated from it is guided to the horizontally placed combustion chamber. A new design was made and printed with a 3D-printer, which can be seen in Figure 5.16. With this set-up, the piezoelectric disc is placed horizontally, which allows to place some liquid on top of it and it will inject the atomized liquid at the other side. The fan, which is placed inside the 3D-printed converging nozzle, is blowing air towards the inlet of the combustion chamber. The airflow will push the atomized liquid from

the piezoelectric disc also to the combustion chamber.

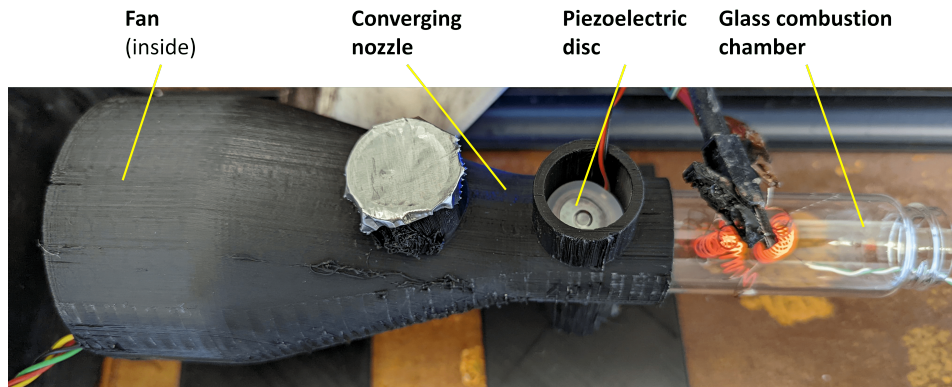


**Figure 5.16:** Horizontal set-up with the fan. The fan is inside the converging nozzle at the left side and blowing air to the right through the glass bottle.

### 5.7.1. Results and observations seventh iteration

The fan speed was adjustable, which allowed to perform the tests with various fan speeds and see how it influences the results. With the lowest setting of the fan, the air blowing was still significantly cooling down the heating coil. Like in the previous iterations, the cooling could be observed by the naked eye since the glowing red color of the heating coil was reducing significantly.

The cooling of the heating coil also prevented the injected hydrogen peroxide to decompose. Different distances of the heating coil and higher electrical power levels were used to observe whether hydrogen peroxide would decompose. In all cases, the airflow caused by the fan was cooling the heating coil too much to decompose hydrogen peroxide. Another problem that was occurring with this design, was because of the converging nozzle shape, some of the injected liquids were rolling back to the side of the fan and not reaching the glass combustion chamber at all. This was even more the case, with lower fan speeds.

This set-up was clearly not working as intended. The only advantage of this set-up was that the piezoelectric disc was significantly cooler and as a result, no piezoelectric discs burned during all the runs of this iteration.

## 5.8. Iteration 8: Impinging method

After concluding that the piezoelectric disc and the fan are cooling down the heating coil too much, other approaches without the piezoelectric disc were sought. The liquid drop from the syringe should be split into smaller droplets. To achieve those smaller droplets, the impinging method was selected for future investigation.

The impinging method typically involves two (or more) streams of liquid impinging on one another. When the two streams collide, the liquid will atomize. However, this will require a relatively high amount of mass flow and two liquid streams of hydrogen peroxide that are impinging. This high mass flow will be beyond the boundaries of this research. Secondly, this could create an unsafe environment in the laboratory with the current set-up and safety measures.

To still make the liquid atomize, two streams of gaseous nitrogen will be impinging and in the middle droplets of hydrogen peroxide will be passing through. The impinging of the two nitrogen streams will make the liquid atomize. However, this adds additional flows of nitrogen (or air) into the system, which will be also reducing the temperature of the heating coil. Since the mass flow of the liquid (that needs to be atomized) is very low, the required amount of gaseous nitrogen will be also low and it is expected that this small amount of nitrogen will not cool the heating coil significantly and decomposition will be

achieved.

### 5.8.1. Set-up eight iteration

Different 3D-designs were made, and with each new design small improvements were realized. For the first design, a trapezoidal shape was made with three lines going through the whole length of the trapezoid. The two lines at the side had an angle of  $30^\circ$ , the line in the middle is vertical. The syringe was placed in the middle and the two outer lines were made for the nitrogen. Because of the angle of the two outer lines, the nitrogen will impinge at the middle just outside the trapezoid shape. This can be also seen in Figure 5.17a. The dotted lines show the lines inside the trapezoidal shape. However, impinging outside was not providing small and consistent droplets. For the next design iteration, the impinging of both nitrogen lines is done inside the design itself as it can be seen in Figure 5.17b, with a cross-section in Figure 5.17d. This updated design was providing smaller droplets compared to the first design, however the angle at which the liquid droplets are ejected are not very consistent. For the final design, which can be seen in Figure 5.17c, the distance of the middle part has been reduced. This puts the needle of the syringe close to the crossing with the nitrogen and results in a better spray cone angle. The cross-sectional design of the bottom part can be seen in Figure 5.17d. The vertical line, in this figure is the place for the syringe, while the two other lines are for the nitrogen supply. All of it will collide inside the small chamber, before leaving at the bottom from the small opening.

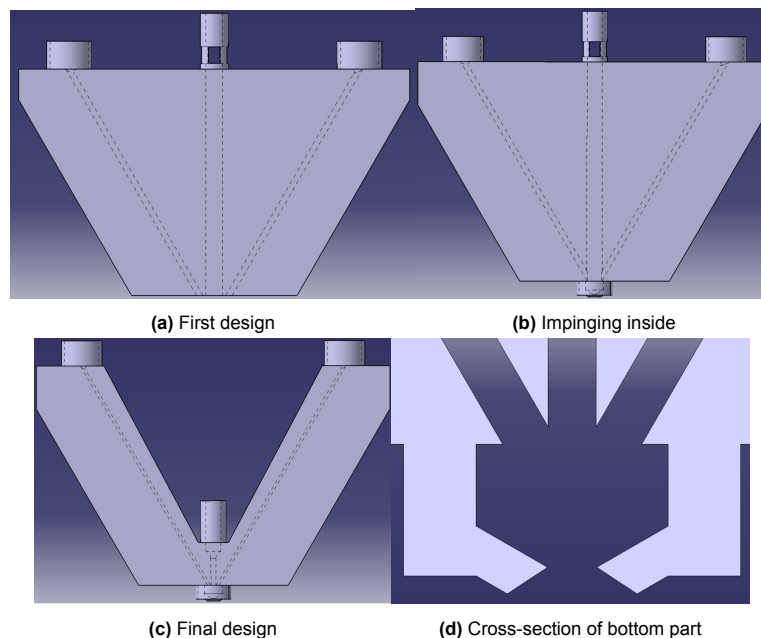


**Figure 5.17:** Three major design changes of the atomizer of the impinging method and the cross-section.

### 5.8.2. Results and observations eighth iteration

The improvements of the spray cone angle over each design iteration can be seen in Figure 5.18. In this figure, a spray test was performed with tap water and without any heat addition to the system. With the later designs, the droplet size decreased significantly and the droplet was more consistent and evenly distributed. Also, the spray cone angle was more stable and consistent in the later design iterations.

With hydrogen peroxide the atomization was not as good as it was with water. Although small droplets were achieved, the drops were also sticking at the edge of the nozzle and influencing other droplets that are expelled out of the nozzle. When the power supply was turned on, and the heat was generated from the heating coil, it was clear that some pressure was occurring due to the fact that more force was required to push the fluid out of the syringe.



A second observation about this set-up was that even a minimum amount of nitrogen required to have the good spray angle, was too much for the heating coil to maintain the high temperature. The nitrogen resulted in significant cooling of the heating coil as it was the case with the piezoelectric disc.

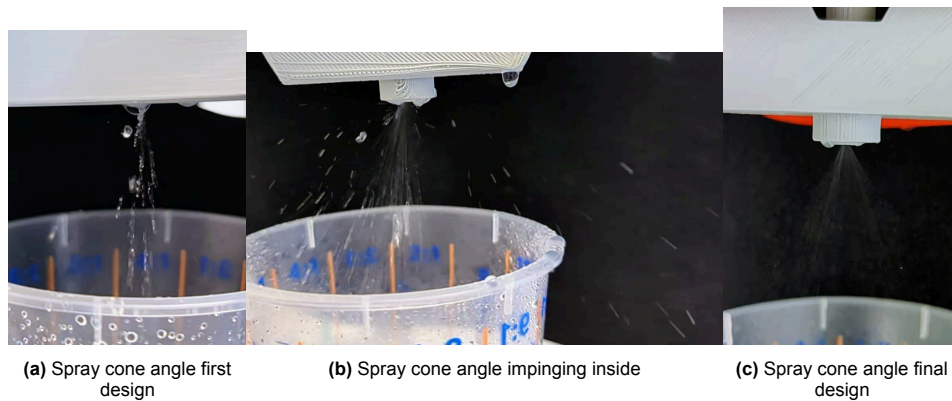


**Figure 5.18:** Spray cone angle with water (and without heat) of the three major versions.

### 5.8.3. Conclusion eighth iteration

The impinging technique produced water droplets that were steady in size and spray cone angle. The spraying was less stable and constant after switching from water to hydrogen peroxide and adding heat to the system. Even with the lowest amount of mass flow of nitrogen to get small droplets was cooling down the heating coil too much to have a proper decomposition of hydrogen peroxide. Both the piezoelectric disc and the impinging method cooling of the heating coil were a problem. It was decided to carry on with the piezoelectric disc, since that method was providing finer droplets with a lower mass flow.

## 5.9. Iteration 9: Hydrogen peroxide and Ethanol combination

Placing the piezoelectric disc very close to the heating coil, will make the rubber ring around the piezoelectric disc catch fire. However, when the set-up is placed horizontally the piezoelectric disc is not exposed to as much heat as it was the case for the vertical set-up. This small change made the rubber ring less likely to catch fire, as it was the case with iteration seventh. However, instead of making use of a fan, it was decided to place the piezoelectric disc in front of the inlet of the combustion chamber.

Two piezoelectric discs would be used for the set-up. One of the piezoelectric discs will be used to inject hydrogen peroxide, while the other will be used to inject ethanol in to the combustion chamber. To hold the two piezoelectric discs and the combustion chamber in place, Y-shaped splitter design was made. This Y-shaped splitter acts as an injector head. The design, which can be seen in Figure 5.19, allows to place two piezoelectric discs at one end. Both will inject the liquid on top to the other side, where the glass combustion chamber is placed. As a result, the atomized liquid will be directly injected inside the combustion chamber.

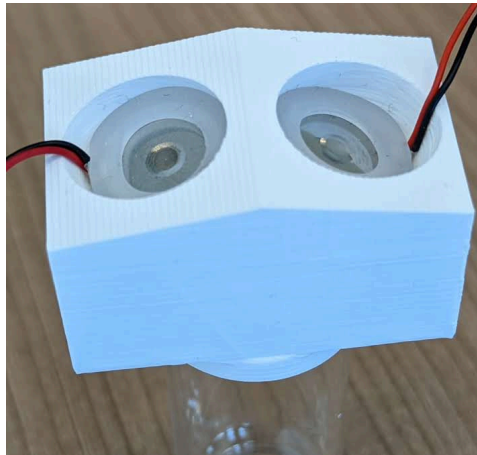


**Figure 5.19:** The splitter allows to place two piezoelectric discs on one side, which injects the liquids on the other side where the glass bottle is placed.

### 5.9.1. Set-up ninth iteration

For this iteration, most of the set-up that was made for the seventh iteration could be reused for this set-up. The converging nozzle, together with the fan, was replaced with the 3D printed splitter. The combustion chamber together with the splitter has been fixed in place with a clamp. Before using two separate piezoelectric discs, first a couple of experiments were performed with a mixture of hydrogen peroxide and ethanol. This mixture was injected with only one piezoelectric disc. During this experiment, one of the holes of the injector head was closed with aluminium tape, to prevent the atomized (hot) liquid escaping from the second hole that was made for the second piezoelectric disc.

### 5.9.2. Results and Observations fuel and oxidizer mixture

Different mixture ratios of ethanol and 88% concentration hydrogen peroxide were used during the experiments. Since it is not yet known how this mixture will behave and react when heat is introduced. For the first couple of experiments, it was decided to have a higher mixture ratio of ethanol instead of hydrogen peroxide. This ratio was step-by-step reduced from 100 *w%* ethanol to 15 *w%* ethanol. During all the experiments, the current going through the heating coil was kept fixed at 4 A.

The first tests were performed with only ethanol, to have an understanding of how ethanol combusts with atmospheric oxygen. This will also allow to compare the combustion and flame of pure ethanol to the different mixture ratios with hydrogen peroxide. When injecting pure ethanol, a very small fire around the hot heating coil occurs and shortly afterwards a flame occurs at the outlet of the combustion chamber. Probably the ethanol is in this case reacting with the atmospheric oxygen that is around the combustion chamber.

The amount of hydrogen peroxide was afterwards increased in steps. With 80% mass ratio ethanol and the other 20% with hydrogen peroxide. The behaviour of the mixture was very comparable to the case with pure ethanol.

However, increasing the mass ratio of hydrogen peroxide to 40%, resulted in a change in the initial behaviour. The first combustion was very short and it seemed like that ethanol was reacting with either the atmospheric oxygen inside the combustion chamber or with the decomposed hydrogen peroxide. The flame was filling the whole volume between the piezoelectric disc and the heating coil. However, this combustion stops soon after and a normal flame at the outlet of the combustion chamber becomes visible. This again shows a weak unstable flame, which means that it is a fuel rich flame. It is probably because the hot ethanol is reacting with the atmospheric oxygen around the combustion chamber. This behaviour can be also seen in Figure 5.20.

Increasing the mass ratio of the mixture to even higher ratios of hydrogen peroxide to 50% was

providing about the same results. However, increasing the hydrogen peroxide ratio to even higher amounts, was only resulting in cooling of the heating coil and no ignition nor flame was observable.



**Figure 5.20:** Combustion of pure ethanol with atmospheric oxygen

To have more oxygen in the mixture, more hydrogen peroxide was added to the mixture. Now the ratio was 50% of ethanol and 50% of hydrogen peroxide. Even in this case, the combustion behaviour was very similar to the case with 60% ethanol. First an initial, very short, flame occurred which quickly extinguished. Afterwards, only a weak unstable flame occurred at the end of the combustion chamber. From the behaviour of the flame, it can be again concluded that it is a fuel rich combustion, which possibly means that the hydrogen peroxide is not (properly) decomposing and the hot ethanol is mainly reacting with the atmospheric oxygen that is around the combustion chamber.

Afterwards the hydrogen peroxide in the mixture has been increased even more to 80%. With this ratio, the heating coil was clearly getting hotter, which is observed by the change in the redness of the coil. But there was no visible flame observable.

To reduce the heat dissipation from the back side of the glass test tube, a glass was used of which the bottom part was not cut off. Only small holes were drilled to avoid the risk of having high pressure build up within the system. With the closed glass set-up, first pure ethanol was injected with the piezoelectric disc. Inside the combustion chamber, an initial flame appeared. After a short time, this flame was getting weaker until it completely extinguished. This is probably caused by the fact that the atmospheric oxygen inside the glass tube was consumed during the initial flame. Adding hydrogen peroxide to the ethanol mixture, was providing very similar results as the experiment with pure ethanol. An initial flame starts, which quickly extinguishes. Increasing the hydrogen peroxide ratio step-by-step until a ratio of 80% hydrogen peroxide and 20% ethanol, allowed to have a sustained combustion happening inside the glass combustion chamber. This was a clear sign, that in case the set-up is a closed system and there is no atmospheric oxygen, the ethanol is reacting with the decomposed hydrogen peroxide.

Some tests have been also performed with a combustion chamber where the heating coil is closer to the injector head. The results were very similar to the earlier experiments with the heating coil at a further distance from the injector head. The only problem with this set-up was, that the heat of the heating coil was melting the 3d-printed part and was not usable anymore in a couple of minutes. Because of this, it was decided to keep the heating coil further away from the inlet of the combustion chamber for the upcoming experiments.

### 5.9.3. Double injector set-up

A second injector was placed in the injector head. Instead of mixing the hydrogen peroxide and ethanol and injecting it from a single injector, the liquids will not be premixed. Instead, it will be injected separately and will be mixing in the combustion chamber itself. The downside of this set-up is that the flow rate of both the fuel and the oxidizer is fixed, since flow rate of the piezoelectric disc can not be adjusted. Compared to the premixed set-up, with this setup significantly better results were achieved. Although it is not possible to vary the injected amount of fuel and oxidizer, there was a combustion and a stable energetic flame which can be seen in Figure 5.21a. This shows that there was much more oxygen available for the ethanol to combust with. This is a clear sign that the hydrogen peroxide decomposed, which provided the additional oxygen in the reaction with ethanol. During the test, the glass combustion

chamber quickly showed cracks and shattered at the end of the experiment. See Figure 5.21b for the picture immediately after the test was finished. This could be caused by the thermal shock caused by the flame.

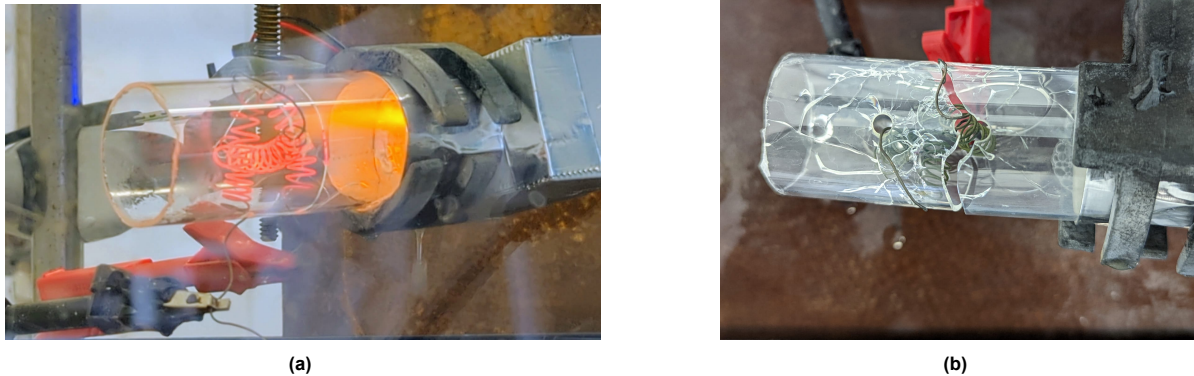


**Figure 5.21:** First successful test with double injector set-up and the shattered glass right after the test.

#### 5.9.4. Reduced power

Until now, three layers of heating coil were used for the ignition and combustion of hydrogen peroxide and ethanol. To reduce the power consumption further, the number of layers was first reduced to two layers. After achieving successful ignitions and combustions, the number of heating coil layers has been reduced to a single layer. With a single layer again successful ignition and combustion were achieved as it can be seen from Figure 5.22. Without any other changes, this reduced the power consumption to about 20 to 22 W, while still maintaining a current of 4 A.

To determine the lowest current at which still ignition is possible, the current was reduced stepwise. With the current set-up, no ignition was achieved with a current of 3 A and a power consumption of 12 W. Increasing the current with 0.25 A and a power consumption of 14 W, was the minimum where ignition and combustion was achieved.

At the 14 W power consumption, also an experiment was performed to turn off the power supply to the heating coil to see whether the combustion would continue to carry on without external power input. Since the experiment is performed within a laboratory environment and because of fire hazards the experiment can not be carried out for more than a couple of seconds. However, after the power supply was turned off after the combustion started, the fire continued for about 1 or 2 seconds until no propellant was left anymore inside the syringes.

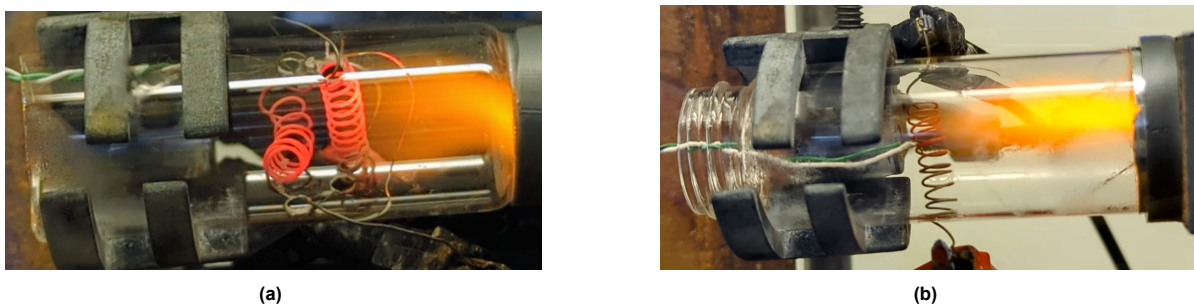
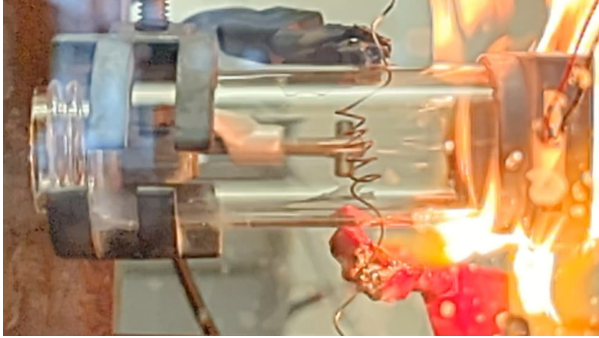


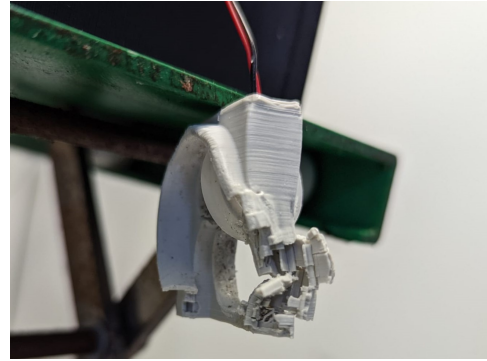
**Figure 5.22:** Successful ignition and combustion with 1 and 2 layers of heating coil.

The same experiments have been repeated with various hydrogen peroxide concentrations ranging from 88 % till 98.5%. The results with varying concentrations are very similar to each other, however

from 94 – 95% concentration and higher the 3D-printed injector head started to react with the decomposed hydrogen peroxide. Resulting in violent burning and exploding injector heads, which can be seen in Figure 5.23. Two different plastics were used for the injector head, PLA and ABS, and both resulted in same failures. For this reason, it was decided not to use concentrations higher than 90% after this incident to have a safe margin from the concentrations where the incidents happened.



(a) Hydrogen peroxide reacting with the plastic



(b) Injector head after the explosion

**Figure 5.23:** Failed experiments with 95 + % concentration hydrogen peroxide.

### 5.9.5. Conclusion ninth iteration

The 3D-printed injector head was proven to result in ignition and combustion of the propellant combination hydrogen peroxide and ethanol. This set-up will be used as the basis for the final experiments that will be performed. It was also confirmed that the distance of the heating coil from the inlet was not influencing the results significantly. Neither is the concentration of hydrogen peroxide of significant influence on the ignition and combustion of the propellant.

For the final set-up that will be performed in the future, the glass combustion chamber will be used the other way around. The current outlet will be used as the inlet and vice versa. This is because the current inlet has a smaller diameter and a thread pattern on the outside, which made it more difficult to have a tight fit of the injector head. Also, some changes will be made to the injector head itself. With the current design, the piezoelectric disc is pushed inside the holes. This is less stable, and small changes in the angle and position of the piezoelectric disc are inevitable. In the new design, the piezoelectric disc will slide into the injector head from the sides, which will provide a fixed angle and position. The final experimental set-up is discussed in detail in Chapter 3.

# 6

## Simulation of thermal igniter for rocket applications

A computer model of a thermal ignition system for a rocket engine application was built. This computer model will be a simplified digital representation of the experimental set-up that was built in the chemical laboratory. The data from the experimental set-up will be used to compare and validate the results obtained from the computer model.

For the simulations of the computer model, the software package COMSOL will be used. COMSOL is a cross-platform finite element analysis, solver and multiphysics simulation software. A desktop with a license for COMSOL 5.6 is provided by the Aerospace faculty of TU Delft to build the model and perform the simulations. The desktop has an eight year old Intel Core i5-4590 processor and uses the integrated graphics processor. The total internal memory of the desktop is 8 GB in a dual channel set-up.

For the computer model, some assumptions and simplifications have been made, which are discussed in Section 6.1. Furthermore, the geometry, including the dimensions, the mesh that is used and the initial- and boundary conditions that are used for the simulations will be discussed. Lastly, the results of the simulations will be discussed and a comparison of the simulations with the experimental set-up will be performed.

### 6.1. Simplifications & Assumptions

The computer model that has been developed during this thesis will serve as a foundation for future development. Because of time and hardware constraints instead of focusing on the decomposition and the chemical reactions that would happen, the focus of this simulation is to reach the auto-ignition temperature of ethanol, which is  $365\text{ }^{\circ}\text{C}$ . This will simplify the model, since no chemical reactions have to be modeled/simulated, however it will still provide information about whether ignition will happen by achieving a temperature that exceeds the auto-ignition temperature of ethanol. In the list below, a short explanation is provided for each simplification/assumption.

- **No atomized liquid**

In the experiments, a piezoelectric disc was used to produce a fine mist of atomized liquid. To reproduce this same fine atomized liquid in COMSOL, is very hard and beyond the scope of this Master's thesis. As a simplification, the liquid ethanol without any atomization has been used for the current simulations. The mass flow rates were the same as the mass flow rates achieved with the piezoelectric disc during the experiments.

- **Ignition assumption**

During the experiment a great number of chemical phenomena happened, which are related to the decomposition of hydrogen peroxide and reaction with ethanol. Modeling all this chemical phenomena/reaction will be very extensive and hard. The main focus of the simulation is to verify whether ignition will occur with a given electrical power to the heating coil. This can be also approached by determining what temperature the injected liquids will achieve. Since the auto ignition temperature, of ethanol, is known to be around  $365\text{ }^{\circ}\text{C}$ , it will be assumed that ignition followed by a combustion will happen. Although hydrogen peroxide will decompose, which will add additional heat to the system, this will be fairly limited since both the ethanol and hydrogen peroxide will be injected (almost) simultaneously. Which results in a limited build-up of decomposed hydrogen peroxide.

- **Injector head angle**

With the experimental set-up, two fluids are injected at a certain angle to improve the mixing of the liquids inside the combustion chamber. Since no simulations will be performed related to the chemical reactions of the fluids, there is no need to inject both liquids in the simulation since no chemical reaction will be simulated. Only using a single liquid, will also imply no mixing of the liquids will happen. As a result, the angle of the injector head is not of interest for the simulation. This will also reduce the complexity of the geometry and as a result, also the number of mesh elements.

## 6.2. Geometry & Mesh

As explained in the previous paragraph, compared to the experimental set-up the computational model will be simplified to a horizontal cylinder with an inlet on one side and an outlet on the other side. The total length of the cylinder is 70 mm, with a diameter of 28 mm. The dimensions are determined by the glass tubes that have been used as the combustion chamber for the experiments. The heating coil is placed at a distance of 30 mm from the inlet, which is similar to the distance that is used during the experiments. The diameter of the coil is set to 0.5106 mm, which is the diameter of a 24 AWG wire. In Figure 6.1 the geometry of the combustion chamber together with the heating coil is shown.

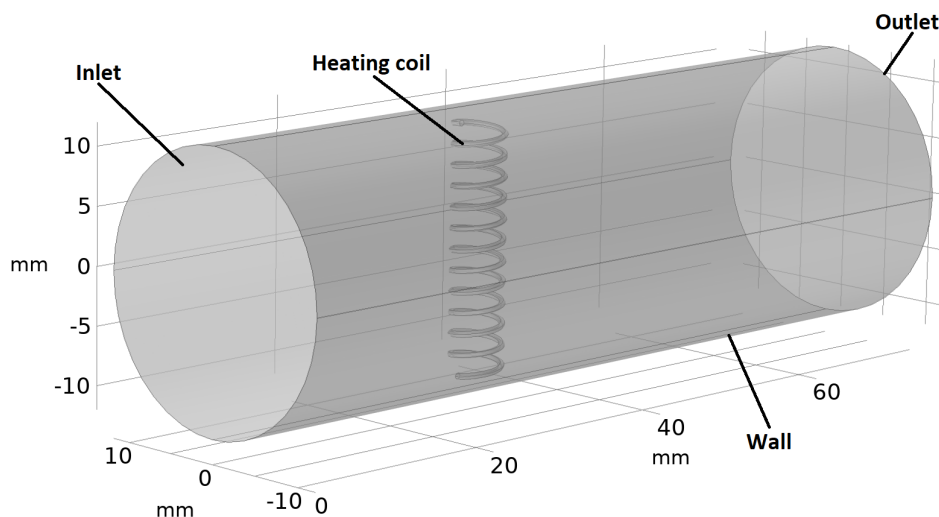


Figure 6.1: Geometry of computational model

The mesh generation is done with the automatic settings of COMSOL. This automatic setting is a physics-controlled mesh. Depending on what kind of multiphysics problem is tried to be solved, the mesh will automatically adapt for it to provide better results. The mesh elements that are used by the automatic mesh generation is a hybrid, which consist of tetrahedrons and hexahedrons. There are

nine levels for the sizing of the mesh elements in the automatic mesh generation mode of COMSOL. Ranging from Extremely coarse to Extremely fine. Because of the hardware limitations the desktop computer has, no finer elements than the Normal pre-set can be selected. For the final simulations itself, the Normal mesh element size was selected, since this was the maximum that the desktop computer was capable of simulating. With the Normal mesh element size, the number of mesh elements are 563969. The simulations were also performed with two other mesh element sizes, to determine the sensitivity of the mesh element size on the results, which are discussed in Section 6.5. The two mesh element sizes are called Extremely coarse and Extra coarse mesh. With 16331 and 56501 number of mesh elements respectively, see Figure 6.2 for the visualization of the three mesh qualities.

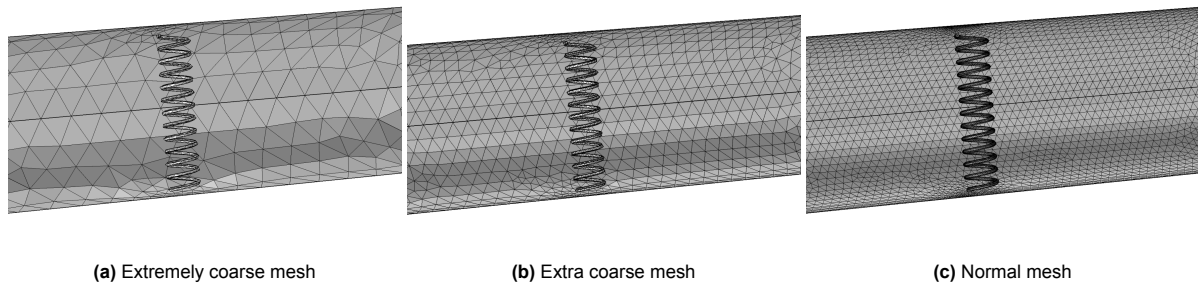


Figure 6.2: Extremely coarse and Normal mesh visualized

## 6.3. COMSOL interfaces & Settings

In COMSOL the physics is divided into various categories, which are called interfaces. Depending on the problem that needs to be solved, one or multiple interfaces are selected. For this computer model, the interfaces that will be used are:

- Heat transfer in Solids and Fluids (ht)
- Laminar flow (spf)
- Surface-to-Surface Radiation (rad)

The combination of all the three interfaces allows to make a model which is able to transfer heat from a solid heating element to a moving fluid, while considering radiation and heat losses at the wall.

### 6.3.1. Initial- & Boundary conditions

Within the selected interfaces of COMSOL, there are various settings and boundary conditions that needs to be defined for the simulation to run. In this section, the most important settings and boundary conditions will be defined and some elaboration will be provided if necessary. For a complete list of settings and boundary conditions that have been used for the simulation, please see Appendix F.

Three different simulations have been performed. All three simulations are time dependent simulations, since the main interest is the temperature change over a short period of time. The difference between the three simulations being the electrical power for the heating coil. Like in the experiments, for the simulation the start was with 20 W. The second simulation used an electrical power of 15 W and for the last simulation, 10 W is used as the electrical power for the heating coil. Besides the electrical power, the initial conditions also change slightly for each power condition. In the list below, a short summation is made of some important settings/conditions that are used for the simulation.

- **Initial volume temperature**

The initial volume temperature is the temperature of the volume within the combustion chamber, right before the liquid is injected inside the combustion chamber. To determine this value, multiple measurements within the experimental set-up in the laboratory were performed with a handheld thermometer. More details about the handheld thermometer can be found in Appendix G. The



temperature inside the combustion chamber was highly dependent on the distance from the heating coil itself. However, the temperature inside the combustion chamber did not change significantly with the changing electrical power output. As a result, for all three simulations an initial temperature inside the combustion chamber was set to  $200\text{ }^{\circ}\text{C}$ , which is in agreement with the measurements performed with the experimental set-up.

- **Initial temperature heating coil**

The temperature of the heating coil is dependent on the electrical power output. Also in this case, a handheld thermometer is used to measure the temperature of the heating coil itself at all three power outputs to determine the initial condition for the simulation. After multiple measurements, the initial temperature of the heating coil was determined to be  $550\text{ }^{\circ}\text{C}$ ,  $500\text{ }^{\circ}\text{C}$  and  $400\text{ }^{\circ}\text{C}$  for the electrical power output of 20 W, 15 W and 10 W respectively. Those temperatures have been used for the three mentioned power outputs as the initial temperature of the heating coil right before the liquid is injected into the combustion chamber.

- **Liquid temperature**

The temperature of the liquid that is injected inside the combustion chamber is equal to room temperature, since no pre-heating of the liquids was performed. The temperature of the liquid is also independent of the electrical power output, therefore for all three simulations the temperature of the liquid was set to  $20\text{ }^{\circ}\text{C}$ .

- **Atmospheric temperature**

The atmospheric temperature, is the temperature outside the combustion chamber. For the model in COMSOL, this is outside the domain. When calculating the heat that is dissipated to its surroundings, the atmospheric temperature is used. Since the experiments were performed at the chemical laboratory, the temperature inside the fume hood was around  $20\text{ }^{\circ}\text{C}$ . This value is also used for the simulation.

- **Flow rate**

As previously explained, the liquid will enter the combustion chamber at the inlet. For the experimental set-up, two piezoelectric discs were used. Tests with water, hydrogen peroxide and ethanol have been performed to determine the flow rate of the piezoelectric disc. For each test, 1 mL of one of the mentioned liquids was filled in a syringe and dropped slowly on the piezoelectric disc to have a continuous flow of atomized liquid droplets. The time it took to atomize the 1 mL liquid was measured with a stopwatch. Independent of which liquid was used, for each test it took about 40 s to atomize 1 mL of fluid. This value has to be multiplied by two, since two injectors were used inside the injector head. This results in a flow rate of 0.05 mL/s from the two injectors that have been used in the experimental set-up and also used for the flow rate in the simulations.

### 6.3.2. Materials

In the materials library of COMSOL there is a wide range of materials available with their properties pre-loaded. In case the required material is not available or small changes is desired to (some of) the properties, from the materials tab within the COMSOL software the desired properties can be defined/changed. For the model for this simulation, a nichrome coil is selected for the heating coil as it was the case for the experimental set-up. For the fluid, ethanol is selected for the final simulations, since the objective of the simulation is to verify whether it will reach the auto-ignition temperature of ethanol at  $365\text{ }^{\circ}\text{C}$ . Additionally, the same simulations have been performed with water and hydrogen peroxide. Since for the experimental set-up both ethanol and hydrogen peroxide are injected, both liquids are simulated separately to have the results of the outer boundaries. If in both cases, the auto-ignition temperature of ethanol is reached, it will mean that a mixture of the fluids will definitely achieve this auto-ignition temperature. More details about the influence of the liquid can be read in Section 6.5.

For the outside of the combustion chamber, glass was used for the experiments. For the simulations this was neglected and instead, it was replaced by a model that simulates heat dissipation. This

had the advantage of simplifying the model even further and requiring fewer mesh elements and thus reducing the required internal memory for the desktop computer and reducing the computational time.

## 6.4. Simulation results

For the final simulations, a time interval of 1 second with steps of 0.01 s was simulated. In this section, the results obtained from all three simulations will be discussed one-by-one and a brief comparison will be performed at the end of this section.

The simulation results show that at the beginning, very close to the heating coil, the liquid is reaching high temperatures. However, the temperature gradient is very high, which means that slightly farther ahead of the heating coil the temperature drops significantly back to the initial temperature condition of  $200\text{ }^{\circ}\text{C}$ . As time advances, the temperature of the heating coil reduces, which also results in a reduction of the peak temperature of the liquid. However, the high temperature zone around the heating coil has now expanded and is now occupying a broader area inside the combustion chamber. This phenomenon is shown in Figure 6.3. At  $t= 0.01\text{ s}$ , only a small portion of the liquid around the coil is heated up to temperatures greater than  $400\text{ }^{\circ}\text{C}$ . At  $t= 0.20\text{ s}$ , the maximum temperature has dropped to about  $365\text{ }^{\circ}\text{C}$ , however, it can be clearly seen from Figure 6.3c, that a wider area around the coil is now heated up. This result was expected, since the heating coil in this model has the highest temperatures and as a result the liquid that is around the heating coil will reach those high temperatures. The same behaviour was observed with the experiments, which is shown in Figure 4.1, the start of the combustion happens very close to the heating coil itself, since that part reaches the auto-ignition temperature of ethanol the quickest.

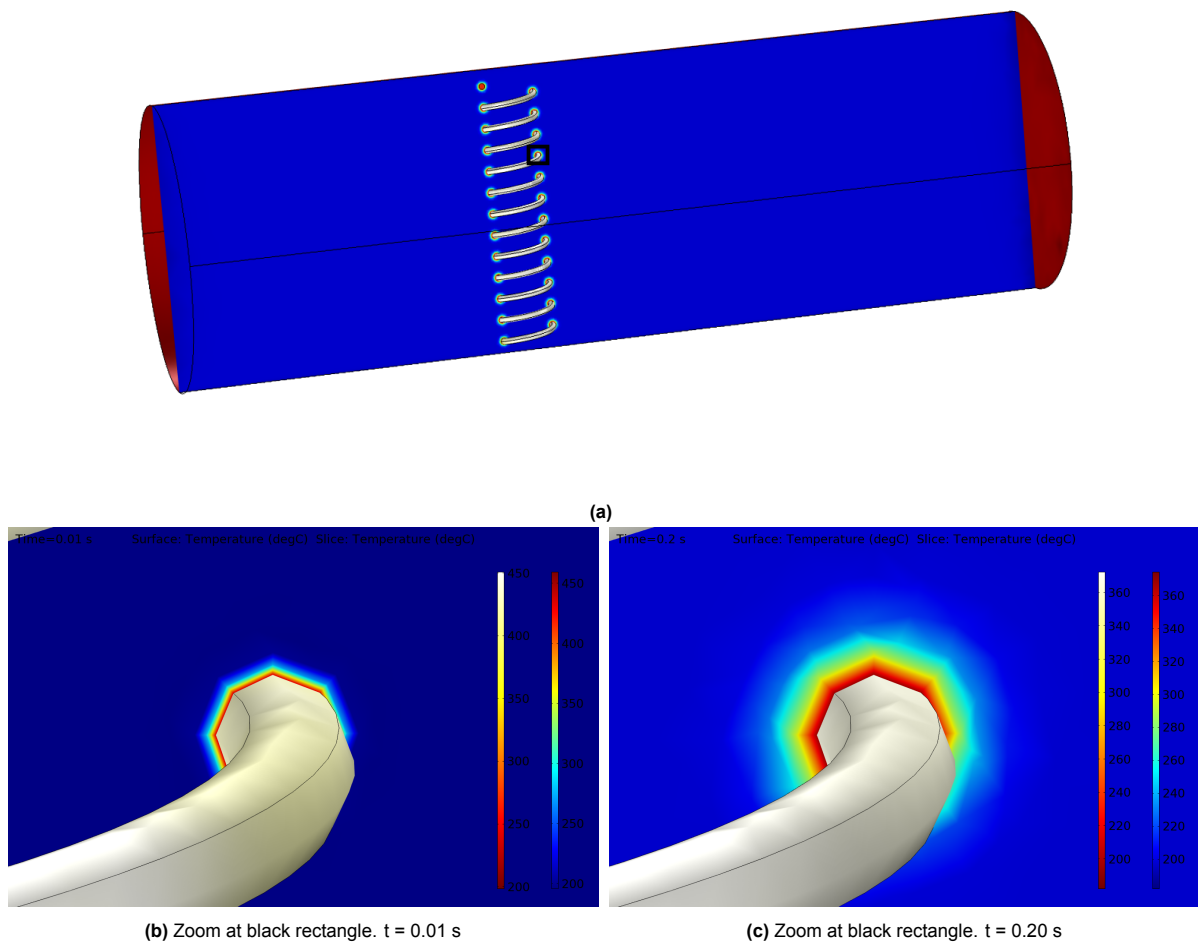


Figure 6.3: Heat distribution around a small part of the heating coil

#### 6.4.1. Comparison of the three simulations

The results of the three simulations show that for both the 20 W as well as 15 W the auto-ignition temperature of ethanol is reached right after the liquid is injected inside the combustion chamber with  $460\text{ }^{\circ}\text{C}$  and  $420\text{ }^{\circ}\text{C}$  respectively. The peak temperature of the liquid drops significantly over time. This is especially the case for the case with 15 W as electrical power input. It is able to maintain a peak temperature higher than  $365\text{ }^{\circ}\text{C}$ , for a period of 0.1 s. While the simulation with the 20 W electrical power input, is able to maintain a peak temperature higher than  $365\text{ }^{\circ}\text{C}$  for 0.25 s. The higher electrical power helps to maintain the higher temperatures for a longer period of time. However, also the higher initial temperatures of the combustion chamber and heating coil help to maintain the higher temperatures for a longer period of time.

The highest temperature that is reached with the 10 W electrical power, is at all times lower than the auto-ignition temperature of ethanol and will result in no ignition. This is similar to the results that were obtained from the experiments. In case the current was lowered, for which the power was close to 10 W, no ignition was achieved. In Figure 6.4, a frame of the three simulations with the temperatures closest to the auto-ignition temperature of ethanol has been shown.

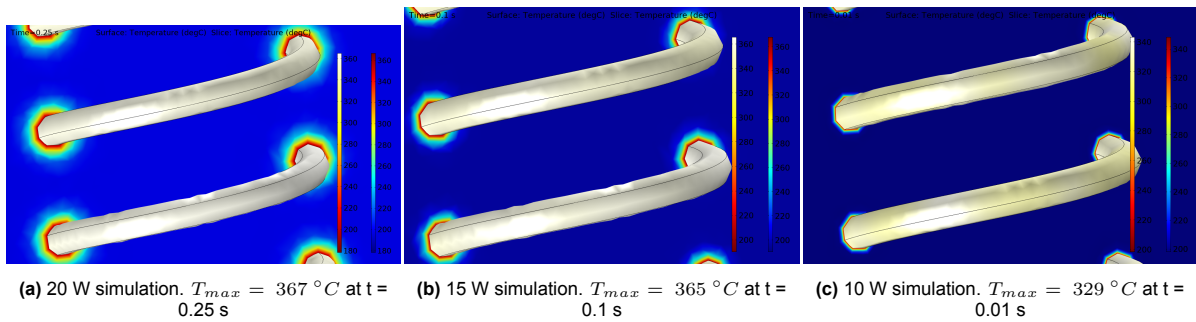


Figure 6.4: Highest temperatures around the heating coil

To compare the temperature over time of all three simulations, an arbitrary point at  $x = 0$ ,  $y = 0.957$ ,  $z = 32.151$  is selected, which is close to the heating coil. This point will be used to obtain the data of the temperature of the liquid over time. From the chart in Figure 6.5 it can be seen that the 20 W simulation is able to maintain a temperature higher than the auto-ignition temperature of ethanol for 0.20 s, while the 15 W simulation can achieve this for 0.08 s. The 10 W simulation, as previously explained never reaches the auto-ignition temperature of ethanol. The slight difference compared to Figure 6.4 is related to the fact that in that case the maximum temperature of the liquid was measured and for the chart, an arbitrary point close to the heating coil was used to probe.

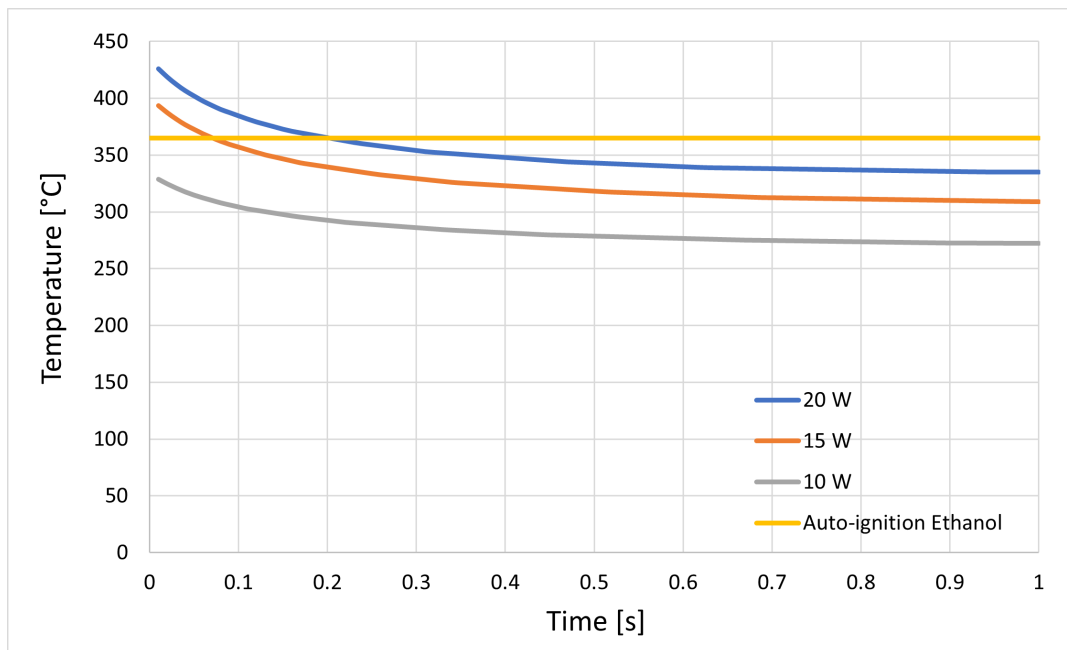


Figure 6.5: Geometry of computational model

## 6.5. Validation & Sensitivity analyses

For the validation of the simulation, the model will be recalculated with different mesh qualities and the distance of the heating coil from the injector head will be changed.

### 6.5.1. Mesh sensitivity

Besides the normal element size that was used for the final simulations, for the validation of the simulator runs have been performed with two other mesh element sizes which are called Extremely coarse and Extra coarse in the COMSOL software. Again, the same arbitrary point has been selected to determine the temperature for each time step and to compare the simulations with the different mesh sizes

with each other. The simulations with the coarser mesh elements, have lower temperatures compared to the Normal mesh elements. The steep temperature gradient that was shown in Figure 6.3, makes it difficult for the coarser mesh to capture the high temperatures very close to heating coil. As a result, the temperatures at the same location with a coarser mesh result in lower temperatures compared to a simulation with finer mesh elements. This can be clearly seen in Figure 6.6. It would have been better to perform the same simulation with even finer mesh elements, however because of internal memory limitations it was not possible to use finer mesh elements.

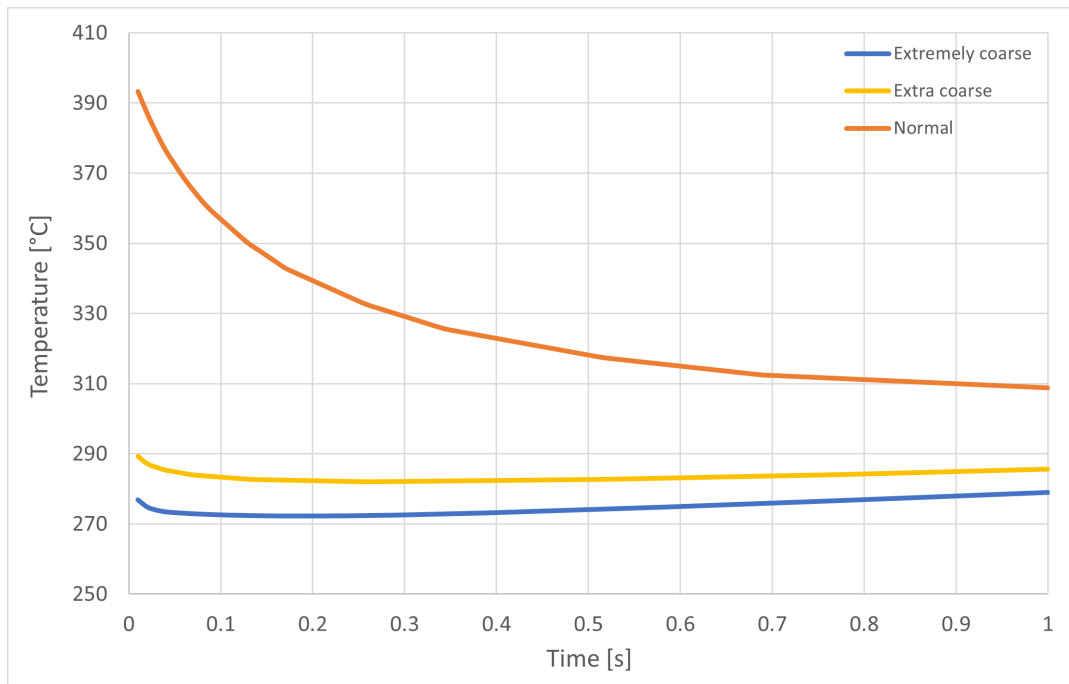


Figure 6.6: Temperature comparison with three different mesh element sizes.

### 6.5.2. Distance heating coil

The distance between the heating coil and the inlet is a second factor that might have an impact on the outcomes of the simulations. Originally, the heating coil was placed at 30 mm from the inlet, since that was also the distance used during the experiments. To determine the influence of the temperature with changing distance of the heating coil relative to the inlet, the distance is reduced from 30 mm to 15 mm and the exact same simulation has been performed with the same settings. As it can be seen from Figure 6.7, there is no significant difference in the temperature pattern at the same arbitrary point relative to the heating coil where the measurement is taken. This could be due to the fact that the flow that is coming from the inlet does not have an angle, which results in the fluid flowing perfectly in the longitudinal direction of the combustion chamber. Secondly, only a single fluid is injected which means no mixing is required as it was the case for experiments in the chemical laboratory. As a result, the temperature of the fluid depends on the residence time near the heating coil. This is independent of the distance in this simulation.

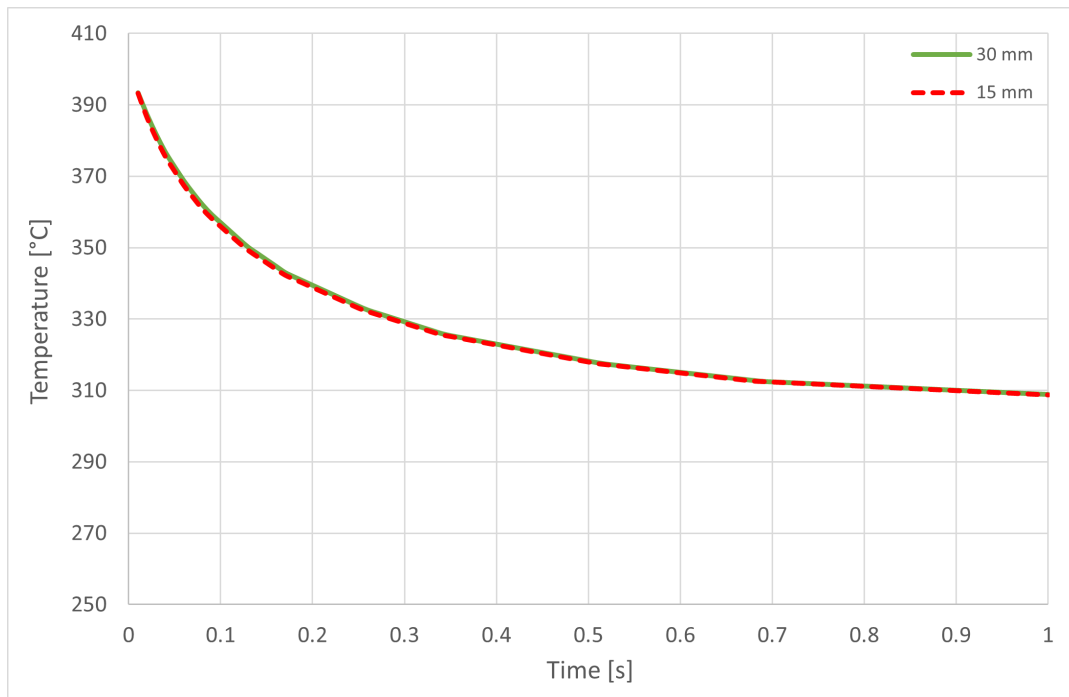


Figure 6.7: Temperature comparison with a simulation at 30 mm and 15 mm distance from the inlet.

### 6.5.3. Influence of the injected fluid

The experimental set-up is a mixture of ethanol and hydrogen peroxide. The properties of this mixture will be also in between the two liquids. By performing the simulations with both liquids separately, the two extremes will be simulated and can be validated whether the liquid will reach temperatures higher than the auto-ignition temperature of ethanol to assume ignition.

As with the previous graphs, again the same arbitrary point close to the heating coil was selected to tabulate the temperature at the same point for the whole duration of the simulation. From Figure 6.8, it can be seen that the highest temperatures are achieved with ethanol with a temperature close to 400 °C. Hydrogen peroxide and water are very close to each other, with hydrogen peroxide reaching a temperature of 366 °C and water 362 °C. Since the temperature is measured at the arbitrary point that has been also used for the previous graphs, those temperatures are not the maximum temperatures of the liquid. The maximum temperature is slightly higher at the beginning, because of the high temperature gradient. This graph shows that both with ethanol as well as with hydrogen peroxide the auto-ignition temperature of ethanol is reached and ignition to be happen can be assumed. Another observation that is made from this graph is that, besides the lower temperature, in case with water and hydrogen peroxide the temperature drop is harder than with ethanol. This could be caused by the fact that the density of water and hydrogen peroxide is higher than ethanol, which requires more energy to heat up and as a result the drop in temperature is more significant.

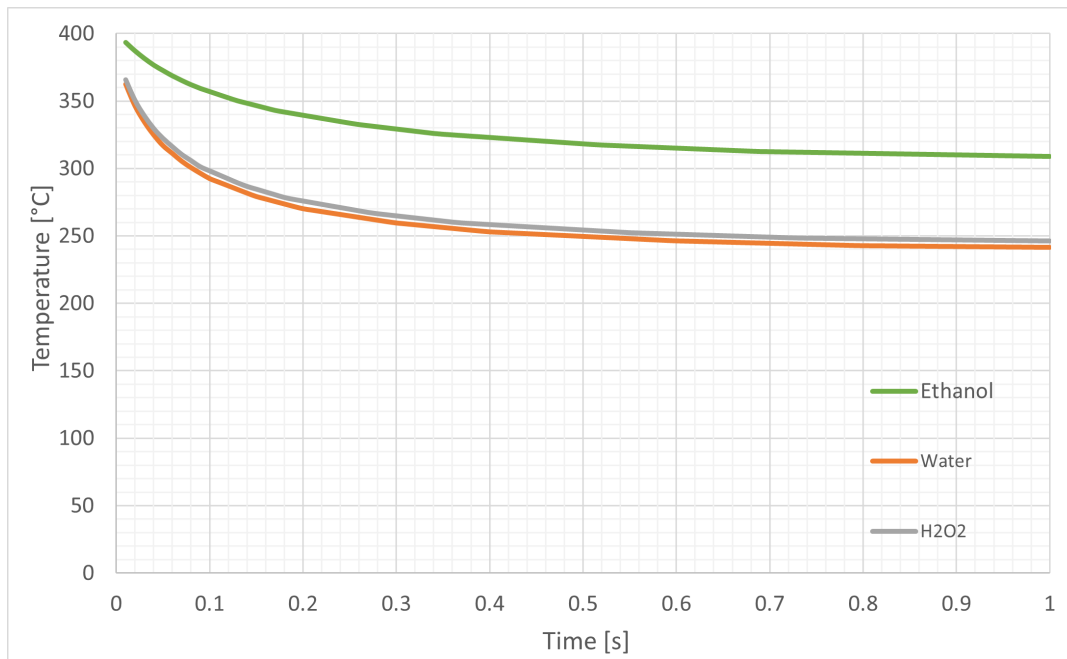


Figure 6.8: Temperature comparison with three different fluids: Water, Hydrogen peroxide and Ethanol

## 6.6. Simulation conclusion

For a computer simulation of the experimental set-up, COMSOL 5.6 is used. The objective of the simulation was to determine with which power output, for the heating coil, ignition can be achieved. The results obtained from the experiments are used to compare it to the results from the simulations to validate it. Some simplifications and assumptions are made for the computer model to reduce the complexity from a time perspective as well as to be within the limits of the provided hardware. Those simplifications include the use of a single fluid that is injected, the assumption that ignition will happen once the liquid reaches the auto ignition temperature of ethanol ( $365\text{ }^{\circ}\text{C}$ ) and no chemical reactions are simulated with the computer model.

Three simulations have been performed. The difference of the three simulations is the electrical power that has been used for the heating coil. The electrical power settings that have been used for the simulations are 20 W, 15 W and 10 W. This makes the power consumption similar to the experiments. Besides the change in the electrical power, also the initial temperature of the heating coil was adjusted for each simulation, which was  $550\text{ }^{\circ}\text{C}$ ,  $500\text{ }^{\circ}\text{C}$  and  $400\text{ }^{\circ}\text{C}$  respectively. The simulation results showed that with both the 20 W as well as 15 W power consumption, the injected temperature reaches temperatures higher than the auto-ignition temperature of ethanol, which is  $365\text{ }^{\circ}\text{C}$ . The simulation with the 10 W electrical power, was not able to reach a temperature of  $365\text{ }^{\circ}\text{C}$ , as a result it can be assumed that no ignition would have happened. This is similar to the results obtained from the experiments, where no ignition was achieved at a power consumption close to 10 W. Only with the optimized heating coil, a combustion with 10 W was achieved. However, the optimized design was not simulated and therefore not comparable.

Performing the same simulations with a different mesh element sizes, showed that the mesh has a significant influence on the results. The lower the number of mesh elements is, the lower the maximum temperature the liquid was reaching. This could be due to the fact that the high temperatures are reached very close to the heating coil itself and the temperature gradient, close to the heating coil, is very high. By increasing the size of the mesh elements, the temperature very close to the heating coil, where the highest temperatures are reached, are not captured properly within the simulation. By making use of finer mesh elements, the temperature close to the heating coil can be properly determined and results in higher temperatures compared to simulations with coarser mesh elements. Furthermore, sensitivity analysis has been performed by changing the fluid that is injected and by changing the dis-

tance of the heating coil relative to the inlet. In the second case, the change in the distance of the heating coil relative to the injector head did not have any influence on the temperature of the liquid close to the heating coil. In case of injecting hydrogen peroxide, instead of ethanol, the temperature dropped significantly but it was still higher than the auto-ignition temperature of ethanol.



# 7

## Conclusion

This chapter will discuss the conclusions of the work that has been performed for this thesis. The objective of this research was to develop a novel ignition system for small green liquid bi-propellant rocket engines that are used for small satellites. First, a literature study was performed on what types of green propellants do exist and are of interest for this thesis work. At the same time, different ignition systems for liquid rocket propulsion systems have been explored and with the aid of a trade-off table, the best ignition system for this application has been selected. After selecting the propellant and ignition system, various experiments have been performed in the chemical laboratory of the Aerospace Faculty at TU Delft to gain an understanding of the characteristics of this propellant and on how to ignite it. Each design iteration of the test set-up improved the design until a set-up was achieved that was reliable and provided consistent results. This final iteration of the set-up allowed to perform test runs to gather data to answer the research question, which is:

*How to develop a simple, reliable and cost effective ignition system that is reusable and also compatible with storable green bi-propellant?*

To briefly answer this research question, it can be said that with a thermal ignition system it is possible to (re-)ignite, with a limited amount of electrical power, the rocket engine that uses green propellants. A more elaborate conclusion on this thesis work will be:

Currently storable (green) bipropellants that are not hypergolic, use mostly a catalytic igniter to start the combustion in a rocket engine. The major drawback of a catalyst is the volume it requires in a rocket engine, the pressure drop and the degradation of the catalyst over time. As an alternative ignition system, the thermal ignition system was selected after a trade-off was performed. For the experiments with the thermal ignition system, hydrogen peroxide and ethanol were selected as the green propellants for the experiments with the thermal ignition system.

Hydrogen peroxide decomposes spontaneously to water vapor and oxygen at temperatures higher than  $150\text{ }^{\circ}\text{C}$ . This decomposition reaction is an exothermic reaction and as a result temperatures of  $900\text{ }^{\circ}\text{C}$  can be achieved, depending on the concentration of hydrogen peroxide that is used. The ethanol will be reacting with the oxygen that is released from the decomposed hydrogen peroxide to have combustion and ignition. Ethanol ignites spontaneously at  $365\text{ }^{\circ}\text{C}$ , which is called the auto-ignition temperature. To have the hydrogen peroxide decompose and react with ethanol, with only heat, the liquids should reach a temperature of at least  $365\text{ }^{\circ}\text{C}$ . This is achieved with a heating coil that is placed inside a glass combustion chamber. Since the experiments were performed in a laboratory environment, no nozzle was used at the end of the combustion chamber to prevent pressure buildup inside the combustion chamber.

Two experiments were performed during this thesis work. For the first experiment, five injector head angles were used varying from  $0^{\circ}$  till  $40^{\circ}$ . With the gathered data, a trade-off has been performed to select which injector head angle is providing the lowest power consumption while still having good flame

characteristics. The  $10^\circ$  injector head angle, had the highest total score and as a result was used for the second experiment. The objective of the second experiment was to determine the minimum power at which successful ignition followed by a self-sustained combustion is achieved. The power consumption was reduced by decreasing the length of the wire, which reduced the required voltage. With the set-up, it was possible to reduce the power consumption to 14 W. After some optimization of the heating coil, successful ignition and self-sustained combustion with a power consumption of 10 W was achieved. The optimization consisted of having only a few windings of the heating coil that are centered in the middle of the combustion chamber.

The data of the experiments are used for the validation of the computer model. A simulation was performed with COMSOL 5.6. To simplify the model, a couple of assumptions and simplifications have been made which are mainly due to the hardware restrictions on which COMSOL software will be doing the calculations. The simplifications that are made for this model are:

- One liquid is injected in the combustion chamber and no injector head angle is used to simplify the design of the set-up in the model.
- It is assumed that an ignition will happen, once the temperature of the liquid reaches  $365^\circ\text{C}$ , since no chemical kinematics calculations will be computed.
- The liquid will not be injected as a spray of atomized liquid, but instead a continuous flow of liquid with the flow rate that matches with the flow rate of the two injectors that have been used for the experimental set-up.

Three simulations have been performed, the power consumption of the heating coil was set to 20 W, 15 W and 10 W. The initial temperature of the heating coil was set to  $550^\circ\text{C}$ ,  $500^\circ\text{C}$  and  $400^\circ\text{C}$  respectively after performing measurements with a thermocouple with the experimental set-up. The results showed that the 20 W and 15 W simulation is reaching temperatures higher than the auto-ignition temperature of ethanol after the liquid has been injected and as a result it is assumed that ignition would have happened in this case. The 10 W simulation, on the other hand never reached the auto-ignition temperature of ethanol and so no ignition would have happened. This result is similar to the experiments that have been performed where ignition was achieved with power consumption higher than 14 W. Although, ignition was also achieved with lower power consumption during the experiment, this was only with the optimized heating coil which is not simulated and as a result not a comparable result.

## 7.1. Future work recommendation

During this thesis work, experiments have been conducted regarding the thermal ignition of storable green liquid bipropellants. The main focus during the experiments was to have a self-sustained combustion, re-ignitability and low power consumption. In this section, recommendations on aspects of possible future work will be provided. The recommendation can be divided into two main categories, the first of which is related to the experiments and experimental set-up. The second category of recommendation is related to the model and simulations.

- **Longer duration experiments**

This study was a preliminary feasibility study to determine whether a thermal ignition system can be a potential alternative to current existing ignition systems. Because of the safety regulations of the laboratory, where the experiments have been performed, and because of design constraints only a short experiment could be performed. Also, in case of longer experiments, the 3D-printed plastic injector head would also heat up and catch fire at some point. Especially for the self-sustained combustion it is important to have longer duration experiments to observe whether the combustion can carry on for longer periods of time without any power consumption. For this, the design of the set-up would need to be redesigned and made out of more heat resistant materials, while still considering the compatibility with hydrogen peroxide. Furthermore, safety of the set-up and environment should be considered in case of longer duration experiments.

- **Pressurized system**

The experiments performed in this study are all done without any pressurized systems. Since a rocket propulsion system will have a pressurized combustion chamber, the next step that should be investigated is on how the thermal ignition system can be implemented in a pressurized combustion chamber, while still maintaining a low power consumption. For this experiment, it would be also of interest if the amount of mass flow could be matched of a small rocket engine that is installed on a small satellite.

- **Optimization power consumption**

Some preliminary study has been performed on the optimization of the power consumption of the thermal ignition system. During this study the focus was mainly on the injector head angle and the length of the heating coil itself. The heat insulation of the combustion chamber was a thin glass wall. A more elaborate study can be performed on how to lower the power consumption of the heating coil even further by also taking into account the position and shape of the heating coil and the thermal insulation of the combustion chamber.

- **Life-time experiments**

The thermal ignition system is in development for small satellite applications. For this application, besides the low power consumption it is also required to have re-ignitability for orbital maneuvers, orbit corrections and/or orientation of the satellite. While during this study, re-ignitability experiments have been performed, it did not take into account how often the thermal igniter can be used to ignite the propellants, without any malfunction of the ignition system. For a future study, it will be first important to know what the average lifespan of a satellite is and how often it needs to re-ignite the rocket engine. This knowledge can be used to perform re-ignitability experiments to simulate a realistic satellite mission.

- **Simulation: Improving the simulation model**

With the current simulation model, no walls have been modeled since this will reduce the required computational power and the use of internal memory. Since the main objective of the simulation for this study was to determine whether ignition would happen, the wall temperature was not of a significant interest. The dissipated heat at the edge of the model, where the wall is supposed to be, is done by a formula that takes into account the heat dissipation at the outer wall. To improve the accuracy of the model and to determine the temperature at the wall itself it would require the wall to be included in the model.

- **Simulation: chemical kinematics**

Simulating chemical reactions is another aspect that was simplified during this study, by assuming that ignition would have happened once it reached the auto-ignition temperature of ethanol. Simulating also the chemical reactions in the computer model, would provide a better understanding of the behaviour of the chemicals on a micro-level and also improve the accuracy of the model. Furthermore, because the chemical kinematics are simulated it will be also of more interest to inject both hydrogen peroxide and ethanol to simulate the mixing and the reaction of those two chemicals. This knowledge could be potentially translated into improving/optimizing the design of the experimental set-up.

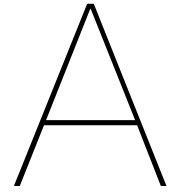
- **Cost (incl mass/volume) estimation**

During the trade-off of the ignition system, a comparison was made of different ignition systems. The grading of the ignition system has been done on the basis of qualitative values. For a better estimation of the cost of a thermal ignition system, including the mass and volume of the igniter system a more elaborate study would be required. This study will help to find within which boundaries this ignition system will be more beneficial compared to its competitors.

# Bibliography

- [1] Alessandro de Iaco Veris. Fundamental concepts on liquid-propellant rocket engines. In *Fundamental Concepts of Liquid-Propellant Rocket Engines*, pages 1–61. Springer, 2021.
- [2] George P Sutton. History of liquid propellant rocket engines in the united states. *Journal of Propulsion and Power*, 19(6):978–1007, 2003.
- [3] Paweł Surmacz. Green rocket propulsion research and development at the institute of aviation: problems and perspectives. *Journal of KONES*, 23:337–344, 2016.
- [4] Lukasz Mezyk, Zbigniew GUT, Przemyslaw PASZKIEWICZ, Piotr WOLANSKI, Grzegorz RARATA, and Aleja Krakowska. Possibility of using thermal decomposition of hydrogen peroxide for low thrust propulsion system application. In *7th European Conference for Aeronautics and Space Sciences*, 2017.
- [5] Dylan DeSantis. Satellite thruster propulsion-h2o2 bipropellant comparison with existing alternatives. *Department of Space Technologies, Institute of Aviation, The Ohio State University, Ohio, USA*, 585, 2014.
- [6] S Frolik, B Austin, J Rusek, and S Heister. Development of hypergolic liquid fuels for use with hydrogen peroxide. In *36th AIAA/ASME/SAE/ASEE Joint Propulsion Conference and Exhibit*, page 3684, 2000.
- [7] ECHA. Classification labeling pbt assessment - hydrazine, 2022.
- [8] ECHA. Candidate list of substances of very high concern for authorisation, 2022.
- [9] Amir S Gohardani, Johann Stanojev, Alain Demairé, Kjell Anflo, Mathias Persson, Niklas Wingborg, and Christer Nilsson. Green space propulsion: Opportunities and prospects. *Progress in Aerospace Sciences*, 71:128–149, 2014.
- [10] Dieter K Huzel. *Modern engineering for design of liquid-propellant rocket engines*, volume 147. AIAA, 1992.
- [11] Olexiy Shynkarenko and Domenico Simone. Oxygen–methane torch ignition system for aerospace applications. *Aerospace*, 7(8):114, 2020.
- [12] C DEXTER and T MCCAY. Space shuttle main engine fuel preburner augmented spark igniter shutdown detonations. In *22nd Joint Propulsion Conference*, page 1445, 1986.
- [13] Larry C Liou. *Combustion-wave ignition for rocket engines*. National Aeronautics and Space Administration, 1992.
- [14] Wen-Li Yuan, Lei Zhang, Guo-Hong Tao, Shuang-Long Wang, You Wang, Qiu-Hong Zhu, Guo-Hao Zhang, Zhang Zhang, Ying Xue, Song Qin, et al. Designing high-performance hypergolic propellants based on materials genome. *Science advances*, 6(49):eabb1899, 2020.
- [15] Stephen M Davis and Nadir Yilmaz. Advances in hypergolic propellants: Ignition, hydrazine, and hydrogen peroxide research. *Advances in Aerospace Engineering*, 2014, 2014.
- [16] Bastien Boust, Jean-Baptiste Lebon, Marc Bellenoue, Alexis Tran, Romain Beauchet, Yann Batonneau, E Labarthe, and Yann Guélou. Catalytic ignition of hydrogen peroxide for storable bipropellant thrusters. In *8th European Conference for Aeronautics and Space Sciences (EUCASS)*, 2019.
- [17] Su-Lim Lee and Choong-Won Lee. Performance characteristics of silver catalyst bed for hydrogen peroxide. *Aerospace Science and Technology*, 13(1):12–17, 2009.

- [18] Lukasz Mezyk, Zbigniew Gut, Kiran Mohan, Jan Kindracki, and Grzegorz Rarata. Initial research on thermal decomposition of 98% concentrated hydrogen peroxide in thruster-like conditions. *Engineering Science and Technology, an International Journal*, 2021.
- [19] Robert Masse, May Allen, Ronald Spores, and Elizabeth A Driscoll. Af-m315e propulsion system advances and improvements. In *52nd AIAA/SAE/ASEE Joint Propulsion Conference*, page 4577, 2016.
- [20] NIST. Isobaric properties for dinitrogen monoxide, 2022.
- [21] NIST. Isothermal properties for dinitrogen monoxide, 2022.
- [22] Mei-feng He, WANG Hao, Hong Jiang, ZHAO Su, and PAN Deng. Effect of hydrogen peroxide concentration on surface properties of ni–cr alloys. *Transactions of Nonferrous Metals Society of China*, 26(5):1353–1358, 2016.
- [23] Pubchem. Ethanol (compound), 2022.
- [24] fishersci. Safety data sheet, 2022.
- [25] Chan-Cheng Chen, Horng-Jang Liaw, Chi-Min Shu, and Yen-Cheng Hsieh. Autoignition temperature data for methanol, ethanol, propanol, 2-butanol, 1-butanol, and 2-methyl-2, 4-pentandiol. *Journal of Chemical & Engineering Data*, 55(11):5059–5064, 2010.
- [26] Paulina Pędziwiatr et al. Decomposition of hydrogen peroxide-kinetics and review of chosen catalysts. *Acta Innovations*, (26):45–52, 2018.
- [27] Wioleta Kopacz, Adam Okninski, Anna Kasztankiewicz, Paweł Nowakowski, Grzegorz Rarata, and Paweł Maksimowski. Hydrogen peroxide—a promising oxidizer for rocket propulsion and its application in solid rocket propellants. *FirePhysChem*, 2022.
- [28] Jaime Quesada Mañas. Propellant grade hydrogen peroxide production and thermo pseudo hypergolicity investigation for dual mode green propulsion systems. 2020.
- [29] Woosuk Jung, Seungkwon Baek, Taesoo Kwon, Juhyeon Park, and Sejin Kwon. Demonstration of ethanol-blended hydrogen peroxide gas generator for ramjet combustor flow simulation. *Journal of Propulsion and Power*, 34(3):591–599, 2018.
- [30] icstation. 20mm 113khz ultrasonic mist maker fogger atomizer ceramic discs with power driver board for desktop mini humidifier, 2022.
- [31] Esteban Guerra-Bravo, Han-Joo Lee, Arturo Baltazar, and Kenneth J Loh. Vibration analysis of a piezoelectric ultrasonic atomizer to control atomization rate. *Applied Sciences*, 11(18):8350, 2021.
- [32] Stefan Kooij, Alina Astefanei, Garry L Corthals, and Daniel Bonn. Size distributions of droplets produced by ultrasonic nebulizers. *Scientific reports*, 9(1):1–8, 2019.



# Commercial Available rocket engines for small satellites/cubesats

Type of propulsion	MONOPROPELLANT	MONOPROPELLANT	MONOPROPELLANT	MONOPROPELLANT	MONOPROPELLANT	MONOPROPELLANT	MONOPROPELLANT	MONOPROPELLANT
Company	Aerojet Rocketdyne	Aerojet Rocketdyne	Aerojet Rocketdyne	Aerojet Rocketdyne	Aerojet Rocketdyne	Aerojet Rocketdyne	Vacco	Vacco
NAME PROP SYSTEM	MPS-130-1U	MPS-130-2U	MPS-135-4U	MPS-120-1U	MPS-120-2U	MPS-125-4U	Green MIPS	ECAPS ADN
Lifespan	3.0kg/thruster	3.0kg/thruster		3.0kg/thruster	3.0kg/thruster			5 hr
Volume [U or L]	1U	2U	4U	1U	2U	4U	3U	1U
Mass (dry,wet) [kg]	(1.06,1.66)	(1.36,2.76)	(3.5,7.2)	(1.06,1.48)	(1.36,2.38)	(3.6,6.2)	(3.5, 5,26)	(0.909, 1.800)
Usable propellant [kg]	0.5	1.4		0.38	0.98		2	0.72
Power (rest,thrust) [W]	(unknown,29)	(unknown,29)	SP				(1, 15)	(0.055, 15)
Thrust [N]	0.25-1.25	0.25-1.25		0.25-1.25	0.25-1.25		0.4	0.4
Impulse [Ns]	1200	3360	7290	775	2000	5240	3320	1828
Number of thrusters [-]	4	4		4	4		4	4
Number of restarts [-]	10000	10000		10000	10000			2000 per thruster
Continuous burntime								30 min/thruster
Pressure [bar]	10.34	10.34		10.34	10.34		5.17	16
Radiation environment L2								
Storage temperature propellant [K]	333 - 278	334 - 278		334 - 278	334 - 278		239 - 333 K	263-333
Launch loads								
Response time								
Safety factor							Pressure (2x)	
Safety margin on prop volume							0.05	
Fuel type	AF-M315E	AF-M315E	AF-M315E	Hydrazine	Hydrazine	Hydrazine	LMP-103S/AF-M315E	LMP-103S
MIB [Ns]	0.004	0.004		0.004	0.004			0.002
ISP [s]	206 - 235	206 - 235		206 - 217	206 - 217			196 - 209
Complete system	Yes	Yes	Yes	Yes	Yes	Yes	Yes	Yes
European	No	No	No	No	No	No	No	No
URL	<a href="#">link</a>	<a href="#">link</a>	<a href="#">link</a>	<a href="#">link</a>	<a href="#">link</a>	<a href="#">link</a>	<a href="#">link</a>	<a href="#">link</a>
URL2	<a href="#">link</a>	<a href="#">link</a>	-	<a href="#">link</a>	<a href="#">link</a>	-	<a href="#">link</a>	<a href="#">link</a>

MONOPROPELLANT	MONOPROPELLANT	MONOPROPELLANT	MONOPROPELLANT	MONOPROPELLANT	MONOPROPELLANT	BIPROPELLANT	BIOPROPELLANT
ECAPS	ECAPS	ECAPS	Busek	Busek	Busek	Hyperion	Tethers Unlimited
100mN HPGP THRUSTER	1N HPGP THRUSTER	5N HPGP THRUSTER	BGT-X1	BGT-X5	BGT-5	PM200	HYDROS-C
5 hr or 1kg	25hr or 24kg	20hr or 100kg					3 years LEO
Can be chosen	Can be chosen	Can be chosen		1U		1U (more propellant possible)	190x130x92 mm = ±2.27L
(0.040, unknown)	(0.38, unknown)	(0.48, unknown)				(1.1, 1.41)	(2.2, 2.7)
Can be chosen	Can be chosen	Can be chosen		0.262*		0.304*	0.5
(unknown, 8)	(unknown, 10)	(unknown, 15-25)	(unknown, 4.5)	(unknown, 20)	(unknown, 50)	(0.1, 12)	(5, 25)
0.1	1	5	0.1	0.5	5	0.5	1.2
Can be chosen	Can be chosen	Can be chosen		565		>850	>2151
1	1	1				1	1
2000	60000	50000					761
30 min	1.5 hr	10 min					
4.5	22	24		27.58			
263-333	263-333	263-333				268-308	Probably>273
						Seconds	
LMP-103S	LMP-103S	LMP-103S	AF-M315E	AF-M315E	AF-M315E	Nitrous oxide and propene	Water
0.005	0.07	<0.1	0.014	0.05		0.035	>1.75
196-209	204-231	239-253	214	220-225	>230	285	310
No	No	No	No	Yes	No	Yes	Yes
Yes	Yes	Yes	No	No	No	Yes	No
<a href="#">link</a>	<a href="#">link</a>	<a href="#">link</a>	<a href="#">link</a>	<a href="#">link</a>	<a href="#">link</a>	<a href="#">link</a>	<a href="#">link</a>
<a href="#">link</a>	<a href="#">link</a>	<a href="#">link</a>		<a href="#">link</a>	-	<a href="#">link</a>	



BIOPROPELLANT	MONOPROPELLANT	BIPROPELLANT	MONOPROPELLANT	MONOPROPELLANT	BIRPROPELLANT	BIRPROPELLANT
Tethers Unlimited	Nanoavionics	DAWN AEROSPACE	DAWN AEROSPACE	MOOG	BENCHMARK SPACE SYSTEMS	BENCHMARK SPACE SYSTEMS
HYDROS-M	EPSS C1	CubeSat Propulsion Module	Small Propulsion Module	MONOPROPELLANT PROPULSION MODULE	HALCYON	PEREGRINE
3 years LEO			93000Ns			
∅ 381 x 191 mm = ±21.78L	U1 (U2 and U3 also available)	0.7/1U	±0.5U, can be chosen	1U scalable to 24x24x24cm		2-3.5-7.8L
(7.7,13.7)	(1,1.2)	(1, 1.17)/(1.1, 1.410)	(0.4+,unknown)	(unknown, 1.01 for 1U)		2.5-4-7.5 wet
6.0	from 0.22	0.17/0.31	Unknown	0.15L for 1U		0,66-1,32-3,77*
(7, 40)	(0.19,9.6)	(unknown,12.5)	(unknown,12)	(unknown,45)	(0.1,10)	(0.1,10)
>1.2	1	0.5	20	0.5 for 1U	0.1-22	0.1-22
>18000	from 400	425/850		500Ns for 1u		1750-3500-10000
1	1	1	1	2	1 to 12	1 to 12
10300			12000			
		7.5Ns	150Ns			
	25	Ox 110, Fuel 40	Ox 72, Fuel 14.7	28		
	20k rad tolerance	50k rads				
Probably>273		operational (273-303)	Operational(286-308)			
	14.1 Grms qualification					
	1.44 on pressure	1.36 on pressure (ox)		1.2 on pressure		
Water	ADN	Nitrous oxide, propene	Propene	Liquid Chemical – Green or Traditional	HTP+Butane	HTP+NHMF
>1.75		0.035	1		0.05	0.0005
310	213	>285	>285	224	140-320	270
Yes	Yes	Yes	No	Yes	Yes	Yes
No	Yes	Yes	Yes	Yes	No	No
<a href="#">link</a>	<a href="#">Link</a>	<a href="#">link</a>	<a href="#">link</a>	<a href="#">link</a>	<a href="#">link</a>	<a href="#">link</a>
		<a href="#">link</a>	<a href="#">link</a>	<a href="#">link</a>	<a href="#">link</a>	<a href="#">link</a>

B

# Hydrogen peroxide Safety Data Sheet

# SAFETY DATA SHEET

## Hydrogen Peroxide 90% HTP

SDS # : 7722-84-1-90-60  
Revision date: 2015-05-28  
Format: NA  
Version 1



### 1. PRODUCT AND COMPANY IDENTIFICATION

#### Product Identifier

**Product Name** Hydrogen Peroxide 90% HTP

#### Other means of identification

**CAS-No** 7722-84-1

#### Recommended use of the chemical and restrictions on use

**Recommended Use:** Monopropellant and bipropellant systems; fuel for rocket engines; rocket boosters / propellants / power source for aircraft; steam generation; rapid source of heat; electronics IC circuits and other military uses

**Restrictions on Use:** Use as recommended by the label.

#### Manufacturer/Supplier

PeroxyChem LLC  
2005 Market Street  
Suite 3200  
Philadelphia, PA 19103  
Phone: +1 267/ 422-2400 (General Information)  
E-Mail: sdsinfo@peroxychem.com

PeroxyChem Canada  
PG Pulp Mill Road  
Prince George, BC V2N2S6  
1+ 250/ 561-4200 (General Information)

#### Emergency telephone number

For leak, fire, spill or accident emergencies, call:  
1 800 / 424 9300 (CHEMTREC - U.S.A.)  
1 703 / 527 3887 (CHEMTREC - Collect - All Other Countries)  
1 613/ 996-6666 (CANUTEC - Canada)  
1 303/ 389-1409 (Medical - U.S. - Call Collect)

1 281 / 474-8750 (Bayport, Texas Plant)  
1 250 / 561-4221 (Prince George, BC, Canada Plant)

### 2. HAZARDS IDENTIFICATION

#### Classification

#### **OSHA Regulatory Status**

This material is considered hazardous by the OSHA Hazard Communication Standard (29 CFR 1910.1200).

Acute toxicity - Oral	Category 4
Acute toxicity - Inhalation (Vapors)	Category 4
Skin corrosion/irritation	Category 1 Sub-category A

## Hydrogen Peroxide 90% HTP

SDS # : 7722-84-1-90-60  
Revision date: 2015-05-28  
Version 1


Serious eye damage/eye irritation	Category 1
Specific target organ toxicity (single exposure)	Category 3
Oxidizing Liquids	Category 1

### GHS Label elements, including precautionary statements

#### EMERGENCY OVERVIEW

**Danger**

**Hazard Statements**  
H314 - Causes severe skin burns and eye damage  
H302 - Harmful if swallowed  
H332 - Harmful if inhaled  
H335 - May cause respiratory irritation  
H272 - May intensify fire; oxidizer



#### **Precautionary Statements - Prevention**

- P271 - Use only outdoors or in a well-ventilated area
- P260 - Do not breathe mist, vapours or spray.
- P280 - Wear protective gloves/ protective clothing/ eye protection/ face protection
- P283 - Wear fire/ flame resistant/ retardant clothing
- P210 - Keep away from heat/sparks/open flames/hot surfaces. - No smoking
- P220 - Keep/Store away from clothing/flammable materials/combustibles
- P221 - Take any precaution to avoid mixing with combustibles/flammables

#### **Precautionary Statements - Response**

- P305 + P351 + P338 - IF IN EYES: Rinse cautiously with water for several minutes. Remove contact lenses, if present and easy to do. Continue rinsing
- P310 - Immediately call a POISON CENTER or doctor
- P303 + P361 + P353 - IF ON SKIN (or hair): Take off immediately all contaminated clothing. Rinse skin with water/ shower
- P306 + P360 - IF ON CLOTHING: rinse immediately contaminated clothing and skin with plenty of water before removing clothes
- P304 + P340 - IF INHALED: Remove person to fresh air and keep comfortable for breathing
- P312 - Call a POISON CENTER or doctor if you feel unwell
- P301 + P330 + P331 - IF SWALLOWED: rinse mouth. Do NOT induce vomiting
- P310 - Immediately call a POISON CENTER or doctor
- P370 + P378 - In case of fire: Use water for extinction
- P371 + P380 + P375 - In case of major fire and large quantities: Evacuate area. Fight fire remotely due to the risk of explosion

#### **Hazards not otherwise classified (HNOC)**

No hazards not otherwise classified were identified.

#### **Other Information**

Keep container in a cool place out of direct sunlight. Store only in vented containers. Do not store on wooden pallets. Do not return unused material to its original container. Avoid contamination - Contamination could cause decomposition and generation of oxygen which may result in high pressure and possible container rupture. Empty drums should be triple rinsed with water before discarding. .

**3. COMPOSITION/INFORMATION ON INGREDIENTS**

Formula HO - OH

Chemical name	CAS-No	Weight %
Hydrogen peroxide	7722-84-1	90
Water	7732-18-5	10

Occupational exposure limits, if available, are listed in section 8

**4. FIRST AID MEASURES**

<b>Eye Contact</b>	Rinse immediately with plenty of water, also under the eyelids, for at least 15 minutes. Remove contact lenses, if present, after the first 5 minutes, then continue rinsing. Seek immediate medical attention/advice.
<b>Skin Contact</b>	Take off contaminated clothing. Rinse skin immediately with plenty of water for 15-20 minutes. Call a poison control center or doctor for further treatment advice.
<b>Inhalation</b>	Move to fresh air. If person is not breathing, contact emergency medical services, then give artificial respiration, preferably mouth-to-mouth if possible. Call a poison control center or doctor for further treatment advice.
<b>Ingestion</b>	Rinse mouth. Do not induce vomiting. If conscious, give 2 glasses of water. Get immediate medical attention. Never give anything by mouth to an unconscious person.
<b>Most important symptoms and effects, both acute and delayed</b>	Hydrogen Peroxide irritates respiratory system and, if inhaled, may cause inflammation and pulmonary edema. The effects may not be immediate. In case of accidental ingestion, necrosis may result from mucous membrane burns (mouth, esophagus and stomach). Oxygen rapid release may cause stomach swelling and hemorrhaging, which may produce major, or even fatal, injury to organs if a large amount has been ingested. Corneal lesions and irreversible damage if contact with the eyes
<b>Indication of immediate medical attention and special treatment needed, if necessary</b>	Hydrogen peroxide at these concentrations is a strong oxidant. Direct contact with the eye is likely to cause corneal damage especially if not washed immediately. Careful ophthalmologic evaluation is recommended and the possibility of local corticosteroid therapy should be considered. Because of the likelihood of corrosive effects on the gastrointestinal tract after ingestion, and the unlikelihood of systemic effects, attempts at evacuating the stomach via emesis induction or gastric lavage should be avoided. There is a remote possibility, however, that a nasogastric or orogastric tube may be required for the reduction of severe distension due to gas formation.

**5. FIRE-FIGHTING MEASURES**

<b>Suitable Extinguishing Media</b>	Water. Do not use any other substance.
<b>Specific Hazards Arising from the Chemical</b>	In closed unventilated containers, risk of rupture due to the increased pressure from decomposition. Contact with combustible material may cause fire. Non-flammable but vapor phase decomposition occurs at 7.6 vol. % for 90% based on flash point.
<b>Hazardous Combustion Products</b>	A severe detonation hazard when mixed with organics. Contact with combustibles will cause fire. While not flammable by OSHA and DOT definitions, contamination, contact with incompatible materials, or high temperatures could cause a rapid decomposition that yields heat and oxygen, which support combustion and will cause a rapid overpressure if confined.
<b>Explosion data</b>	
<b>Sensitivity to Mechanical Impact</b>	Not sensitive.
<b>Sensitivity to Static Discharge</b>	Static discharge can potentially initiate decomposition in vapor mixtures.
<b>Protective equipment and</b>	Use water spray to cool fire exposed surfaces and protect personnel. Move containers from

**precautions for firefighters** fire area if you can do it without risk. As in any fire, wear self-contained breathing apparatus and full protective gear.

**6. ACCIDENTAL RELEASE MEASURES**

**Personal Precautions** Avoid contact with skin, eyes and clothing. Wear personal protective equipment. Isolate and post spill area. Keep people away from and upwind of spill/leak. Eliminate all sources of ignition and remove combustible materials.

**Other** Combustible materials exposed to hydrogen peroxide should be immediately submerged in or rinsed with large amounts of water to ensure that all hydrogen peroxide is removed. Residual hydrogen peroxide that is allowed to dry (upon evaporation hydrogen peroxide can concentrate) on organic materials such as paper, fabrics, cotton, leather, wood or other combustibles can cause the material to ignite and result in fire.

**Environmental Precautions** Prevent material from entering into soil, ditches, sewers, waterways, and/or groundwater. See Section 12, Ecological Information for more detailed information.

**Methods for Containment** Dike to collect large liquid spills. Stop leak and contain spill if this can be done safely. Small spillage: Dilute with large quantities of water.

**Methods for cleaning up** Flush area with flooding quantities of water. Hydrogen peroxide may be decomposed by adding sodium metabisulfite or sodium sulfite after diluting to about 5%.

**7. HANDLING AND STORAGE**

**Handling** CONSULT PEROXYCHEM FOR APPROVED PERSONAL PROTECTIVE EQUIPMENT AND HANDLING AND STORAGE PROCEDURES. Wear chemical splash-type monogoggles and full face shield, Gortex®, polyester or acrylic full cover clothing and approved rubber or nitrile gloves and shoes. Do not use cotton, wool or leather for these materials react rapidly with hydrogen peroxide concentrations greater than 90%. Avoid contamination and heat as these will cause decomposition and generation of oxygen gas which will result in high pressures and possible container rupture. Hydrogen peroxide should be stored only in vented containers and transferred only in a prescribed manner (contact Peroxychem for procedures). Never return unused hydrogen peroxide to original container. Empty aluminum drums should be returned to Peroxychem. Utensils used for handling hydrogen peroxide should be made only of clean glass, pre-approved passivated aluminum or stainless steel, or approved plastics such as polytetrafluoroethylene. Do not discard 90% or higher concentrations without first diluting to less than 5%.

**Storage** Keep containers in cool areas out of direct sunlight and away from combustibles. Provide mechanical general and/or local exhaust ventilation to prevent release of vapor or mist into work environment. Containers must be vented. Keep/store only in original container. Store rooms or warehouses should be made of non-combustible materials with impermeable floors. In case of release, spillage should flow to safe area. Containers should be visually inspected on a regular basis to detect any abnormalities (swollen drums, increases in temperature, etc.).

**Incompatible products** Combustible materials. Copper alloys, galvanized iron. Strong reducing agents. Heavy metals. Iron. Copper alloys. Contact with metals, metallic ions, alkalis, reducing agents and organic matter (such as alcohols or terpenes) may produce self-accelerated thermal decomposition.

**8. EXPOSURE CONTROLS/PERSONAL PROTECTION**

Control parameters

**Exposure Guidelines** Ingredients with workplace control parameters.

Chemical name	ACGIH TLV	OSHA PEL	NIOSH	Mexico
Hydrogen peroxide 7722-84-1	TWA: 1 ppm	TWA: 1 ppm TWA: 1.4 mg/m <sup>3</sup>	IDLH: 75 ppm TWA: 1 ppm TWA: 1.4 mg/m <sup>3</sup>	Mexico: TWA 1 ppm Mexico: TWA 1.5 mg/m <sup>3</sup> Mexico: STEL 2 ppm

# Hydrogen Peroxide 90% HTP

SDS # : 7722-84-1-90-60  
Revision date: 2015-05-28  
Version 1

Chemical name	British Columbia	Quebec	Ontario TWAEV	Mexico: STEL 3 mg/m <sup>3</sup> Alberta
Hydrogen peroxide 7722-84-1	TWA: 1 ppm	TWA: 1 ppm TWA: 1.4 mg/m <sup>3</sup>	TWA: 1 ppm	TWA: 1 ppm TWA: 1.4 mg/m <sup>3</sup>

## Appropriate engineering controls

**Engineering measures** Showers. Eyewash stations. Ventilation systems.

## Individual protection measures, such as personal protective equipment

<b>Eye/Face Protection</b>	Use chemical splash-type monogoggles and a full-face shield made of polycarbonate, acetate, polycarbonate/acetate, PETG or thermoplastic.
<b>Skin and Body Protection</b>	For body protection wear impervious clothing such as an approved splash protective suit made of SBR rubber, PVC (PVC Outershell w/Polyester Substrate), Gore-Tex (Polyester trilaminate w/Gore-Tex), or a specialized HAZMAT Splash or Protective Suite (Level A, B, or C). DO NOT wear any form of splash suit or rainwear made of nylon or nylon-blends. For foot protection, wear approved boots made of NBR, PVC, Polyurethane, or neoprene. Overboots made of Latex or PVC, as well as firefighter boots or specialized HAZMAT boots are also permitted. DO NOT wear any form of boot or overboot made of nylon or nylon blends. DO NOT USE cotton, wool or leather as these materials react RAPIDLY with 90% or higher concentrations of hydrogen peroxide. Completely submerge hydrogen peroxide contaminated clothing or other materials in water prior to drying. Residual hydrogen peroxide, if allowed to dry on materials such as paper, fabrics, cotton, leather, wood or other combustibles, can cause the material to ignite and result in a fire.
<b>Hand Protection</b>	For hand protection, wear approved gloves made of nitrile, PVC, or neoprene. DO NOT use cotton, wool or leather for these materials react RAPIDLY with higher concentrations of hydrogen peroxide. Thoroughly rinse the outside of gloves with water prior to removal. Inspect regularly for leaks.
<b>Respiratory Protection</b>	If concentrations in excess of 10 ppm are expected, use NIOSH/DHHS approved self-contained breathing apparatus (SCBA) or other approved air-supplied respirator (ASR) equipment (e.g., a full-face airline respirator (ALR)). DO NOT use any form of air-purifying respirator (APR) or filtering facepiece (dust mask), especially those containing oxidizable sorbants such as activated carbon.
<b>Hygiene measures</b>	Avoid breathing vapors, mist or gas. Clean water should be available for washing in case of eye or skin contamination. .
<b>General information</b>	Protective engineering solutions should be implemented and in use before personal protective equipment is considered.

## 9. PHYSICAL AND CHEMICAL PROPERTIES

### Information on basic physical and chemical properties

<b>Appearance</b>	Clear, colorless liquid
<b>Physical State</b>	Liquid
<b>Color</b>	Colorless
<b>Odor</b>	odorless
<b>Odor threshold</b>	Not applicable
<b>pH</b>	<= 1
<b>Melting point/freezing point</b>	-12 °C
<b>Boiling Point/Range</b>	141 °C
<b>Flash point</b>	Seta Closed Cup: (90% ) 82 - 85°C. No visible flame observed. Reaction attributed to rapid decomposition.
<b>Evaporation Rate</b>	> 1 (n-butyl acetate=1)
<b>Flammability (solid, gas)</b>	Non-flammable but vapor phase decomposition occurs at 7.6 vol. % for 90 % based on flash point.
<b>Flammability Limit in Air</b>	Not applicable
<b>Upper flammability limit:</b>	

## Hydrogen Peroxide 90% HTP

SDS # : 7722-84-1-90-60  
Revision date: 2015-05-28  
Version 1

<b>Lower flammability limit:</b>	
<b>Vapor pressure</b>	5 mm Hg @ 30 °C
<b>Vapor density</b>	No information available
<b>Density</b>	1.39 g/cm <sup>3</sup> @ 20°C
<b>Specific gravity</b>	1.39
<b>Water solubility</b>	completely soluble
<b>Solubility in other solvents</b>	No information available
<b>Partition coefficient</b>	No data available
<b>Autoignition temperature</b>	ASTM E 659-78: 99% - 210°C (in air) 169°C (in oxygen). Reaction was attributed to rapid decomposition of vapors.
<b>Decomposition temperature</b>	740 °C
<b>Viscosity, kinematic</b>	1.15 cP @ 25 °C
<b>Viscosity, dynamic</b>	No information available
<b>Explosive properties</b>	No information available
<b>Oxidizing properties</b>	Powerful oxidizer
<b>Molecular weight</b>	34
<b>Bulk density</b>	Not applicable

## 10. STABILITY AND REACTIVITY

<b>Reactivity</b>	Reactive and oxidizing agent.
<b>Chemical Stability</b>	Stable under normal conditions. Decomposes on heating. Stable under recommended storage conditions.
<b>Possibility of Hazardous Reactions</b>	A severe detonation hazard when mixed with organics. Contact with combustibles will cause fire. While not flammable by OSHA and DOT definitions, contamination, contact with incompatible materials, or high temperatures could cause a rapid decomposition that yields heat and oxygen, which support combustion and will cause a rapid overpressure if confined.
<b>Hazardous polymerization</b>	Hazardous polymerization does not occur.
<b>Conditions to avoid</b>	Excessive heat; Contamination; Exposure to UV-rays; pH variations.
<b>Incompatible materials</b>	Combustible materials. Copper alloys, galvanized iron. Strong reducing agents. Heavy metals. Iron. Copper alloys. Contact with metals, metallic ions, alkalis, reducing agents and organic matter (such as alcohols or terpenes) may produce self-accelerated thermal decomposition.
<b>Hazardous Decomposition Products</b>	Oxygen which supports combustion. Liable to produce overpressure in container.

## 11. TOXICOLOGICAL INFORMATION

### Product Information

<b>LD50 Oral</b>	50% solution: LD50: > 225 mg/kg bw (rat) 35 % solution: LD50 1193 mg/kg bw (rat) 70 % solution: LD50 1026 mg/kg bw (rat)
<b>LD50 Dermal</b>	35% solution: LD50 > 2000 mg/kg bw (rabbit) 70 % solution: LD50 9200 mg/kg bw (rabbit)
<b>LC50 Inhalation</b>	50% solution: LC50 > 170 mg/m <sup>3</sup> (rat) (4-hr) Hydrogen Peroxide vapors: LC0 9400 mg/m <sup>3</sup> (mouse) (5 - 15 minutes) Hydrogen Peroxide vapors: LC50 > 2160 mg/m <sup>3</sup> (mouse)
<b>Sensitization</b>	Did not cause sensitization on laboratory animals.

### Information on toxicological effects

<b>Symptoms</b>	Vapors, mists, or aerosols of hydrogen peroxide can cause upper airway irritation, inflammation of the nose, hoarseness, shortness of breath, and a sensation of burning or tightness in the chest. Prolonged exposure to concentrated vapor or to dilute solutions can
-----------------	---



## Hydrogen Peroxide 90% HTP

SDS # : 7722-84-1-90-60  
Revision date: 2015-05-28  
Version 1

cause irritation and temporary bleaching of skin and hair. Exposure to vapor, mist, or aerosol can cause stinging pain and tearing of eyes.

### Delayed and immediate effects as well as chronic effects from short and long-term exposure

**Carcinogenicity** This product contains hydrogen peroxide. The International Agency for Research on Cancer (IARC) has concluded that there is inadequate evidence for carcinogenicity of hydrogen peroxide in humans, but limited evidence in experimental animals (Group 3 - not classifiable as to its carcinogenicity to humans). The American Conference of Governmental Industrial Hygienists (ACGIH) has concluded that hydrogen peroxide is a 'Confirmed Animal Carcinogen with Unknown Relevance to Humans' (A3).

Chemical name	ACGIH	IARC	NTP	OSHA
Hydrogen peroxide 7722-84-1	A3	3		

**Mutagenicity** This product is not recognized as mutagenic by Research Agencies  
In vivo tests did not show mutagenic effects

**Reproductive toxicity** This product is not recognized as reprotox by Research Agencies.

**STOT - single exposure** May cause respiratory irritation.  
**STOT - repeated exposure** Not classified.

**Target organ effects** Eyes, Respiratory System, Skin.

**Aspiration hazard** Aspiration risk: may cause lung damage if swallowed.

## 12. ECOLOGICAL INFORMATION

### Ecotoxicity

**Ecotoxicity effects** Hydrogen peroxide is naturally produced by sunlight (between 0.1 and 4 ppb in air and 0.001 to 0.1 mg/L in water). Not expected to have significant environmental effects.

Hydrogen peroxide (7722-84-1)				
Active Ingredient(s)	Duration	Species	Value	Units
Hydrogen peroxide	96 h LC50	Fish Pimephales promelas	16.4	mg/L
Hydrogen peroxide	72 h LC50	Fish Leuciscus idus	35	mg/L
Hydrogen peroxide	48 h EC50	Daphnia pulex	2.4	mg/L
Hydrogen peroxide	24 h EC50	Daphnia magna	7.7	mg/L
Hydrogen peroxide	72 h EC50	Algae Skeletonema costatum	1.38	mg/L
Hydrogen peroxide	21 d NOEC	Daphnia magna	0.63	mg/L

**Persistence and degradability** Hydrogen peroxide in the aquatic environment is subject to various reduction or oxidation processes and decomposes into water and oxygen. Hydrogen peroxide half-life in freshwater ranged from 8 hours to 20 days, in air from 10 - 20 hours, and in soils from minutes to hours depending upon microbiological activity and metal contamination.

**Bioaccumulation** Material may have some potential to bioaccumulate but will likely degrade in most environments before accumulation can occur.

**Mobility** Will likely be mobile in the environment due to its water solubility but will likely degrade over time.

**Other Adverse Effects** Decomposes into oxygen and water. No adverse effects.

**13. DISPOSAL CONSIDERATIONS**

**Waste disposal methods** Dispose of in accordance with local regulations. Can be disposed as waste water, when in compliance with local regulations.

**US EPA Waste Number** D001 D002

**Contaminated Packaging** Dispose of in accordance with local regulations. Drums - Empty as thoroughly as possible. Triple rinse drums before disposal. Avoid contamination; impurities accelerate decomposition. Never return product to original container.

**14. TRANSPORT INFORMATION**

DOT

**UN/ID no** 2015  
**Proper Shipping Name** HYDROGEN PEROXIDE, AQUEOUS SOLUTION, STABILIZED  
**Hazard class** 5.1 (Oxidizer)  
**Subsidiary class** 8  
**Packing Group** I

TDG

**UN/ID no** UN 2015  
**Proper Shipping Name** HYDROGEN PEROXIDE, AQUEOUS SOLUTION, STABILIZED  
**Hazard class** 5.1 (Oxidizer)  
**Subsidiary class** 8  
**Packing Group** I

ICAO/IATA

Hydrogen peroxide (>40%) is forbidden on Passenger and Cargo Aircraft.

IMDG/IMO

**UN/ID no** 2015  
**Proper Shipping Name** HYDROGEN PEROXIDE, AQUEOUS SOLUTION, STABILIZED  
**Hazard class** 5.1  
**Subsidiary Hazard Class** 8  
**Packing Group** I

**OTHER INFORMATION**

Protect from physical damage. Keep drums in upright position. Drums should not be stacked in transit. Do not store drums on wooden pallets.

**15. REGULATORY INFORMATION**

**U.S. Federal Regulations**

**SARA 313**

Section 313 of Title III of the Superfund Amendments and Reauthorization Act of 1986 (SARA). This product does not contain any chemicals which are subject to the reporting requirements of the Act and Title 40 of the Code of Federal Regulations, Part 372

**SARA 311/312 Hazard Categories**

<b>Acute health hazard</b>	Yes
<b>Chronic health hazard</b>	No
<b>Fire hazard</b>	Yes
<b>Sudden release of pressure hazard</b>	No
<b>Reactive Hazard</b>	No

**Clean Water Act**

This product does not contain any substances regulated as pollutants pursuant to the Clean Water Act (40 CFR 122.21 and 40 CFR 122.42)

# Hydrogen Peroxide 90% HTP

SDS # : 7722-84-1-90-60  
 Revision date: 2015-05-28  
 Version 1

## CERCLA

This material, as supplied, contains one or more substances regulated as a hazardous substance under the Comprehensive Environmental Response Compensation and Liability Act (CERCLA) (40 CFR 302):

Chemical name	Hazardous Substances RQs	Extremely Hazardous Substances RQs	SARA RQ
Hydrogen peroxide 7722-84-1		1000 lb	

Hydrogen Peroxide RQ is for concentrations of > 52% only

## International Inventories

Component	TSCA (United States)	DSL (Canada)	EINECS/EL INCS (Europe)	ENCS (Japan)	China (IECSC)	KECL (Korea)	PICCS (Philippines)	AICS (Australia)	NZIoC (New Zealand)
Hydrogen peroxide 7722-84-1 ( 90 )	X	X	X	X	X	X	X	X	X

Mexico - Grade Serious risk, Grade 3

## CANADA

WHMIS Hazard Class C - Oxidizing materials  
 D1B - Toxic materials  
 E - Corrosive material  
 F - Dangerously reactive material



## 16. OTHER INFORMATION

NFPA	Health Hazards 3	Flammability 0	Stability 3	Special Hazards OX
HMIS	Health Hazards 3	Flammability 0	Physical hazard 3	Special precautions H

### NFPA/HMIS Ratings Legend

Severe = 4; Serious = 3; Moderate = 2; Slight = 1; Minimal = 0

Special Hazards: OX = Oxidizer

Protection = H (Safety goggles, gloves, apron, the use of supplied air or SCBA respirator is required in lieu of a vapor cartridge respirator)

Uniform Fire Code Oxidizer: Class 3--Liquid

Revision date: 2015-05-28  
 Revision note Initial Release

### Disclaimer

PeroxyChem believes that the information and recommendations contained herein (including data and statements) are accurate as of the date hereof. **NO WARRANTY OF FITNESS FOR ANY PARTICULAR PURPOSE, WARRANTY OF MERCHANTABILITY OR ANY OTHER WARRANTY, EXPRESSED OR IMPLIED, IS MADE CONCERNING THE INFORMATION PROVIDED HEREIN.** The information provided herein relates only to the specified product designated and may not be applicable where such product is used in combination with any other materials or in any process. Further, since the conditions and methods of use are beyond the control of PeroxyChem, PeroxyChem expressly disclaims any and all liability as to any results obtained or arising from any use of the products or reliance on such information.

Prepared By:

PeroxyChem  
 © 2015 PeroxyChem. All Rights Reserved.

**End of Safety Data Sheet**

**Hydrogen Peroxide 90% HTP**

**SDS # :** 7722-84-1-90-60  
**Revision date:** 2015-05-28  
**Version** 1

C

# Ethanol Label

TechniSolv  
**Ethanol absolute**

Ethanol absolu  
Ethanol absolut

**83813.360 | Size: 5 L**

Lot: 21J224009 | Use by: 2026-Oct-18

CAS: 64-17-5 | MW: 46,07  
Formula:  $H_3CCH_2OH$   
EC number: 200-578-6 | Density: 0,79 kg/l  
Date opened:

Assay (V/V)	100.0 %
Density (20/20)	0.791
Water	< 0.1 %



**Ethyl alcohol 100% technical grade**  
**000001170** (5th)

051

01. Hal 0.32/CCabinet 8/S4  
SC280110 ADR: 3  
TUDelft

Danger - Highly flammable liquid and vapour. Causes serious eye irritation. Keep away from heat, hot surfaces, sparks, open flames and other ignition sources. No smoking. Take precautionary measures against static discharge. Wear protective gloves/protective clothing/eye protection/face protection. IF IN EYES: Rinse cautiously with water for several minutes. Remove contact lenses, if present and easy to do. Continue rinsing. Store in a well-ventilated place. Keep cool.

Danger - Liquide et vapeurs très inflammables. Provoque une sévère irritation des yeux. Tenir à l'écart de la chaleur, des surfaces chaudes, des étincelles, des flammes nues et de toute autre source d'inflammation. Ne pas fumer. Prendre des mesures de précaution contre les décharges électrostatiques. Porter des gants de protection/des vêtements de protection/un équipement de protection des yeux/du visage. EN CAS DE CONTACT AVEC LES YEUX: rincer avec précaution à l'eau pendant plusieurs minutes. Enlever les lentilles de contact si la victime en porte et si elles peuvent être facilement enlevées. Continuer à rincer. Stocker dans un endroit bien ventilé. Tenir au frais.

Gefahr - Flüssigkeit und Dampf leicht entzündbar. Verursacht schwere Augenreizung. Von Hitze, heißen Oberflächen, Funken, offenen Flammen sowie anderen Zündquellenarten fernhalten. Nicht rauchen. Maßnahmen gegen elektrostatische Aufladungen treffen. Schutzhandschuhe/Schutzkleidung/Augenschutz/Gesicht tragen. BEI KONTAKT MIT DEN AUGEN: Einige Minuten lang behutsam mit Wasser spülen. Vorhandene Kontaktlinsen nach Möglichkeit entfernen. Weiter spülen. Kühl an einem gut belüfteten Ort aufbewahren.

H+P: H225+H319+P210+P243+P280+P305+P351+P338+P403+P235

For Specifications, C of A and SDS please go to [vwr.com](http://vwr.com) or scan the QR code on the right. For Professional use in Laboratory or Manufacturing. Not for use as an Active Pharmaceutical Ingredient or Food or Animal Feed.

Manufactured by: VWR International S.A.S. 1-3 Rue d'Aurion - F-93114 Rosny-sous-Bois-cedex FRANCE +33145148500  
Made in FRANCE

ETHANOL 3, II  
**UN1170**



D

## Nichrome Data Sheet

# Resistance Heating Wire Nickel-Chromium Alloy 80% Nickel/20% Chromium

- ✓ Withstands High Temperatures up to 1150°C (2100°F)
- ✓ Quick Heating, Long Life
- ✓ Corrosion Resistant
- ✓ Used to Make Straight or Helical Coil Resistance Heaters
- ✓ Convenient 15 m and 60 m Spools Available

OMEGA® NIC80 wire is a resistance heating wire comprised of 80% Nickel and 20% Chromium. NIC80 wire is commonly used as a resistor at elevated temperatures. NI/CR-80/20 is essential for resistor elements in high temperature applications such as electric furnaces, electric ranges and radiant heaters operating at temperatures up to 1150°C (2100°F).

In addition to these qualities and standard uses, it has found wide application in technical applications due to its combination of high electrical resistance and its temperature coefficient of resistance much less than that of Nickel-Chrome 60.



See Page G-39  
for Coiled  
Resistance Wire

## Specifications

**Composition:** 80% Ni, 20% Cr

**Specific Resistance:**

650 Ohms per circular mil-foot at 20°C (68°F). See table below for multiplication factors to obtain resistance at other temperatures.

**Specific Gravity:** 8.41

**Density:** 8.4g/cm<sup>3</sup>

**Melting Point:** approx.  
1400°C (2550°F)

**Nominal Coefficient of Linear Expansion:** 0.000017 (10-1000°C)

**Tensile Strength (Kg/cm<sup>2</sup>) 20°C:**

Hard Drawn: 14,060

Soft Annealed: 7,030

**Nominal Temperature**

**Coefficient of Resistance:**

0.00011 Ohms/Ohm/°C (20-500°C)

Factor by Which Resistance at Room Temperature Is to Be Multiplied to Obtain Resistance at Indicated Temperatures (These figures are given as a basis for engineering calculations and represent average material as supplied.)											
Temp. °F	68	200	400	600	800	1000	1200	1400	1600	1800	2000°F
Temp. °C	20	93	204	315	427	538	649	760	871	982	1093°C
Factor	1.000	1.016	1.037	1.054	1.066	1.070	1.064	1.062	1.066	1.072	1.078

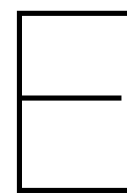
To Order (Specify Model Number)										IN STOCK FOR FAST DELIVERY!	
AWG	Dia. mm	Ohms per 30cm @ 20°C (68°F)	Current Temperature Characteristics* °C (°F)						Model No.	Price	
			425 (800)	550 (1000)	650 (1200)	750 (1400)	875 (1600)	1100 (2000)		15 m	60 m
18	1 (.040)	.4062	8.32	10.17	12.48	15.11	18.06	24.03	NI80-040-(†)	£17.25	£52.00
20	.8 (.032)	.6348	6.17	7.56	9.24	11.13	13.23	17.57	NI80-032-(†)	13.00	39.50
22	.64 (.0253)	1.015	4.62	5.62	6.85	8.20	9.69	12.85	NI80-025-(†)	13.00	39.50
24	.5 (.0201)	1.609	3.46	4.18	5.06	6.04	7.10	9.40	NI80-020-(†)	13.00	39.50
26	.4 (.0159)	2.571	2.62	3.12	3.76	4.49	5.27	6.90	NI80-015-(†)	8.20	24.50
28	.3 (.0126)	4.094	1.98	2.38	2.84	3.37	3.93	5.09	NI80-012-(†)	8.20	24.50
30	.25 (.010)	6.50	1.50	1.81	2.14	2.53	2.93	3.75	NI80-010-(†)	8.20	24.50

\* Showing approximate amperes necessary to produce a given temperature, applying only to a straight wire stretched horizontally in free air.

Note: This wire is not intended for use in making thermocouple elements. † Specify desired length in metres: 15m or 60m

Ordering Example: NI80-040-15m is a 15 m spool of 1.0mm bare wire, £17.25.





# Photron FASTCAM NOVA S6 Data Sheet



## PRODUCT DATASHEET

# NOVA<sup>S</sup>

FASTCAM series by Photron



FASTCAM NOVA S16 / S12 / S9 / S6

### 1-Megapixel CMOS Image Sensor:

1024 x 1024 pixels at 16,000fps (Model S16)

1024 x 1024 pixels at 12,800fps (Model S12)

1024 x 1024 pixels at 9,000fps (Model S9)

1024 x 1024 pixels at 6,400fps (Model S6)

### Maximum Frame Rate:

1,100,000fps (Nova S16 type 1100K)

1,000,000fps (Nova S12 type 1000K)

900,000fps (Nova S9 type 900K)

800,000fps (Nova S6 type 800K)

500,000fps (Nova S16 / S12 / S9 / S6 type 500K)

200,000fps (Nova S16 / S12 / S9 / S6 type 200K)

### Class Leading Light Sensitivity:

ISO 64,000 monochrome

ISO 16,000 color

### Global Electronic Shutter:

1ms to 0.2 $\mu$ s independent of frame

rate (sub-microsecond shutter available subject to export control)

### Dynamic Range (ADC):

12-bit monochrome

36-bit color

### Compact and Lightweight:

120mm (H) x 120mm (W) x 217.2mm (D)

4.72" (H) x 4.72" (W) x 8.55" (D)

Weight: 3.3kg (7.2 lbs.)

### Internal Recording Memory:

8GB, 16GB, 32GB, 64GB, 128GB

### Optional FASTDrive Removable High Capacity Data Storage:

4TB High-speed Solid State Drive

### Fast 10-Gigabit Ethernet Interface:

Provides camera control and high-speed image download to standard PC

### Fan Stop Function:

Remotely switch off cooling fans to eliminate vibration when recording at high magnifications

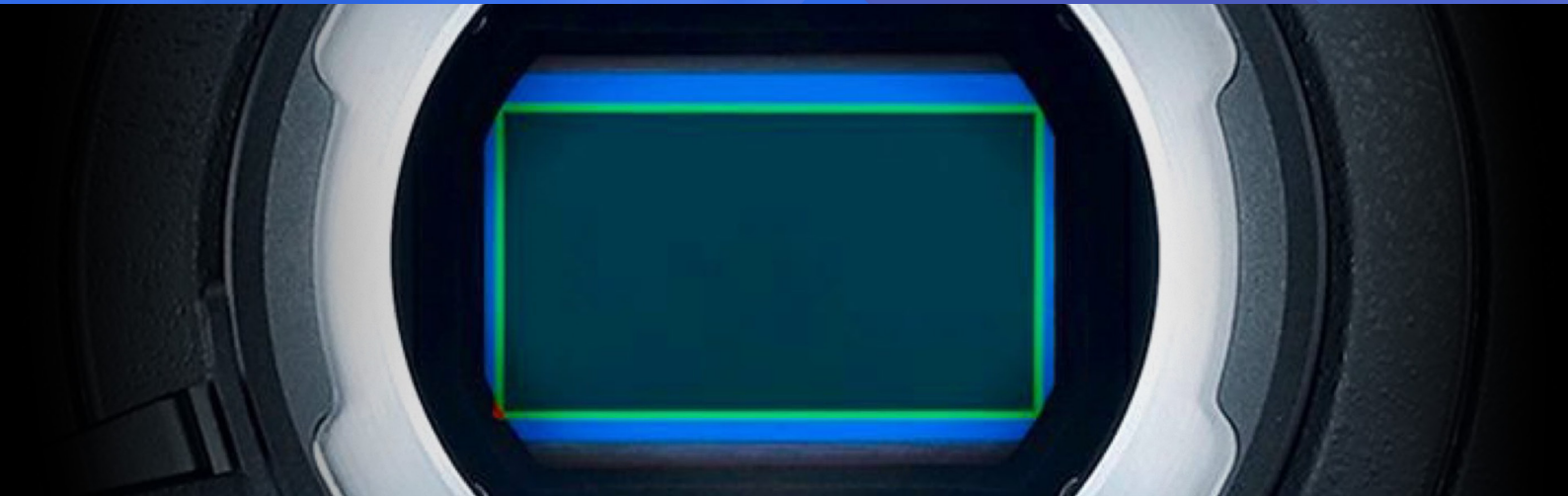
## COMPACT AND VERSATILE HIGH PERFORMANCE CAMERA SYSTEM

The FASTCAM NOVA brings together unique CMOS image sensor technologies and extensive high-speed digital imaging expertise to provide a camera with the flexibility to be used in a wide variety of applications. Available in four different models, the FASTCAM NOVA offers 12-bit image recording rates up to 16,000 frames per second (fps) at megapixel image resolution, and shutter speeds to 0.2 $\mu$ s. Recording rates to 1,100,000fps are available at reduced image resolution. All of this available from a camera that is rugged, compact, lightweight and provides the best light sensitivity in its class.

Standard features of the FASTCAM NOVA include an internal mechanical shutter to allow remote system calibration, a high-performance 10-Gigabit Ethernet interface for camera control and high-speed image download, memory segmentation that allows recording into one memory partition while downloading from another, and compatibility with a number of industry standard lens formats to allow the use of Nikon G-Type, C-mount and Canon EF lenses.

The FASTCAM NOVA also features a "sealed body" design that prevents dust and corrosive particles from contaminating sensitive electronics. An optional FASTDrive SSD can be used for the download of images at up to 1GB per second.

Intuitive and feature rich Photron FASTCAM Viewer (PFV) software is included with each FASTCAM NOVA camera. Also included is a Photron Device Control SDK that allows integration of the camera with user-specific software, and libraries for controlling the camera within a MATLAB® or LabView environment.



## Light Sensitivity:

### FASTCAM NOVA

Monochrome models	ISO 64,000
Color models	ISO 16,000

Monochrome sensors used in the FASTCAM NOVA are supplied without an IR absorbing filter, extending the camera spectral response beyond 900nm. When the sensitivity of the FASTCAM NOVA is measured to tungsten light including near IR response an equivalent value of ISO 160,000 is obtained.

### Image Sensor:

The FASTCAM NOVA uses an advanced CMOS image sensor optimized for light sensitivity and high image quality that is unique to Photron.

A 20-micron pixel pitch gives a sensor size at full image resolution of 20.48 x 20.48mm (diagonal 28.96mm).

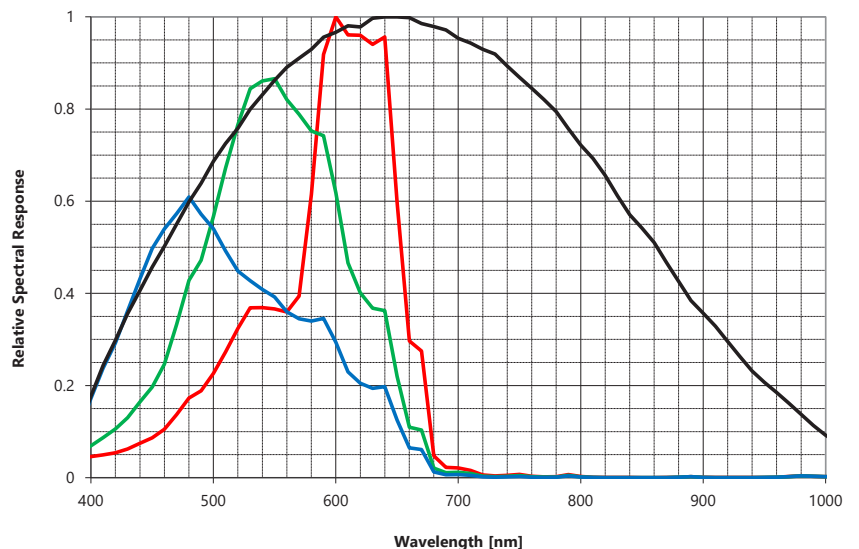
Lenses designed for both FX (35mm full frame) and also DX (APS-C digital SLR) formats are fully compatible with the FASTCAM NOVA at full image resolution.

Sensor Type	Proprietary Design Advanced CMOS
Maximum Resolution (pixels)	1024 x 1024 pixels
Sensor Size / Diagonal	20.48 x 20.48mm / 28.96mm
Pixel Size (microns)	20µm x 20µm
Quantum Efficiency	78.5% at 590nm
Fill Factor	Effective Fill Factor 94.5%
Color Matrix	Bayer CFA (single sensor)
Light Sensitivity	ISO 64,000 monochrome ISO 16,000 color (monochrome sensor equivalent ISO 160,000 including near IR response)

### Shutter

Global Electronic Shutter 1ms to 0.2µs independent of frame rate (sub-microsecond shutter available subject to export control)

FASTCAM Nova Relative Spectral Response Curves – Monochrome and Color



Specifications subject to change.

# Camera Performance Specifications

## Camera Performance Specifications

Model	FASTCAM Nova S16	FASTCAM Nova S12	FASTCAM Nova S9	FASTCAM Nova S6
Full Frame Performance	16,000fps 1024 x 1024 pixels	12,800fps 1024 x 1024 pixels	9,000fps 1024 x 1024 pixels	6,400fps 1024 x 1024 pixels
Maximum Frame Rate	1,100,000fps (128 x 16 pixels)*	1,000,000fps (128 x 16 pixels)*	900,000fps (128 x 16 pixels) *	800,000fps (128 x 16 pixels) *
Minimum Exposure Time	Global electronic shutter to 0.2µs selectable independent of frame rate (subject to export control)			
Ruggedized Mechanical Calibration Shutter	Standard feature			
Dynamic Range (ADC)	12-bit monochrome 36-bit color			
Memory Capacity Options	8GB, 16GB, 32GB, 64GB, or 128GB			
Memory Partitions	Up to 128 memory segments			
Region of Interest	Selectable in steps of 128 pixels (horizontal) x 16 pixels (vertical)			
Trigger Inputs	Selectable +/- TTL 5V and switch input (may be configured NO or NC)			
Trigger Delay	Programmable on selected input / output triggers: 100ns resolution			
Input / Output	Input: Trigger (TTL/Switch), sync, ready, event, IRIG Output: trigger, sync, ready, rec, exposure			
Trigger Modes	Start, end, center, manual, random, random reset			
Time Code Input	IRIG-B (selectable at beginning or end of frame exposure)			
External Sync	+/- TTL 5Vp-p Variable frequency sync			
Camera Control Interface	High-speed 1/10 Gigabit Ethernet			
Image Data Display	Frame rate, shutter speed, trigger mode, date/time, status, real time / IRIG time, frame count, resolution			
Saved Image Formats	BMP, TIFF, JPEG, PNG, RAWW, MRAW, AVI, MOV - Images can be saved with or without image data and in 8-bit, 16-bit or bit depth of sensor			
Supported OS	Microsoft Windows operating system including: 8.1, 10 (32/64-bit)			

\* Frame rates above 225,000fps and exposure times below 1µs may be subject to export control regulations in some areas

### Optional Removable Data Storage:

The FASTCAM NOVA can be supplied with the Photron FASTDrive high capacity removable SSD. The ultra-high data rate FASTDrive allows a 64GB camera recording to be transferred to a removable SSD drive in approximately 1 minute. Recorded data can then be directly accessed while coupled to the camera or the drive may be removed and inserted into the portable FASTDock station connected to any Windows PC.



### High-Speed 10-Gigabit Ethernet Interface:

The FASTCAM NOVA camera system is equipped with a high-speed Gigabit Ethernet Interface to provide reliable camera control and fast download of image data.

### Dedicated I/O:

A dedicated BNC connection for a contact closure hardware trigger input is provided. In addition, two programmable inputs and two programmable output channels provide direct connection for common tasks such as synchronization of multiple cameras and operation in conjunction with Data Acquisition (DAQ) hardware.

### Ruggedized Mechanical Calibration Shutter:

The ruggedized mechanical shutter fitted as standard to the FASTCAM NOVA camera allows sensor black balance calibration to be carried out remotely from the system control software.

### Nikon G-Type Compatible Lens Mount:

The FASTCAM NOVA camera is equipped with an objective lens mount compatible with readily available Nikon G-type lenses. Controls provided within the lens mount allow the control of lens aperture on lenses without external iris control.

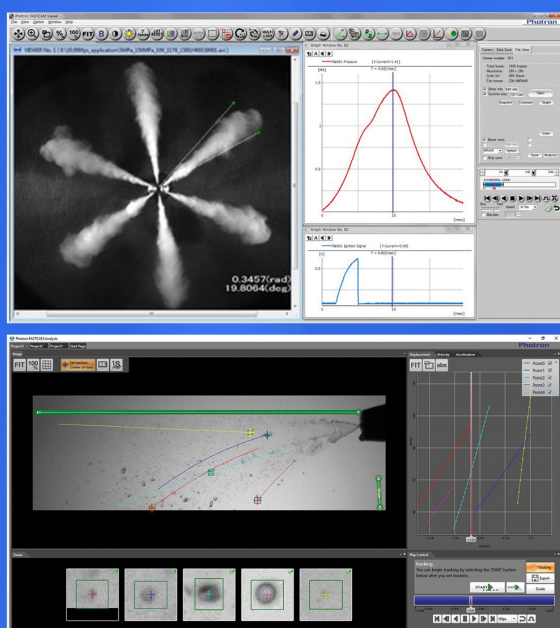


## Camera Operation Features

Frame Synchronization	Accurate frame synchronization with other cameras and with external and unstable frequencies.
Dual Slope Shutter (Extended Dynamic Range)	Selectable in 20 steps (0 to 95% in 5% increments) to prevent pixel overexposure without post processing.
Memory Partitions	Up to 128 memory segments allow multiple events to be stored in camera memory before downloading, with automatic progression to the next available partition.
Low Light Mode	Operation at minimum frame rate with separately adjustable shutter time to allow easy camera set-up and focus in ambient lighting.
Video Output	1080p live and playback via HD-SDI output
IRIG Phase Lock	Enables multiple cameras to be synchronized together with other instrumentation equipment or to a master external time source.
Internal Time Delay Generator	Allows programmable delays to be set on input and output triggers; 100ns resolution.
Event Markers	Up to ten user-entered event markers to define specific events within the recorded image sequence .
Download While Recording	FASTCAM NOVA supports Partition Recording Mode, allowing image data captured in one memory partition to be downloaded while at the same time recording into another partition.
Automatic Download	The system can be set to automatically download image data to the control PC and, when download is complete to re-arm in readiness for the next trigger with automatically incremented file names.
Software Binning	Virtual pixel binning (2x2, 4x4 etc.) allows increased light sensitivity with reduced image resolution without changing camera field of view.
FASTDrive	4TB solid state drive (SSD) memory pack provides ultra high data rate transfer to removable media.

## Operation Software Features

Image Calibration	2D image calibration allows the measurement of distance and angle from the image. A calibration grid overlay can be superimposed on the image.
Image Overlay	A stored reference image may be overlaid on the live image to allow accurate camera positioning to achieve the same view as a previous test.
Import of Multiple Image Sequences	Multiple image sequences can be loaded and simultaneously replayed. Timing of image sequences can be adjusted to create a common time reference. Time based synchronization allows images captured at different frame rates to be synchronized.
High Dynamic Range Mode	Making use of the full sensor dynamic range, HDR mode allows enhanced detail in both light and dark areas of an image to be displayed simultaneously.
Background Subtraction	In order to highlight subtle changes in an image, Background Subtraction allows a reference image to be subtracted from a recorded sequence. Details including propagation of shock waves and surface changes during impact can be visualized using the feature.
Line Profile	A line profile representing grey levels along a line drawn across any region of the image is displayed. In live mode the Line Profile can be used to ensure optimum image focus is achieved.
Histogram	A histogram displaying grey levels within a user-defined image area is displayed. In live mode the Histogram can be used to ensure that optimum exposure levels are set for the scene being recorded.



### Photron FASTCAM Viewer:

Photron FASTCAM Viewer software (PFV) has been designed to provide an intuitive and feature rich user interface for the control of Photron high-speed cameras, data saving, image replay and simple motion analysis. Advanced operation menus provide access to features for advanced camera operation and image enhancement. Tools are provided to allow image calibration and easy measurement of angles and distances from image data. Also included are a C++ SDK and wrappers for LabView and MATLAB ®.

An optional software plug-in module provides synchronization between Photron high-speed cameras and data acquired through National Instruments data acquisition systems. Synchronized data captured by the DAQ system provides waveform information which can be viewed alongside high-speed camera images.

### Photron FASTCAM Analysis:

PFV software allows image sequences to be exported directly to optional Photron FASTCAM Analysis (PFA) Motion Analysis software. This entry level Motion Analysis software with an on screen 'step by step guide' function provides automated tracking of up to 5 points using feature or correlation tracking algorithms for the automated analysis of motion within an image sequence.

### Variable Region of Interest:

Region of Interest (ROI) or sub-windowing allows a user-specified portion of the sensor to be defined to capture images. By using a reduced portion of the image area, the frame rate at which images are recorded can be increased. FASTCAM NOVA allows the ROI to be set in increments of 128 pixels horizontal and 16 pixels vertical.

### Square Image Sensor Format:

Unlike broadcast and media applications where image formats such as 16:9 have now become standard, in scientific and industrial imaging applications an image sensor with a 1:1 image format is generally accepted to be advantageous. To capture the maximum useful image data in applications including microscopy, detonics, combustion imaging and many others, a 1:1 sensor format provides greater flexibility than 'letterbox' image formats. The FASTCAM NOVA image sensor allows the user to choose either square or rectangular image formats in order to obtain the maximum subject information.

### External Frame Synchronization:

The FASTCAM NOVA can be fully synchronized with an external event to allow the timing of when each individual image is captured to be precisely referenced. The camera can be accurately synchronized to unstable frequencies allowing complex events such as combustion in rapidly accelerating or decelerating engines to be recorded and studied.

### Record During Download Operation:

FASTCAM NOVA recording memory can be divided into multiple active sections. The user can record an on-going event in one memory partition while at the same time downloading a previously recorded image sequence in order to improve workflow and optimize camera operation.



FASTCAM NOVA Model Comparison - Frame Rate				
Resolution (h x v pixels)	Frame Rate			
	Nova S16	Nova S12	Nova S9	Nova S6
1024 x 1024	16,000	12,800	9,000	6,400
1024 x 896	18,000	15,000	10,000	8,000
1024 x 768	20,000	18,000	12,000	9,000
1024 x 512	30,000	25,000	18,000	12,800
896 x 896	20,000	16,000	10,000	8,000
768 x 768	26,400	22,500	15,000	10,000
640 x 640	36,000	30,000	20,000	16,000
640 x 480	48,000	40,000	25,000	20,000
512 x 512	52,800	40,000	30,000	22,500
512 x 384	66,000	50,000	38,400	30,000
384 x 384	82,500	64,000	45,000	36,000
384 x 256	100,000	80,000	57,600	45,000
256 x 256	144,000	115,200	80,000	64,000
256 x 128	264,000	225,000	160,000	125,000
128 x 128	330,000	288,000	200,000	160,000
128 x 96	396,000	320,000	250,000	200,000
128 x 64	600,000	500,000	400,000	320,000
128 x 48	660,000	576,000	480,000	400,000
128 x 32	825,000	750,000	576,000	500,000
128 x 16	1,100,000	1,000,000	900,000	800,000

\* Specifications subject to change without notice.

FASTCAM NOVA Model Comparison - Recording Memory					
Resolution (h x v pixels)	Recording Duration (frames)				
	128GB	64GB	32GB	16GB	8GB
1024 x 1024	87,357	43,666	21,821	10,898	5,437
1024 x 896	99,836	49,904	24,938	12,455	6,214
1024 x 768	116,476	58,222	29,095	14,531	7,249
1024 x 512	174,714	87,333	43,642	21,797	10,874
896 x 896	114,099	57,034	28,501	14,234	7,101
768 x 768	155,301	77,629	38,793	19,375	9,666
640 x 640	223,634	111,786	55,862	27,900	13,919
640 x 480	298,179	149,048	74,483	37,200	18,559
512 x 512	349,429	174,666	87,285	43,594	21,749
512 x 384	465,905	232,888	116,380	58,126	28,999
384 x 384	621,207	310,518	155,173	77,501	38,665
384 x 256	931,811	465,777	232,760	116,252	57,998
256 x 256	1,397,717	698,666	349,141	174,378	86,997
256 x 128	2,795,434	1,397,333	698,282	348,757	173,994
128 x 128	5,590,869	2,794,666	1,396,565	697,514	347,989
128 x 96	7,454,492	3,726,222	1,862,087	930,019	463,985
128 x 64	11,181,738	5,589,333	2,793,130	1,395,029	695,978
128 x 48	14,908,984	7,452,444	3,724,174	1,860,039	927,971
128 x 32	22,363,477	11,178,666	5,586,261	2,790,058	1,391,957
128 x 16	44,726,954	22,357,333	11,172,522	5,580,117	2,783,914

**Note:** Recording duration (sec) = Recording duration (frames) / Frame rate (fps)

\*\* Recording time is an estimate and may be different depending on recording conditions and settings.

# Mechanical and Environmental Specifications

## Mechanical and Environmental Specifications

Mechanical	
Lens Mount	F-mount (G-type lens compatible) and C-mount provided - Optional lens mounts available include Canon EF remote control mount
Camera Mountings	4 x M6 (base and side), 2 x 1/4 - 20 UNC (top),
External Dimensions	
Camera Body (excluding protrusions)	120mm (H) x 120mm (W) x 217.2mm (D) 4.72" (H) x 4.72" (W) x 8.55" (D)
Weight	
Camera Body	3.3kg (7.2lbs)
Environmental	
Operating Temperature	0 to 50C, 32° to 122°F
Storage Temperature	-20 to 60C, -4° to 140°F
Humidity	85% or less (non-condensing)
Cooling	Internal fan cooling (fan-off mode supported)
Operational Shock	30G, 11ms, 6-axes 10 times/axis
Power	
AC Power (with supplied adapter)	100 to 240V, 50 to 60Hz
DC Power (primary input)	22 to 32V, 150VA
DC Power (battery input)	22 to 32V, 150VA



### Nikon G-Type Compatible Lens Mount:

The FASTCAM NOVA camera is equipped with an objective lens mount compatible with readily available Nikon G-type lenses. Controls provided within the lens mount allow the control of lens aperture on lenses without external iris control.

### Canon EF Lens Mount Option:

An optional lens mount supporting Canon EF lenses is available for the FASTCAM NOVA providing remote control of lens aperture and iris through Photron PFV software.

### Operation Environments:

The 'sealed body' design of the FASTCAM NOVA ensures optimum air flow and prevents dust and corrosive particles from being ingested within the internal camera body where they can damage sensitive electronics. The fans may be disabled during recording for any vibration sensitive measurements.

The FASTCAM NOVA camera has been extensively tested to ensure operation for extended periods in ambient temperatures up to 50 degrees C.

### Auto-sensing Secondary DC Input:

Two power supply connectors "DC IN" and "BATTERY" are provided. "DC IN" is the primary input and has priority. The camera automatically senses when the power supply to "DC IN" fails and switches without interruption to the secondary "BATTERY" connection.

### Versatile Mounting of Camera:

The FASTCAM NOVA has equal mounting positions on the base and one side. This permits the camera to be rotated through 90 degrees for those applications requiring maximum resolution with a vertical aspect ratio e.g. tensile testing.

Specifications subject to change without notice.

PHOTRON USA, INC.  
9520 Padgett Street, Suite 110  
San Diego, CA 92126  
USA

Tel: 858.684.3555 or 800.585.2129  
Fax: 858.684.3558  
Email: [image@photron.com](mailto:image@photron.com)  
[www.photron.com](http://www.photron.com)

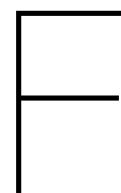
PHOTRON EUROPE LIMITED  
The Barn, Bottom Road  
West Wycombe  
Bucks. HP14 4BS  
United Kingdom

Tel: +44 (0) 1494 481011  
Fax: +44 (0) 1494 487011  
Email: [image@photron.com](mailto:image@photron.com)  
[www.photron.com](http://www.photron.com)

PHOTRON (Shanghai)  
Room 20C, Zhao-Feng  
World Trade Building  
No. 369, JiangSu Road  
Chang Ning District  
Shanghai, 200050 China  
Tel: +86 (21) 5268-3700  
Fax: +86 (21) 5268-3702  
Email: [info@photron.cn.com](mailto:info@photron.cn.com)  
[www.photron.cn.com](http://www.photron.cn.com)

PHOTRON LIMITED  
21F, Jinbocho Mitsui Bldg.  
1-105 Kanda Jimbocho  
Chiyoda-ku, Tokyo 101-0051  
Japan

Tel: +81 (3) 3518-6271  
Fax: +81 (3) 3 3518-6279  
Email: [image@photron.co.jp](mailto:image@photron.co.jp)  
[www.photron.co.jp](http://www.photron.co.jp)



## Comsol Simulation Settings

# 1 Component 1

## SETTINGS

Description	Value
Unit system	Same as global system (SI)

## 1.1 DEFINITIONS

### 1.1.1 Coordinate Systems

#### Boundary System 1

Coordinate system type	Boundary system
Tag	sys1

#### COORDINATE NAMES

First	Second	Third
t1	t2	n

## 1.2 GEOMETRY 1

### UNITS

Length unit	mm
Angular unit	deg

### GEOMETRY STATISTICS

Description	Value
Space dimension	3
Number of domains	2
Number of boundaries	12
Number of edges	24
Number of vertices	16

### 1.2.1 Cylinder 1 (cyl1)

#### POSITION

Description	Value
Position	{0, 0, 0}

#### AXIS

Description	Value
Axis type	z - axis

#### SIZE AND SHAPE

Description	Value
Radius	12
Height	75

### 1.2.2 Helix 1 (hel1)

#### POSITION

Description	Value
Position	{0, -11, 30}

#### AXIS

Description	Value
Axis type	y - axis

#### SIZE AND SHAPE

Description	Value
Number of turns	12
Major radius	2.15
Minor radius	0.2553
Axial pitch	1.8
Radial pitch	0
Chirality	Right - handed

## 1.3 MATERIALS

### 1.3.1 Water, liquid

#### SELECTION

Geometric entity level	Domain
Selection	Geometry geom1: Dimension 3: No domains

#### BASIC

Description	Value
Coefficient of thermal expansion	{{alpha_p(T), 0, 0}, {0, alpha_p(T), 0}, {0, 0, alpha_p(T)}}
Bulk viscosity	muB(T)
thermalexpansioncoefficient_symmetry	3
bulkviscosity_symmetry	0
Dynamic viscosity	eta(T)
dynamicviscosity_symmetry	0
Ratio of specific heats	gamma_w(T)
ratioofspecificheat_symmetry	0
Electrical conductivity	{{5.5e-6[S/m], 0, 0}, {0, 5.5e-6[S/m], 0}, {0, 0, 5.5e-6[S/m]}}
electricconductivity_symmetry	3
Heat capacity at constant pressure	Cp(T)
heatcapacity_symmetry	0
Density	rho(T)
density_symmetry	0
Thermal conductivity	{{k(T), 0, 0}, {0, k(T), 0}, {0, 0, k(T)}}
thermalconductivity_symmetry	3
Speed of sound	cs(T)
soundspeed_symmetry	0

### 1.3.2 Nichrome [solid,steady-state]

#### SELECTION

Geometric entity level	Domain
Selection	Geometry geom1: Dimension 3: Domain 2

#### MATERIAL PARAMETERS

Name	Value	Unit
Density	rho(T[1/K])[kg/m^3]	kg/m^3
Thermal conductivity	11.3	W/(m-K)
Heat capacity at constant pressure	480	J/(kg-K)

#### BASIC

Description	Value
Resistivity	{{res(T[1/K])[ohm*m], 0, 0}, {0, res(T[1/K])[ohm*m], 0}, {0, 0, res(T[1/K])[ohm*m]}}
resistivity_symmetry	0
Electrical conductivity	{{sigma(T[1/K])[S/m], 0, 0}, {0, sigma(T[1/K])[S/m], 0}, {0, 0, sigma(T[1/K])[S/m]}}
electricconductivity_symmetry	0
Density	rho(T[1/K])[kg/m^3]
density_symmetry	0
Thermal conductivity	{{11.3, 0, 0}, {0, 11.3, 0}, {0, 0, 11.3}}
thermalconductivity_symmetry	0
Heat capacity at constant pressure	480
heatcapacity_symmetry	0



### 1.3.3 Ethanol

#### SELECTION

Geometric entity level	Domain
Selection	Geometry geom1: Dimension 3: No domains

#### BASIC

Description	Value
Dynamic viscosity	eta(T)
dynamicviscosity_symmetry	0
Heat capacity at constant pressure	Cp(T)
heatcapacity_symmetry	0
Density	rho(T)
density_symmetry	0
Thermal conductivity	{{k(T), 0, 0}, {0, k(T), 0}, {0, 0, k(T)}}
thermalconductivity_symmetry	3
Ratio of specific heats	1.174
ratioofspecificeat_symmetry	0

### 1.3.4 H2O2 [liquid]

#### SELECTION

Geometric entity level	Domain
Selection	Geometry geom1: Dimension 3: Domain 1

#### MATERIAL PARAMETERS

Name	Value	Unit
Density	rho(T[1/K])[kg/m^3]	kg/m^3
Heat capacity at constant pressure	2619	J/(kg-K)
Thermal conductivity	0.58576	W/(m-K)
Dynamic viscosity	0.001145886	Pa-s
Ratio of specific heats	1.10293	1

#### BASIC

Description	Value
Coefficient of thermal expansion	{{(alpha(T[1/K])[1/K] + (Tempref - 293[K])*if(abs(T - Tempref)>1e-3, (alpha(T[1/K])[1/K] - alpha(Tempref[1/K])[1/K])/(T - Tempref), d(alpha(T[1/K])[1/K], T)))/(1 + alpha(Tempref[1/K])[1/K]*(Tempref - 293[K])), 0, 0), {0, (alpha(T[1/K])[1/K] + (Tempref - 293[K])*if(abs(T - Tempref)>1e-3, (alpha(T[1/K])[1/K] - alpha(Tempref[1/K])[1/K])/(T - Tempref), d(alpha(T[1/K])[1/K], T)))/(1 + alpha(Tempref[1/K])[1/K]*(Tempref - 293[K])), 0}, {0, 0, (alpha(T[1/K])[1/K] + (Tempref - 293[K])*if(abs(T - Tempref)>1e-3, (alpha(T[1/K])[1/K] - alpha(Tempref[1/K])[1/K])/(T - Tempref), d(alpha(T[1/K])[1/K], T)))/(1 + alpha(Tempref[1/K])[1/K]*(Tempref - 293[K]))}}
thermalexpansioncoefficient_symmetry	0
VP	VP(T[1/K])[Pa]
VP_symmetry	0
Density	rho(T[1/K])[kg/m^3]
density_symmetry	0
SurfF	SurfF(T[1/K])[N/m]
SurfF_symmetry	0
Heat capacity at constant pressure	2619

Description	Value
heatcapacity_symmetry	0
Thermal conductivity	{{0.58576, 0, 0}, {0, 0.58576, 0}, {0, 0, 0.58576}}
thermalconductivity_symmetry	0
Dynamic viscosity	0.001145886
dynamicviscosity_symmetry	0
Ratio of specific heats	1.10293
ratioofspecificeat_symmetry	0

#### THERMAL EXPANSION

Description	Value
Tangent coefficient of thermal expansion	{{CTE(T[1/K])[1/K], 0, 0}, {0, CTE(T[1/K])[1/K], 0}, {0, 0, CTE(T[1/K])[1/K]}}
Thermal strain	{{(dL(T[1/K]) - dL(Tempref[1/K]))/(1 + dL(Tempref[1/K])), 0, 0}, {0, (dL(T[1/K]) - dL(Tempref[1/K]))/(1 + dL(Tempref[1/K])), 0}, {0, 0, (dL(T[1/K]) - dL(Tempref[1/K]))/(1 + dL(Tempref[1/K]))}}
alphatan_symmetry	0
dL_symmetry	0

## 1.4 HEAT TRANSFER IN SOLIDS AND FLUIDS

#### USED PRODUCTS

COMSOL Multiphysics
Heat Transfer Module

#### SELECTION

Geometric entity level	Domain
Selection	Geometry geom1: Dimension 3: All domains

#### EQUATIONS

$$\rho C_p \frac{\partial T}{\partial t} + \rho C_p \mathbf{u} \cdot \nabla T + \nabla \cdot \mathbf{q} = Q$$

$$\mathbf{q} = -k \nabla T$$

### 1.4.1 Interface Settings

#### Discretization

##### SETTINGS

Description	Value
Temperature	Linear

#### Physical Model

##### SETTINGS

Description	Value
Isothermal domain	Off
Reference temperature	User defined
Reference temperature	293.15[K]

### 1.4.2 Solid 1

#### SELECTION

Geometric entity level	Domain
Selection	Geometry geom1: Dimension 3: All domains

#### EQUATIONS

$$\rho C_p \frac{\partial T}{\partial t} + \rho C_p \mathbf{u} \cdot \nabla T + \nabla \cdot \mathbf{q} = Q + Q_{ted}$$

$$\mathbf{q} = -k \nabla T$$

#### Heat Conduction, Solid

##### SETTINGS

Description	Value
Thermal conductivity	From material

### Thermodynamics, Solid

#### SETTINGS

Description	Value
Density	From material
Heat capacity at constant pressure	From material

### Coordinate System Selection

#### SETTINGS

Description	Value
Coordinate system	Global coordinate system

### Model Input

#### SETTINGS

Description	Value
Volume reference temperature	Common model input

#### USED PRODUCTS

COMSOL Multiphysics

#### PROPERTIES FROM MATERIAL

Property	Material	Property group
Thermal conductivity	Nichrome [solid,steady-state]	Basic
Density	Nichrome [solid,steady-state]	Basic
Heat capacity at constant pressure	Nichrome [solid,steady-state]	Basic

### 1.4.3 Fluid 1

#### SELECTION

Geometric entity level	Domain
Selection	Geometry geom1: Dimension 3: Domain 1

#### EQUATIONS

$$\rho c_p \frac{\partial T}{\partial t} + \rho c_p \mathbf{u} \cdot \nabla T + \nabla \cdot \mathbf{q} = Q + Q_p + Q_{vd}$$

$$\mathbf{q} = -k \nabla T$$

$$\rho = \frac{p_A}{R_s T} \text{ in ideal gas domains}$$

### Heat Conduction, Fluid

#### SETTINGS

Description	Value
Thermal conductivity	From material

### Thermodynamics, Fluid

#### SETTINGS

Description	Value
Fluid type	From material

### Coordinate System Selection

#### SETTINGS

Description	Value
Coordinate system	Global coordinate system

### Model Input

#### SETTINGS

Description	Value
Volume reference temperature	User defined
Volume reference temperature	293.15[K]

#### PROPERTIES FROM MATERIAL

Property	Material	Property group
----------	----------	----------------

Property	Material	Property group
Thermal conductivity	H2O2 [liquid]	Basic
Density	H2O2 [liquid]	Basic
Heat capacity at constant pressure	H2O2 [liquid]	Basic
Ratio of specific heats	H2O2 [liquid]	Basic

### 1.4.4 Initial Values 1

#### SELECTION

Geometric entity level	Domain
Selection	Geometry geom1: Dimension 3: All domains

### Initial Values

#### SETTINGS

Description	Value
Temperature	User defined
Temperature	200[degC]

#### USED PRODUCTS

COMSOL Multiphysics

### Variables

Name	Expression	Unit	Description	Selection
ht.Tinit	200[degC]	K	Temperature	Domain 1

### 1.4.5 Thermal Insulation 1

#### SELECTION

Geometric entity level	Boundary
Selection	Geometry geom1: Dimension 2: All boundaries

#### EQUATIONS

$$-\mathbf{n} \cdot \mathbf{q} = 0$$

#### USED PRODUCTS

COMSOL Multiphysics

### 1.4.6 Inflow 1

#### SELECTION

Geometric entity level	Boundary
Selection	Geometry geom1: Dimension 2: Boundary 3

#### EQUATIONS

$$-\mathbf{n} \cdot \mathbf{q} = \rho \Delta H \mathbf{u} \cdot \mathbf{n}$$

$$\Delta H = \int_{T_{ustr}}^T C_p dT$$

### Upstream Properties

#### SETTINGS

Description	Value
Upstream temperature	User defined
Upstream temperature	293.15[K]
Specify upstream absolute pressure	Off

### 1.4.7 Outflow 1

#### SELECTION

Geometric entity level	Boundary
Selection	Geometry geom1: Dimension 2: Boundary 4

#### EQUATIONS

$$-\mathbf{n} \cdot \mathbf{q} = 0$$

#### USED PRODUCTS

COMSOL Multiphysics

### 1.4.8 Heat Source 1

#### SELECTION

Geometric entity level	Domain
Selection	Geometry geom1: Dimension 3: Domain 2

EQUATIONS  
 $Q = Q_0$

Heat Source

SETTINGS

Description	Value
Heat source	Heat rate
Heat rate	15

USED PRODUCTS

COMSOL Multiphysics

1.4.9 Heat Flux 1

SELECTION

Geometric entity level	Boundary
Selection	Geometry geom1: Dimension 2: Boundaries 1–2, 5, 12

EQUATIONS  
 $-\mathbf{n} \cdot \mathbf{q} = q_0$   
 $q_0 = h(T_{\text{ext}} - T)$

Heat Flux

SETTINGS

Description	Value
Heat flux	Convective heat flux
Heat transfer coefficient	User defined
Heat transfer coefficient	30
External temperature	User defined
External temperature	293.15[K]

USED PRODUCTS

COMSOL Multiphysics

1.4.10 Initial Values 2

SELECTION

Geometric entity level	Domain
Selection	Geometry geom1: Dimension 3: Domain 2

Initial Values

SETTINGS

Description	Value
Temperature	User defined
Temperature	500[degC]

USED PRODUCTS

COMSOL Multiphysics

Variables

Name	Expression	Unit	Description	Selection
ht.Tinit	500[degC]	K	Temperature	Domain 2

1.4.11 Heat Flux 2

SELECTION

Geometric entity level	Boundary
Selection	Geometry geom1: Dimension 2: Boundary 4

EQUATIONS  
 $-\mathbf{n} \cdot \mathbf{q} = q_0$   
 $q_0 = h(T_{\text{ext}} - T)$

Heat Flux

SETTINGS

Description	Value
Heat flux	Convective heat flux
Heat transfer coefficient	User defined
Heat transfer coefficient	500
External temperature	User defined
External temperature	293.15[K]

USED PRODUCTS

COMSOL Multiphysics

1.5 LAMINAR FLOW

USED PRODUCTS

COMSOL Multiphysics

Heat Transfer Module

SELECTION

Geometric entity level	Domain
Selection	Geometry geom1: Dimension 3: Domain 1

EQUATIONS

$$\rho \frac{\partial \mathbf{u}}{\partial t} + \rho(\mathbf{u} \cdot \nabla)\mathbf{u} = \nabla \cdot [-p\mathbf{I} + \mathbf{K}] + \mathbf{F}$$

$$\frac{\partial \rho}{\partial t} + \nabla \cdot (\rho \mathbf{u}) = 0$$

1.5.1 Interface Settings

Discretization

SETTINGS

Description	Value
Discretization of fluids	P1 + P1

Physical Model

SETTINGS

Description	Value
Neglect inertial term (Stokes flow)	Off
Compressibility	Weakly compressible flow
Enable porous media domains	Off
Include gravity	Off
Reference pressure level	1[atm]

Turbulence

SETTINGS

Description	Value
Turbulence model type	None

Advanced Settings

SETTINGS

Description	Value
Use pseudo time stepping for stationary equation form	Automatic from physics
CFL number expression	Automatic

1.5.2 Fluid Properties 1

SELECTION

Geometric entity level	Domain
Selection	Geometry geom1: Dimension 3: All domains

EQUATIONS

$$\rho \frac{\partial \mathbf{u}}{\partial t} + \rho(\mathbf{u} \cdot \nabla)\mathbf{u} = \nabla \cdot [-p\mathbf{I} + \mathbf{K}] + \mathbf{F}$$

$$\frac{\partial \rho}{\partial t} + \nabla \cdot (\rho \mathbf{u}) = 0$$

$$\mathbf{K} = \mu(\nabla \mathbf{u} + (\nabla \mathbf{u})^T) - \frac{2}{3}\mu(\nabla \cdot \mathbf{u})\mathbf{I}$$

#### Fluid Properties

##### SETTINGS

Description	Value
	Newtonian
Dynamic viscosity	From material

#### Model Input

##### SETTINGS

Description	Value
Volume reference temperature	User defined
Volume reference temperature	293.15[K]

##### USED PRODUCTS

COMSOL Multiphysics
---------------------

##### PROPERTIES FROM MATERIAL

Property	Material	Property group
Dynamic viscosity	H2O2 [liquid]	Basic

### 1.5.3 Initial Values 1

##### SELECTION

Geometric entity level	Domain
Selection	Geometry geom1: Dimension 3: All domains

#### Initial Values

##### SETTINGS

Description	Value
Velocity field, x component	0
Velocity field, y component	0
Velocity field, z component	0
Pressure	0

#### Coordinate System Selection

##### SETTINGS

Description	Value
Coordinate system	Global coordinate system

##### USED PRODUCTS

COMSOL Multiphysics
---------------------

Name	Expression	Unit	Description	Selection
spf.u_initx	0	m/s	Velocity field, x component	Domain 1
spf.u_inity	0	m/s	Velocity field, y component	Domain 1
spf.u_initz	0	m/s	Velocity field, z component	Domain 1
spf.p_init	0	Pa	Pressure	Domain 1

### 1.5.4 Wall 1

##### SELECTION

Geometric entity level	Boundary
Selection	Geometry geom1: Dimension 2: All boundaries

##### EQUATIONS

$$\mathbf{u} = \mathbf{0}$$

#### Boundary Condition

##### SETTINGS

Description	Value
Wall condition	No slip

#### Wall Movement

##### SETTINGS

Description	Value
Translational velocity	Automatic from frame
Sliding wall	Off

#### Constraint Settings

##### SETTINGS

Description	Value
Constraints	Default
Apply reaction terms on	Individual dependent variables
Constraint method	Elemental

##### USED PRODUCTS

COMSOL Multiphysics
---------------------

### 1.5.5 Inlet 1

##### SELECTION

Geometric entity level	Boundary
Selection	Geometry geom1: Dimension 2: Boundary 3

##### EQUATIONS

$$\mathbf{u} \cdot \mathbf{t} = 0$$

$$[-p\mathbf{I} + \mathbf{K}]\mathbf{n} = -p_{\text{grad}}\mathbf{n}$$

#### Boundary Condition

##### SETTINGS

Description	Value
Boundary condition	Fully developed flow
Apply condition on each disjoint selection separately	On

#### Fully Developed Flow

##### SETTINGS

Description	Value
Fully developed flow option	Flow rate
Flow rate	5e-8

#### Constraint Settings

##### SETTINGS

Description	Value
Use weak constraints	Off
Constraint method	Elemental

### 1.5.6 Outlet 1

##### SELECTION

Geometric entity level	Boundary
Selection	Geometry geom1: Dimension 2: Boundary 4

##### EQUATIONS

$$[-p\mathbf{I} + \mathbf{K}]\mathbf{n} = -\hat{p}_0\mathbf{n}$$

$$\hat{p}_0 \leq p_0,$$

#### Boundary Condition

##### SETTINGS

Description	Value
Boundary condition	Pressure

#### Pressure Conditions

##### SETTINGS

Description	Value
Pressure	0
Normal flow	Off
Suppress backflow	On

### Constraint Settings

#### SETTINGS

Description	Value
Apply reaction terms on	All physics (symmetric)
Use weak constraints	Off
Constraint method	Elemental

#### USED PRODUCTS

COMSOL Multiphysics

## 1.6 SURFACE-TO-SURFACE RADIATION

#### USED PRODUCTS

COMSOL Multiphysics

Heat Transfer Module

#### SELECTION

Geometric entity level	Boundary
Selection	Geometry geom1: Dimension 2: All boundaries

#### EQUATIONS

$$J = \varepsilon e_b(T) + \rho_d G$$

$$G = G_m(J) + G_{amb} + G_{ext}$$

$$G_{amb} = F_{amb} e_b(T_{amb})$$

$$e_b(T) = \sigma T^4$$

### 1.6.1 Interface Settings

#### Discretization

#### SETTINGS

Description	Value
Surface radiosity	Linear
Value type when using splitting of complex variables	Real

#### Radiation Settings

#### SETTINGS

Description	Value
Use radiation groups	Off
Surface-to-surface radiation method	Hemicube
Radiation resolution	256
Transparent media refractive index	1
Wavelength dependence of radiative properties	Constant
Expression	0
Tolerance	0

### 1.6.2 Diffuse Surface 1

#### SELECTION

Geometric entity level	Boundary
Selection	Geometry geom1: Dimension 2: All boundaries

#### EQUATIONS

$$J = \varepsilon e_b(T) + \rho_d G$$

$$\varepsilon + \rho_d = 1$$

$$G = G_m(J) + G_{amb} + G_{ext}$$

$$G_{amb} = F_{amb} \varepsilon_{amb} e_b(T_{amb})$$

$$G_{ext} = q_s + I_{diff}$$

$$e_b(T) = \sigma T^4$$

$$q_{r,net} = \varepsilon(G - e_b(T))$$

#### Radiation Direction

#### SETTINGS

Description	Value
Radiation direction	Opacity controlled

### Ambient

#### SETTINGS

Description	Value
Define ambient temperature on each side	Off
Ambient temperature	User defined
Ambient temperature	293.15[K]
Define ambient emissivity on each side	Off
Ambient emissivity	Blackbody
Include diffuse irradiance	On
Diffuse irradiance	User defined
Diffuse irradiance	0

#### Surface Emissivity

#### SETTINGS

Description	Value
Define surface emissivity on each side	Off
Surface emissivity	User defined
Surface emissivity	0.8

#### Constraint Settings

#### SETTINGS

Description	Value
Use weak constraints	Off
Constraint method	Elemental

### 1.6.3 Initial Values 1

#### SELECTION

Geometric entity level	Boundary
Selection	Geometry geom1: Dimension 2: All boundaries

#### Initial Values

#### SETTINGS

Description	Value
Initial value	Blackbody/Graybody

## 1.7 MULTIPHYSICS

### 1.7.1 Nonisothermal Flow 1

#### USED PRODUCTS

COMSOL Multiphysics

#### SELECTION

Geometric entity level	Domain
Selection	Geometry geom1: Dimension 3: All domains

#### EQUATIONS

$$Q_{vd} = \tau : \nabla \mathbf{u}$$

#### Material Properties

#### SETTINGS

Description	Value
Specify density	From heat transfer interface
Specify reference temperature	From heat transfer interface

#### Flow Heating

#### SETTINGS

Description	Value
Include viscous dissipation	On

#### Coupled Interfaces

#### SETTINGS

Description	Value
Fluid flow	Laminar Flow (spf)
Fluid showDependencies	Off
Heat transfer	Heat Transfer in Solids and Fluids (ht)

## 1.7.2 Heat Transfer with Surface-to-Surface Radiation 1

### USED PRODUCTS

COMSOL Multiphysics
Heat Transfer Module

### SELECTION

Geometric entity level	Boundary
Selection	Geometry geom1: Dimension 2: All boundaries

### EQUATIONS

$$-\mathbf{n} \cdot \mathbf{q} = q_{r,\text{net}}$$

### Coupled Interfaces

### SETTINGS

Description	Value
Heat transfer	Heat Transfer in Solids and Fluids (ht)
Surface-to-surface radiation	Surface-to - Surface Radiation (rad)

## 1.8 MESH 1

### 1.8.1 Size (size)

#### SETTINGS

Description	Value
Maximum element size	7.5
Minimum element size	1.35
Curvature factor	0.6
Resolution of narrow regions	0.5
Maximum element growth rate	1.5

### 1.8.2 Size 1 (size1)

#### SELECTION

Geometric entity level	Domain
Selection	Geometry geom1: Dimension 3: Domain 1

#### SETTINGS

Description	Value
Calibrate for	Fluid dynamics
Maximum element size	2.4
Minimum element size	0.72
Curvature factor	0.7
Resolution of narrow regions	0.6
Maximum element growth rate	1.2
Predefined size	Coarse

### 1.8.3 Size 2 (size2)

#### SELECTION

Geometric entity level	Boundary
Selection	Geometry geom1: Dimension 2: Boundaries 1–2, 5–12

#### SETTINGS

Description	Value
Calibrate for	Fluid dynamics
Maximum element size	1.27
Minimum element size	0.24
Curvature factor	0.5
Resolution of narrow regions	0.8
Maximum element growth rate	1.13
Predefined size	Fine

### 1.8.4 Corner Refinement 1 (cr1)

#### SELECTION

Geometric entity level	Domain
Selection	Geometry geom1: Dimension 3: Domain 1

### 1.8.5 Free Tetrahedral 1 (ftet1)

#### SELECTION

Geometric entity level	Domain
Selection	Remaining

#### SETTINGS

Description	Value
Avoid inverted curved elements	On

### 1.8.6 Boundary Layers 1 (bl1)

#### SELECTION

Geometric entity level	Domain
Selection	Geometry geom1: Dimension 3: Domain 1

#### SETTINGS

Description	Value
Handling of sharp edges	Trimming

### Boundary Layer Properties 1 (blp1)

#### SELECTION

Geometric entity level	Boundary
Selection	Geometry geom1: Dimension 2: Boundaries 1–2, 5–12

#### SETTINGS

Description	Value
Number of boundary layers	2
Thickness adjustment factor	5

G

## Thermometer Data Sheet

## FEATURES

- Type K thermocouple input - the most common thermocouple junction is the type K as it provides the widest operating temperature range
- Measurement range - 50 to 1300°C
- °C / °F selectable display
- Data memory and read function direct from the display (150 sets)
- Display HOLD function
- Operating temperature range 0 to +40 °C
- Input protection 20 V maximum
- Auto power off to conserve battery life
- Flip up stand
- Dual LCD display
- Power source 6 x AAA batteries
- Battery life approximately 110 hours
- Dimensions 150 x 72 x 35 mm
- Weight 235 g

## RS PRO Digital Thermometer - 1319A Digital Thermometer

RS Stock No.: 1232215



RS Professionally Approved Products bring to you professional quality parts across all product categories. Our product range has been tested by engineers and provides a comparable quality to the leading brands without paying a premium price.



## Product Description

### RS PRO K-Type Digital Thermometer

RS PRO 1319A is a great value, high accuracy digital thermometer for use with any K-type thermocouple as a temperature sensor. It features a dual LCD display which shows temperature reading (main display) and MAX /MIN / AVERAGE or offset reference value - in RELATIVE mode (secondary display). A digital thermometer can measure temperature to a decimal point rather than a whole number meaning its results are more accurate. The RS PRO 1319A digital thermometer is ideal for areas where accurate temperature readings are required.

## General Specifications

<b>Model Number</b>	<b>1319A</b>
<b>Thermometer Type</b>	<b>Handheld</b>
<b>Probe Type</b>	<b>K</b>
<b>Number of Temperature Inputs</b>	<b>1</b>
<b>Absolute Maximum Temperature Measurement</b>	<b>+1300 °C, +1999 °F</b>
<b>Temperature Scale</b>	<b>Centigrade, Fahrenheit</b>
<b>Display type</b>	<b>LCD display with backlight</b>
<b>Resolution</b>	<b>0.1 K</b>
<b>Best Accuracy</b>	<b>0.3 % ± 1 °C, 0.3 % ± 2 °F</b>
<b>Temperature Coefficient</b>	<b>0.1x specified accuracy / per °C at 0°C to 18°C &amp; 28°C to 40°C</b>
<b>Data Storage Memory</b>	<b>150 sets (Direct reading from LCD display)</b>
<b>Minimum/Maximum Recordings</b>	<b>Yes</b>
<b>Automatic Shut-Off</b>	<b>Yes Auto power off to conserve battery life</b>
<b>Calibrated Certificate</b>	<b>Yes</b>
<b>Operating Temperature</b>	<b>0 to 50°C (32 to 122°F)</b>
<b>Storage Temperature</b>	<b>10 to 60°C, 14 to 140°F</b>
<b>Operating Humidity</b>	<b>Below 80% RH</b>
<b>Applications</b>	<b>General purpose temperature monitoring</b>

## Electrical Specifications

<b>Battery Type</b>	<b>AAA</b>
<b>Battery Life</b>	<b>Approx. 110 hours</b>

## Mechanical Specifications

<b>Dimensions</b>	<b>150(L) x72(W) x35(H)mm</b>
<b>Length</b>	<b>150mm</b>
<b>Width</b>	<b>72mm</b>
<b>Height</b>	<b>35mm</b>
<b>Weight</b>	<b>Approx. 235g</b>

## Approvals

<b>Declarations</b>	<b>RoHS Certificate of Compliance</b>
---------------------	---------------------------------------

## Similar Products

Stock No.	Brand	Product Name	Thermometer Type	Absolute Maximum Temperature Measurement	Probe Type
1232211	RS PRO	1313 Digital Thermometer	Handheld	+400 (T) °C, +752 (T) °F, +870 (E) °C, +1090 (J) °C, +1300 (N) °C, +1370 (K) °C, +1598 (E) °F, +1767 (R) °C, +1767 (S) °C, +1994 (J) °F, +1999.9 (K) °F, +1999.9 (N) °F, +1999.9 (R) °F, +1999.9 (S) °F	E, J, K, N, R, S, T
1232212	RS PRO	1314 Digital Thermometer	Handheld	+400 (T) °C, +752 (T) °F, +870 (E) °C, +1090 (J) °C, +1300 (N) °C, +1370 (K) °C, +1598 (E) °F, +1767 (R) °C, +1767 (S) °C, +1994 (J) °F, +1999.9 (K) °F, +1999.9 (N) °F, +1999.9 (R) °F, +1999.9 (S) °F	E, J, K, N, R, S, T